

IOW-40-199-2
Revision 0
December 1982
25.2640.0199

DUANE ARNOLD ENERGY CENTER
PLANT UNIQUE ANALYSIS REPORT
VOLUME 2
SUPPRESSION CHAMBER ANALYSIS

Prepared for:
Iowa Electric Light and Power Company

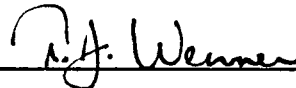
Prepared by:
NUTECH Engineers, Inc.
San Jose, California

Prepared by:



H. H. Shah, S.E.
Engineering Manager

Approved by:



T. J. Wenner, P.E.
Engineering Director


Issued by:



H. J. Sund
Project Manager



for Dr. A. B. Higginbotham, P.E.
Senior Vice President
San Jose Operations



K. A. Hoedeman, P.E.
Project General Manager

Date 12/15/82

8301040098 821230
PDR ADOCK 05000331
P PDR

nutech
ENGINEERS

REVISION CONTROL SHEET

TITLE : Duane Arnold Energy Center
Plant Unique Analysis Report
Volume 2

<u>Vijid Ahij</u> V. Ahuja/Specialist	<u>VA</u> INITIALS
<u>L. S. Chang</u> L. S. Chang/Consultant II	<u>LSC</u> INITIALS
<u>Alan Chau</u> A. N. Chau/Consultant I	<u>ANC</u> INITIALS
<u>Chris W. Fong</u> C. W. Fong/Specialist	<u>cwf</u> INITIALS
<u>P. N. Kaul</u> P. N. Kaul/Principal Engineer	<u>PK</u> INITIALS
<u>Vijay Kumar</u> V. Kumar/Project Engineer	<u>VK</u> INITIALS
<u>Reggie R. Lee</u> V. R. R. Lee/Engineer	<u>VRRL</u> INITIALS
<u>G. S. Ma</u> G. S. Ma/Consultant II	<u>BSM</u> INITIALS
<u>S. H. Rosenblum</u> S. H. Rosenblum/Consultant II	<u>SRH</u> INITIALS
<u>H. H. Shah</u> H. H. Shah/Engineering Manager	<u>HS</u> INITIALS
<u>W. J. Steffy</u> W. J. Steffy/Principal Engineer	<u>WJS</u> INITIALS

EFFEC-TIVE PAGE (S)	REV	PRE-PARED	ACCURACY CHECK	CRITERIA CHECK	EFFEC-TIVE PAGE (S)	REV	PRE-PARED	ACCURACY CHECK	CRITERIA CHECK
2-v	0	PK	LSC	SRH	2-1.2	0	PK	BSM	HS
2-vi	0	PK	LSC	SRH	2-1.3	0	PK	BSM	HS
2-vii	0	BSM	PK	LSC	2-1.4	0	PK	BSM	HS
2-viii	0	PK	BSM	LSC	2-1.5	0	PK	BSM	HS
2-ix	0	PK	BSM	LSC	2-1.6	0	PK	BSM	HS
2-x	0	PK	BSM	LSC	2-1.7	0	PK	BSM	HS
2-xi	0	PK	BSM	LSC	2-2.1	0	PK	BSM	HS
2-xii	0	PK	BSM	LSC	2-2.2	0	PK	BSM	HS
2-xiii	0	PK	BSM	LSC	2-2.3	0	PK	BSM	HS
2-xiv	0	PK	BSM	LSC	2-2.4	0	PK	BSM	HS
2-xv	0	PK	BSM	LSC	2-2.5	0	PK	BSM	HS
2-1.1	0	PK	BSM	SRH	2-2.6	0	PK	BSM	HS
					2-2.7	0	PK	BSM	HS
					2-2.8	0	PK	BSM	HS

REVISION CONTROL SHEET
(Continuation)

TITLE: Duane Arnold Energy Center
Plant Unique Analysis Report
Volume 2

EFFECTIVE PAGE(S)	REV	PRE-PARED	ACCURACY CHECK	CRITERIA CHECK	EFFECTIVE PAGE(S)	REV	PRE-PARED	ACCURACY CHECK	CRITERIA CHECK
2-2.9	0	WJS	Pnk	LSC	2-2.50	0	BSM	ANC	Pnk
2-2.10	↓	↓	↓	↓	2-2.51	↓	↓	↓	↓
2-2.11	↓	↓	↓	↓	2-2.52	↓	ANC	BSM	LSC
2-2.12	↓	↓	↓	↓	2-2.53	↓	↓	↓	LSC
2-2.13	↓	↓	↓	↓	2-2.54	↓	↓	ANC	LSC
2-2.14	↓	↓	↓	↓	2-2.55	↓	BSM	↓	Pnk
2-2.15	↓	↓	↓	↓	2-2.56	↓	↓	↓	↓
2-2.16	↓	↓	↓	↓	2-2.57	↓	↓	↓	↓
2-2.17	↓	↓	↓	↓	2-2.58	↓	↓	↓	↓
2-2.18	↓	↓	↓	LSC	2-2.59	↓	↓	↓	↓
2-2.19	↓	Pnk	BSM	↓	2-2.60	↓	↓	↓	VK
2-2.20	↓	↓	↓	↓	2-2.61	↓	↓	↓	↓
2-2.21	↓	↓	↓	↓	2-2.62	↓	↓	↓	↓
2-2.22	↓	↓	↓	↓	2-2.63	↓	↓	↓	LSC
2-2.23	↓	↓	↓	↓	2-2.64	↓	↓	↓	LSC
2-2.24	↓	↓	↓	↓	2-2.65	↓	↓	↓	LSC
2-2.25	↓	↓	↓	↓	2-2.66	↓	↓	↓	↓
2-2.26	↓	↓	↓	↓	2-2.67	↓	ANC	↓	BSM
2-2.27	↓	↓	↓	↓	2-2.68	↓	↓	↓	↓
2-2.28	↓	↓	↓	↓	2-2.69	↓	Pnk	↓	VK
2-2.29	↓	↓	↓	↓	2-2.70	↓	↓	↓	↓
2-2.30	↓	↓	↓	↓	2-2.71	↓	↓	↓	↓
2-2.31	↓	↓	↓	↓	2-2.72	↓	↓	↓	↓
2-2.32	↓	↓	↓	↓	2-2.73	↓	↓	↓	↓
2-2.33	↓	↓	↓	↓	2-2.74	↓	↓	↓	↓
2-2.34	↓	↓	↓	↓	2-2.75	↓	↓	↓	↓
2-2.35	↓	↓	↓	↓	2-2.76	↓	↓	↓	↓
2-2.36	↓	↓	↓	↓	2-2.77	↓	↓	↓	↓
2-2.37	↓	↓	↓	↓	2-2.78	↓	↓	↓	↓
2-2.38	↓	↓	↓	↓	2-2.79	↓	↓	↓	↓
2-2.39	↓	↓	↓	↓	2-2.80	↓	↓	↓	↓
2-2.40	↓	↓	↓	↓	2-2.81	↓	↓	↓	↓
2-2.41	↓	↓	↓	↓	2-2.82	↓	↓	↓	↓
2-2.42	↓	↓	↓	↓	2-2.83	↓	↓	↓	↓
2-2.43	↓	↓	↓	VK	2-2.84	↓	↓	↓	↓
2-2.44	↓	↓	↓	↓	2-2.85	↓	↓	↓	↓
2-2.45	↓	↓	↓	↓	2-2.86	↓	↓	↓	↓
2-2.46	↓	↓	↓	↓	2-2.87	↓	↓	↓	↓
2-2.47	↓	BSM	ANC	Pnk	2-2.88	↓	↓	↓	↓
2-2.48	↓	↓	↓	↓	2-2.89	↓	↓	↓	↓
2-2.49	0	ANC	BSM	LSC	2-2.90	0	↓	↓	↓

QEP-001.4-00

IOW-40-199-2
Revision 0



REVISION CONTROL SHEET
(Continuation)

TITLE: Duane Arnold Energy Center
Plant Unique Analysis Report
Volume 2

EFFECTIVE PAGE (S)	REV	PRE-PARED	ACCURACY CHECK	CRITERIA CHECK	EFFECTIVE PAGE (S)	REV	PRE-PARED	ACCURACY CHECK	CRITERIA CHECK
2-2.91	0	VA	VKRL	VA	2-2.132	0	VA	CWF	VK
2-2.92	↓	↓	↓	VA	2-2.133	↓	↓	↓	↓
2-2.93	↓	Pnk	AVC	LSC	2-2.134	↓	Pnk	GSM	VA
2-2.94	↓	↓	GSM	VA	2-2.135	↓	↓	↓	↓
2-2.95	↓	↓	↓	↓	2-2.136	↓	↓	↓	↓
2-2.96	↓	↓	↓	↓	2-2.137	↓	↓	↓	↓
2-2.97	↓	↓	↓	↓	2-2.138	↓	↓	↓	↓
2-2.98	↓	↓	↓	↓	2-2.139	↓	AVC	AVC	GSM
2-2.99	↓	↓	↓	↓	2-2.140	↓	GSM	Pnk	VK
2-2.100	↓	↓	↓	↓	2-2.141	↓	↓	↓	LSC
2-2.101	↓	↓	↓	↓	2-2.142	↓	↓	↓	LSC
2-2.102	↓	↓	↓	↓	2-2.143	↓	Pnk	GSM	LSC
2-2.103	↓	↓	↓	↓	2-2.144	↓	↓	↓	VA
2-2.104	↓	↓	↓	↓	2-2.145	↓	↓	↓	↓
2-2.105	↓	↓	↓	↓	2-2.146	↓	↓	↓	↓
2-2.106	↓	↓	↓	↓	2-2.147	↓	Pnk	↓	↓
2-2.107	↓	AVC	↓	Pnk	2-3.1	0	↓	↓	LSC
2-2.108	↓	↓	↓	↓					
2-2.109	↓	↓	↓	↓					
2-2.110	↓	↓	Pnk	GSM					
2-2.111	↓	↓	↓	↓					
2-2.112	↓	↓	↓	↓					
2-2.113	↓	↓	↓	↓					
2-2.114	↓	Pnk	AVC	VA					
2-2.115	↓	↓	↓	↓					
2-2.116	↓	↓	↓	↓					
2-2.117	↓	↓	↓	↓					
2-2.118	↓	↓	↓	↓					
2-2.119	↓	↓	↓	↓					
2-2.120	↓	AVC	Pnk	LSC					
2-2.121	↓	↓	↓	↓					
2-2.122	↓	↓	↓	↓					
2-2.123	↓	Pnk	LSC	VA					
2-2.124	↓	↓	LSC	↓					
2-2.125	↓	↓	LSC	↓					
2-2.126	↓	↓	LSC	↓					
2-2.127	↓	↓	GSM	VK					
2-2.128	↓	↓	↓	↓					
2-2.129	↓	↓	↓	↓					
2-2.130	↓	↓	↓	↓					
2-2.131	0	↓	↓	↓					

ABSTRACT

The primary containment for the Duane Arnold Energy Center (DAEC) was designed, erected, pressure-tested, and ASME Code N-stamped during the early 1970's for the Iowa Electric Light and Power Company by the Chicago Bridge and Iron Company. Since that time new requirements have been generated. These requirements affect the design and operation of the primary containment system and are defined in the Nuclear Regulatory Commission's Safety Evaluation Report NUREG-0661. The requirements to be addressed include an assessment of additional containment design loads postulated to occur during a loss-of-coolant accident or a safety relief valve discharge event, as well as an assessment of the effects that these postulated events have on the operational characteristics of the containment system.

This plant unique analysis report documents the efforts undertaken to address and resolve each of the applicable NUREG-0661 requirements and demonstrates, in accordance with NUREG-0661 acceptance criteria, that the design of the primary containment system is adequate and that original design safety margins have been restored. The report is composed of the following six volumes and appendix.

- o Volume 1 - GENERAL CRITERIA AND LOADS METHODOLOGY
- o Volume 2 - SUPPRESSION CHAMBER ANALYSIS
- o Volume 3 - VENT SYSTEM ANALYSIS
- o Volume 4 - INTERNAL STRUCTURES ANALYSIS
- o Volume 5 - SAFETY RELIEF VALVE DISCHARGE LINE
PIPING ANALYSIS
- o Volume 6 - TORUS ATTACHED PIPING AND SUPPRESSION
CHAMBER PENETRATIONS ANALYSES
- o Appendix A - DAEC RESPONSES TO CURRENT CONTAINMENT
AND PIPING LICENSING ISSUES

Volume 2 documents the evaluation of the suppression chamber and has been prepared by NUTECH Engineers, Inc. (NUTECH), acting as an agent to the Iowa Electric Light and Power Company.

IOW-40-199-2
Revision 0

2-vi

nutech
ENGINEERS

TABLE OF CONTENTS

	<u>Page</u>
ABSTRACT	2-v
LIST OF ACRONYMS	2-viii
LIST OF TABLES	2-xi
LIST OF FIGURES	2-xiii
2-1.0 INTRODUCTION	2-1.1
2-1.1 Scope of Analysis	2-1.3
2-1.2 Summary and Conclusions	2-1.5
2-2.0 SUPPRESSION CHAMBER ANALYSIS	2-2.1
2-2.1 Component Description	2-2.2
2-2.2 Loads and Load Combinations	2-2.20
2-2.2.1 Loads	2-2.21
2-2.2.2 Load Combinations	2-2.69
2-2.3 Analysis Acceptance Criteria	2-2.87
2-2.4 Methods of Analysis	2-2.94
2-2.4.1 Analysis for Major Loads	2-2.95
2-2.4.2 Analysis for Lateral Loads	2-2.114
2-2.4.3 Methods for Evaluating Analysis Results	2-2.123
2-2.5 Analysis Results	2-2.128
2-2.5.1 Discussion of Analysis Results	2-2.143
2-2.5.2 Closure	2-2.146
2-3.0 LIST OF REFERENCES	2-3.1

LIST OF ACRONYMS

ADS	Automatic Depressurization System
ACI	American Concrete Institute
AISC	American Institute of Steel Construction
ASME	American Society of Mechanical Engineers
CDF	Cumulative Distribution Function
CO	Condensation Oscillation
DAEC	Duane Arnold Energy Center
DC	Downcomer
DBA	Design Basis Accident
DBE	Design Basis Earthquake
DLF	Dynamic Load Factor
EQ	Earthquake
FSAR	Final Safety Analysis Report
FSI	Fluid-Structure Interaction
FSTF	Full-Scale Test Facility
IBA	Intermediate Break Accident
ID	Inside Diameter
IELP	Iowa Electric Light and Power
IR	Inside Radius
LDR	Load Definition Report
LOCA	Loss-of-Coolant Accident
MC	Midcylinder
MJ	Miter Joint

LIST OF ACRONYMS

(Continued)

MVA	Multiple Valve Actuation
NEP	Non-Exceedance Probability
NOC	Normal Operating Conditions
NRC	Nuclear Regulatory Commission
NVB	Non-Vent Bay
NWL	Normal Water Level
OBE	Operating Basis Earthquake
OD	Outside Diameter
PSD	Power Spectral Density
PUA	Plant Unique Analysis
PUAAG	Plant Unique Analysis Application Guide
PUAR	Plant Unique Analysis Report
PULD	Plant Unique Load Definition
QSTF	Quarter-Scale Test Facility
RPV	Reactor Pressure Vessel
RSEL	Resultant-Static-Equivalent Load
SBA	Small Break Accident
SER	Safety Evaluation Report
SRSS	Square Root of the Sum of Squares
SRV	Safety Relief Valve
SRVDL	Safety Relief Valve Discharge Line

LIST OF ACRONYMS

(Concluded)

SSE	Safe Shutdown Earthquake
SVA	Single Valve Actuation
TAP	Torus-Attached Piping
VB	Vent Bay
VH	Vent Header
VL	Vent Line

LIST OF TABLES

<u>Number</u>	<u>Title</u>	<u>Page</u>
2-2.2-1	Suppression Chamber Component Loading Identification	2-2.43
2-2.2-2	Suppression Pool Temperature Response Analysis Results - Maximum Temperatures	2-2.44
2-2.2-3	Torus Shell Pressures Due to Pool Swell at Key Times and Selected Locations	2-2.45
2-2.2-4	Ring Beam LOCA Air Clearing Submerged Structure Load Distribution	2-2.46
2-2.2-5	DBA Condensation Oscillation Torus Shell Pressure Amplitudes	2-2.47
2-2.2-6	Ring Beam DBA Condensation Oscillation Submerged Structure Load Distribution	2-2.49
2-2.2-7	Post-Chug Torus Shell Pressure Amplitudes	2-2.50
2-2.2-8	Ring Beam Pre-Chug Submerged Structure Load Distribution	2-2.52
2-2.2-9	Ring Beam Post-Chug Submerged Structure Load Distribution	2-2.53
2-2.2-10	Ring Beam SRV Submerged Structure Load Distribution	2-2.54
2-2.2-11	Mark I Containment Event Combinations	2-2.80
2-2.2-12	Controlling Suppression Chamber Load Combinations	2-2.81
2-2.2-13	Enveloping Logic for Controlling Suppression Chamber Load Combinations	2-2.83
2-2.3-1	Allowable Stresses for Suppression Chamber Components and Supports	2-2.91
2-2.3-2	Suppression Chamber Vertical Support System Allowable Loads	2-2.93

LIST OF TABLES
(Concluded)

<u>Number</u>	<u>Title</u>	<u>Page</u>
2-2.4-1	Suppression Chamber Frequency Analysis Results	2-2.108
2-2.5-1	Maximum Suppression Chamber Shell Stresses for Governing Loads	2-2.130
2-2.5-2	Maximum Vertical Support Reactions for Governing Suppression Chamber Loadings	2-2.131
2-2.5-3	Maximum Suppression Chamber Stresses for Controlling Load Combinations	2-2.132
2-2.5-4	Maximum Vertical Support Reactions for Controlling Suppression Chamber Load Combinations	2-2.134
2-2.5-5	Maximum Suppression Chamber Shell Stresses Due to Lateral Loads	2-2.135
2-2.5-6	Maximum Seismic Restraint Reactions Due to Lateral Loads	2-2.136
2-2.5-7	Maximum Suppression Chamber Shell Stresses and Seismic Restraint Reactions for Controlling Load Combinations with Lateral Loads	2-2.137
2-2.5-8	Maximum Stresses in Seismic Restraint Components for Controlling Load Combinations with Lateral Loads	2-2.138
2-2.5-9	Maximum Fatigue Usage Factors for Suppression Chamber Components and Welds	2-2.139

LIST OF FIGURES

<u>Number</u>	<u>Title</u>	<u>Page</u>
2-2.1-1	Plan View of Containment	2-2.9
2-2.1-2	Elevation View of Containment	2-2.10
2-2.1-3	Suppression Chamber Section - Midbay - Vent Bay	2-2.11
2-2.1-4	Suppression Chamber Section - Miter Joint	2-2.12
2-2.1-5	Suppression Chamber Ring Beam and Vertical Supports - Partial Elevation View	2-2.13
2-2.1-6	Suppression Chamber Ring Beam Stiffener Details	2-2.14
2-2.1-7	Suppression Chamber Vertical Support Base Plates - Partial Plan View and Details	2-2.15
2-2.1-8	Suppression Chamber Seismic Restraint	2-2.16
2-2.1-9	Locations of T-Quenchers	2-2.17
2-2.1-10	Developed View of Suppression Chamber Segment	2-2.18
2-2.1-11	T-quencher and T-quencher Supports - Plan View and Details	2-2.19
2-2.2-1	Suppression Chamber Internal Pressures for SBA Event	2-2.55
2-2.2-2	Suppression Chamber Internal Pressures for IBA Event	2-2.56
2-2.2-3	Suppression Chamber Internal Pressures for DBA Event	2-2.57
2-2.2-4	Suppression Chamber Temperatures for SBA Event	2-2.58
2-2.2-5	Suppression Chamber Temperatures for IBA Event	2-2.59

LIST OF FIGURES
(Continued)

<u>Number</u>	<u>Title</u>	<u>Page</u>
2-2.2-6	Suppression Chamber Temperatures for DBA Event	2-2.60
2-2.2-7	Pool Swell Torus Shell Pressure Transient at Suppression Chamber Miter Joint - Bottom Dead Center Location	2-2.61
2-2.2-8	Pool Swell Torus Shell Pressure Transient for Suppression Chamber Airspace	2-2.62
2-2.2-9	Normalized Torus Shell Pressure Distribution for DBA Condensation Oscillation and Post-Chug Loadings	2-2.63
2-2.2-10	FSI Pool Acceleration Profile for Dominant Suppression Chamber Frequency at Midbay Location	2-2.64
2-2.2-11	Circumferential Torus Shell Pressure Distribution for Symmetric and Asymmetric Pre-Chug Loadings	2-2.65
2-2.2-12	Longitudinal Torus Shell Pressure Distribution for Asymmetric Pre-Chug Loadings	2-2.66
2-2.2-13	SRV Discharge Torus Shell Loads for Case A1.1/A1.3 - Single Valve Actuation	2-2.67
2-2.2-14	SRV Discharge Torus Shell Loads for Case A1.2/C3.2 - Multiple Valve Actuation	2-2.68
2-2.2-15	Suppression Chamber SBA Event Sequence	2-2.84
2-2.2-16	Suppression Chamber IBA Event Sequence	2-2.85
2-2.2-17	Suppression Chamber DBA Event Sequence	2-2.86
2-2.4-1	Suppression Chamber 1/32 Segment Finite Element Model - Isometric View	2-2.111
2-2.4-2	Suppression Chamber Fluid Model - Isometric View	2-2.112

LIST OF FIGURES
(Concluded)

<u>Number</u>	<u>Title</u>	<u>Page</u>
2-2.4-3	Modal Correction Factors Used for Analysis of SRV Discharge Torus Shell Loads	2-2.113
2-2.4-4	Methodology for Suppression Chamber Lateral Load Application	2-2.120
2-2.4-5	Typical Chugging Cycle Load Transient Used for Asymmetric Pre-Chug Dynamic Amplification Factor Determination	2-2.121
2-2.4-6	Dynamic Load Factor Determination for Suppression Chamber Unbalanced Lateral Load Due to SRV Discharge	2-2.122
2-2.4-7	Allowable Number of Stress Cycles for Suppression Chamber Fatigue Evaluation	2-2.127
2-2.5-1	Suppression Chamber Response Due to Pool Swell Loads - Total Vertical Load Per Mitered Cylinder	2-2.140
2-2.5-2	Suppression Chamber Response Due to Single Valve SRV Discharge Torus Shell Loads - Total Vertical Load Per Mitered Cylinder	2-2.141
2-2.5-3	Suppression Chamber Response Due to Multiple Valve SRV Discharge Torus Shell Loads - Total Vertical Load Per Mitered Cylinder	2-2.142

2-1.0 INTRODUCTION

In conjunction with Volume 1 of the Plant Unique Analysis Report (PUAR), this volume documents the efforts undertaken to address the NUREG-0661 requirements which affect the DAEC suppression chamber. The suppression chamber PUAR is organized as follows:

- o INTRODUCTION
 - Scope of Analysis
 - Summary and Conclusions
- o SUPPRESSION CHAMBER ANALYSIS
 - Component Description
 - Loads and Load Combinations
 - Analysis Acceptance Criteria
 - Methods of Analysis
 - Analysis Results

The INTRODUCTION section contains an overview of the scope of the suppression chamber evaluation, as well as a summary of the conclusions derived from the comprehensive evaluation of the suppression chamber. The SUPPRESSION CHAMBER ANALYSIS section contains a comprehensive discussion of the suppression chamber loads and load combinations and a description of the

suppression chamber components affected by these loads. The section also contains a discussion of the methodology used to evaluate the effects of these loads, the evaluation results, and the acceptance limits to which the results are compared.

IOW-40-199-2
Revision 0

2-1.2

nutech
ENGINEERS

2-1.1 Scope of Analysis

The criteria presented in Volume 1 are used as the basis for the DAEC suppression chamber evaluation. The suppression chamber is evaluated for the effects of LOCA-related and SRV discharge-related loads defined by the NRC Safety Evaluation Report NUREG-0661 (Reference 1) and by the "Mark I Containment Program Load Definition Report" (LDR) (Reference 2).

The LOCA and SRV discharge loads used in this evaluation are formulated using the methodology discussed in Volume 1 of this report. The loads are developed using the plant unique geometry, operating parameters, and test results contained in the "Mark I Containment Program Plant Unique Load Definition" (PULD) report (Reference 3). Other loads and methodology, such as the evaluation for seismic loads, are taken from the plant's Final Safety Analysis Report (FSAR) (Reference 4). The effects of increased suppression pool temperatures which occur during SRV discharge events are also evaluated. These temperatures are taken from the plant's suppression pool temperature response analysis.

The evaluation includes a structural analysis of the suppression chamber for the effects of LOCA-related and SRV discharge-related loads to confirm that the design of the modified suppression chamber is adequate. Rigorous analytical techniques are used in this evaluation, including the use of detailed analytical models for computing the dynamic response of the suppression chamber. Effects such as fluid-structure interaction are considered in the suppression chamber analysis.

The results of the structural evaluation of the suppression chamber for each load are used to evaluate load combinations and fatigue effects in accordance with the "Mark I Containment Program Structural Acceptance Criteria Plant Unique Analysis Application Guide" (PUAAG) (Reference 5). The analysis results are compared with the acceptance limits specified by the PUAAG and the applicable sections of the ASME Code (Reference 6).

2-1.2 Summary and Conclusions

The evaluation documented in this report is based on the modified DAEC suppression chamber as described in Section 1-2.1. The overall load-carrying capacity of the suppression chamber and its supports is substantially greater than that of the original suppression chamber design described in the plant's FSAR.

The loads considered in the original design of the suppression chamber include dead loads, OBE and DBE loads, and pressure and temperature loads associated with normal operating conditions (NOC) and a postulated LOCA event. Additional loadings, which affect the design of the suppression chamber, are postulated to occur during SBA, IBA, or DBA LOCA events and during SRV discharge events. These loadings are defined generically in NUREG-0661. Each of these events results in hydrodynamic pressure loadings on the suppression chamber shell, hydrodynamic drag loadings on the submerged suppression chamber components, and in reaction loadings caused by loads acting on structures attached to the suppression chamber.

The methodology used to develop plant unique loadings for the suppression chamber evaluation is discussed in Section 1-4.0. Applying this methodology results in conservative values for each of the significant NUREG-0661 loadings which envelop those postulated to occur during an actual LOCA or SRV discharge event.

The LOCA-related and SRV discharge-related loads are grouped into event combinations using the NUREG-0661 criteria discussed in Section 1-3.2. The event sequencing and event combinations specified and evaluated envelop the actual events expected to occur throughout the life of the plant.

Some of the loads contained in the postulated event combinations are major contributors to the total response of the suppression chamber. These include LOCA internal pressure loads, DBA pool swell suppression chamber shell loads, DBA condensation oscillation suppression chamber shell loads, and SRV discharge suppression chamber shell loads. Although considered in the evaluation, other loadings, such as temperature loads, seismic loads, chugging suppression chamber shell loads, submerged structure loads, and containment structure reaction loads, have a lesser effect on the total response of the suppression chamber.

The suppression chamber evaluation is based on the NUREG-0661 acceptance criteria discussed in Section 1-3.2. These acceptance limits are at least as restrictive as those used in the original suppression chamber design documented in the plant's FSAR. Use of these criteria ensures that the original suppression chamber design margins have been restored.

The controlling event combinations for the suppression chamber are those which include the loadings found to be major contributors to the response of the suppression chamber. The evaluation results for these controlling event combinations show that all of the suppression chamber stresses and support reactions are within acceptable limits.

As a result, the suppression chamber described in Section 1-2.1 is adequate to restore the margins of safety inherent in the original design of the suppression chamber documented in the plant's FSAR. The NUREG-0661 requirements, as they affect the design adequacy and safe operation of the DAEC suppression chamber, are met.

Evaluations of each NUREG-0661 requirement affecting the design adequacy of the DAEC suppression chamber are presented in the following sections. The criteria used in this evaluation are presented in Volume 1 of this report.

The suppression chamber (torus) components examined are described in Section 2-2.1. The loads and load combinations for which the suppression chamber is evaluated are presented in Section 2-2.2. The acceptance limits to which the analysis results are compared are described in Section 2-2.3. The methodology used to evaluate the effects of these loads and load combinations on the suppression chamber is discussed in Section 2-2.4. The analysis results and the corresponding suppression chamber design margins are presented in Section 2-2.5.

2-2.1 Component Description

The DAEC suppression chamber (torus) is constructed from 16 mitered cylindrical shell segments joined together in the shape of a torus. Figure 2-2.1-1 shows the plan view of the suppression chamber. Figure 2-2.1-2 shows the proximity of the suppression chamber to other components of the containment.

The major radius of the suppression chamber is 49'4", measured at midbay of each mitered cylinder (Figure 2-2.1-1). The inside diameter of the mitered cylinders which make up the suppression chamber is 25'8". The suppression chamber shell thickness is typically 0.500" above the horizontal centerline and 0.534" below the horizontal centerline (Figure 2-2.1-3), except at penetrations where it is locally thicker.

The suppression chamber is connected to the drywell by eight vent lines, which in turn are connected to a common vent header within the suppression chamber. A bellows assembly is provided at the penetration of the vent line to the suppression chamber to allow differential movement of the suppression chamber and vent system to occur (Figure 2-2.1-3). Attached to the

vent header are downcomers which terminate below the surface of the suppression pool. The vent system is supported vertically at each miter joint by two support columns, which transfer reaction loads to the suppression chamber (Figure 2-2.1-4).

The suppression chamber shell is reinforced at each miter joint location by a T-shaped ring beam (Figures 2-2.1-4 and 2-2.1-5). A typical ring beam is located in a plane 4" from the miter joint and on the non-vent bay side of each miter joint. The inner flange of the ring beam is an 8" wide, 1-1/4" thick plate rolled to a constant inside radius of 11'4-3/4". Thus a ring beam web depth varies from 16" to 19" and has a constant thickness of 1-1/4". As such, the intersection of a ring beam web and the suppression chamber shell is an ellipse. The ring beam is attached to the suppression chamber shell with 5/16" fillet welds.

The ring beams are braced laterally with 1" and 1-1/4" thick stiffeners connecting the ring beam webs to the suppression chamber shell. The stiffener plates are spaced intermittently around the circumference of the

ring beams, concentrated in areas where lateral submerged drag loads and flange compressive stresses occur (Figure 2-2.1-6).

The suppression chamber is supported vertically at each miter joint location by inside and outside columns and by saddle supports adjacent to the columns (Figures 2-2.1-4 and 2-2.1-5). The columns, column connection plates, and saddle supports are located parallel to the associated miter joint in the plane of the ring beam web. At each miter joint, the ring beam, columns, column connections, and saddle support form an integral support system which takes vertical loads acting on the suppression chamber shell and transfers them to the reactor building basemat. The support system provides full vertical support for the suppression chamber, allowing lateral movement and thermal expansion to occur. The addition of saddles to the vertical support system provides a load transfer mechanism which reduces local suppression chamber shell stresses and distributes reaction loads more evenly to the basemat.

The inside and outside column supports are W10 X 89 rolled sections. The connection of the column supports to the suppression chamber shell consists of 5/8" web

and flange plates. The web plates are welded to the suppression chamber shell with full penetration welds, and the flange plates are connected to the web plate using fillet welds. The 2-1/2" column base plate is supported by a 2-3/4" bearing plate which rests on the basemat. A 1/4" thick lubrite plate is provided between the base plate and the bearing plate to permit free thermal movement of the column base with respect to the basemat. Steel hold-down brackets welded to the columns are anchored to the basemat to provide more uplift capacity. The brackets have slotted holes to allow free horizontal thermal movement between the brackets and anchor bolts. In addition to the two cast-in-place 1-3/4" diameter anchor bolts, two 1-1/4" diameter anchor bolts (Maxi-Bolts) are provided at 12 of the outside columns to transmit additional uplift forces, resulting from hydrodynamic loads, to the basemat (Figures 2-2.1-5 and 2-2.1-7).

Each saddle support is composed of a 1-1/4" thick stiffened web plate and saddle base plate assemblies (Figures 2-2.1-4 and 2-2.1-5). The saddle support web plates are attached to the suppression chamber shell with full penetration welds and are also welded to the suppression chamber support columns. The saddle support

web plates are stiffened to ensure that buckling does not occur during peak load transfer. The base plate assembly immediately under the saddle webs is identical to that provided under the columns. A system of base plate assemblies and brackets are welded to the saddle web stiffeners at one end and anchored to the basemat at the other end, helping to transmit saddle uplift loads to the basemat. Anchor bolts (Maxi-Bolts), 1-1/4" in diameter, are provided in groups of 6 and 10 for the outside saddles and in groups of 6 and 8 for the inside saddles (Figures 2-2.1-5 and 2-2.1-7). Thus, the number of anchor bolts at the miters, including column anchor bolts, varies from 16 to 24.

Four seismic restraints, which provide lateral support for the suppression chamber, are located 90° apart (Figure 2-2.1-1). Each seismic restraint consists of a 1-1/2" thick pad plate welded to the bottom of the suppression chamber shell, a system of interlaced pin plates joined together by an 8" diameter pin, and a 2-1/4" thick base plate with shear bars keyed and grouted into the basemat (Figure 2-2.1-8). The seismic restraints permit vertical and radial movement of the suppression chamber, at the same time restraining longitudinal movement resulting from lateral loads acting on the suppression chamber. The pad plates

distribute loads over a large area of the suppression chamber shell and provide an effective means of transferring suppression chamber lateral loads to the basemat.

The T-quencher used for DAEC is described in Section 1-4.2 and also in Volume 5. Six T-quenchers (with ramsheads) are located at the midbay with the associated quencher arms aligned along the suppression chamber axis. Each T-quencher device is supported by a beam that spans the ring girders and each SRV line is supported near the elbow by a beam that spans between ring girders. Figures 2-2.1-9 through 2-2.1-11 show location and details of the six DAEC T-quenchers.

The suppression chamber provides support for many other containment-related structures, such as the vent system, catwalk, monorail and attached piping. Loads acting on the suppression chamber cause motions at the attachment points of these structures to the suppression chamber. Loads acting on these structures also cause reaction loads on the suppression chamber. These containment interaction effects are evaluated in the analysis of the suppression chamber.

The overall load-carrying capacities of the suppression chamber components described in the preceding paragraphs are substantially greater than those of the original suppression chamber design described in the plant's FSAR.

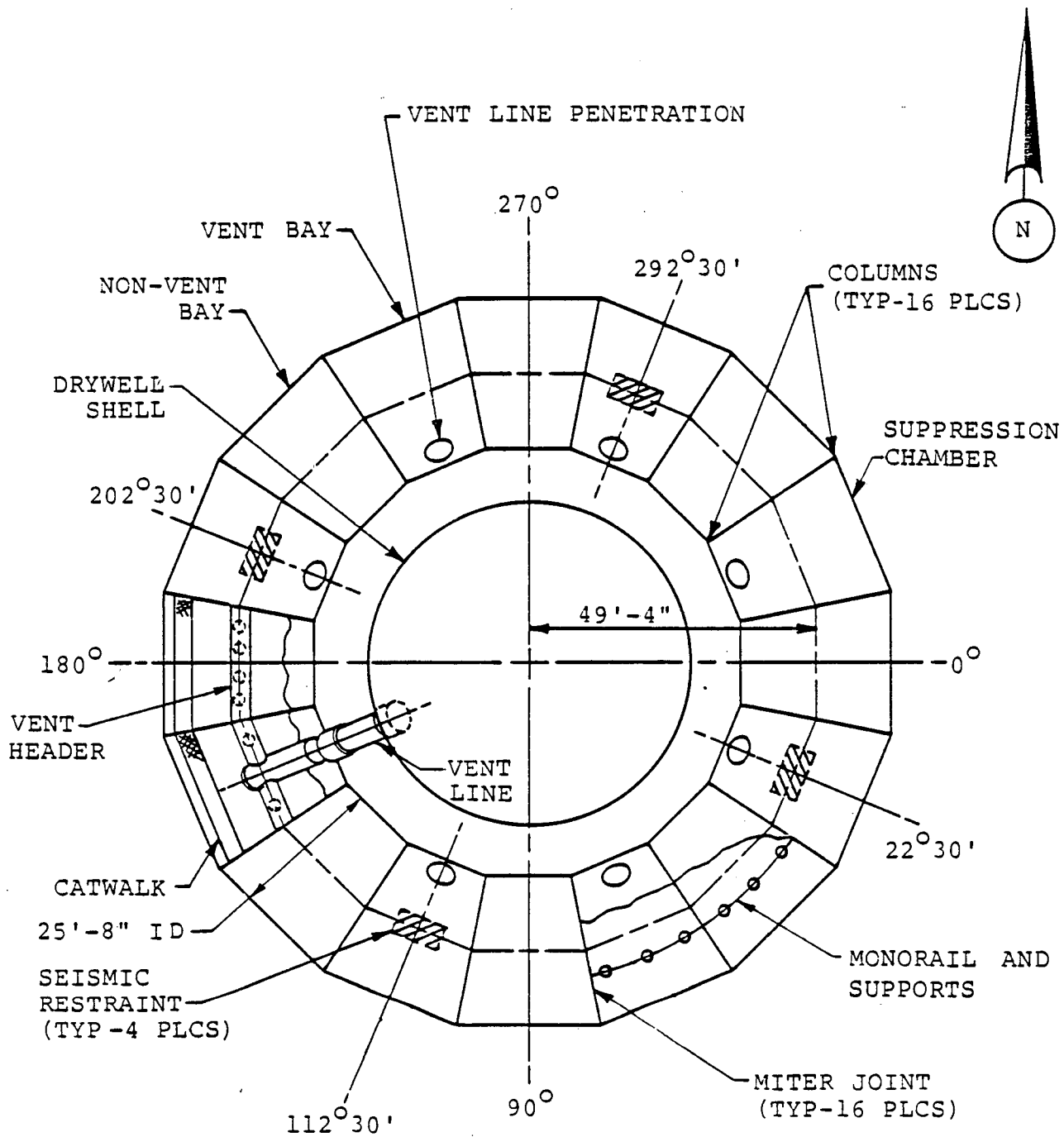


Figure 2-2.1-1
PLAN VIEW OF CONTAINMENT

IOW-40-199-2
 Revision 0

2-2.9

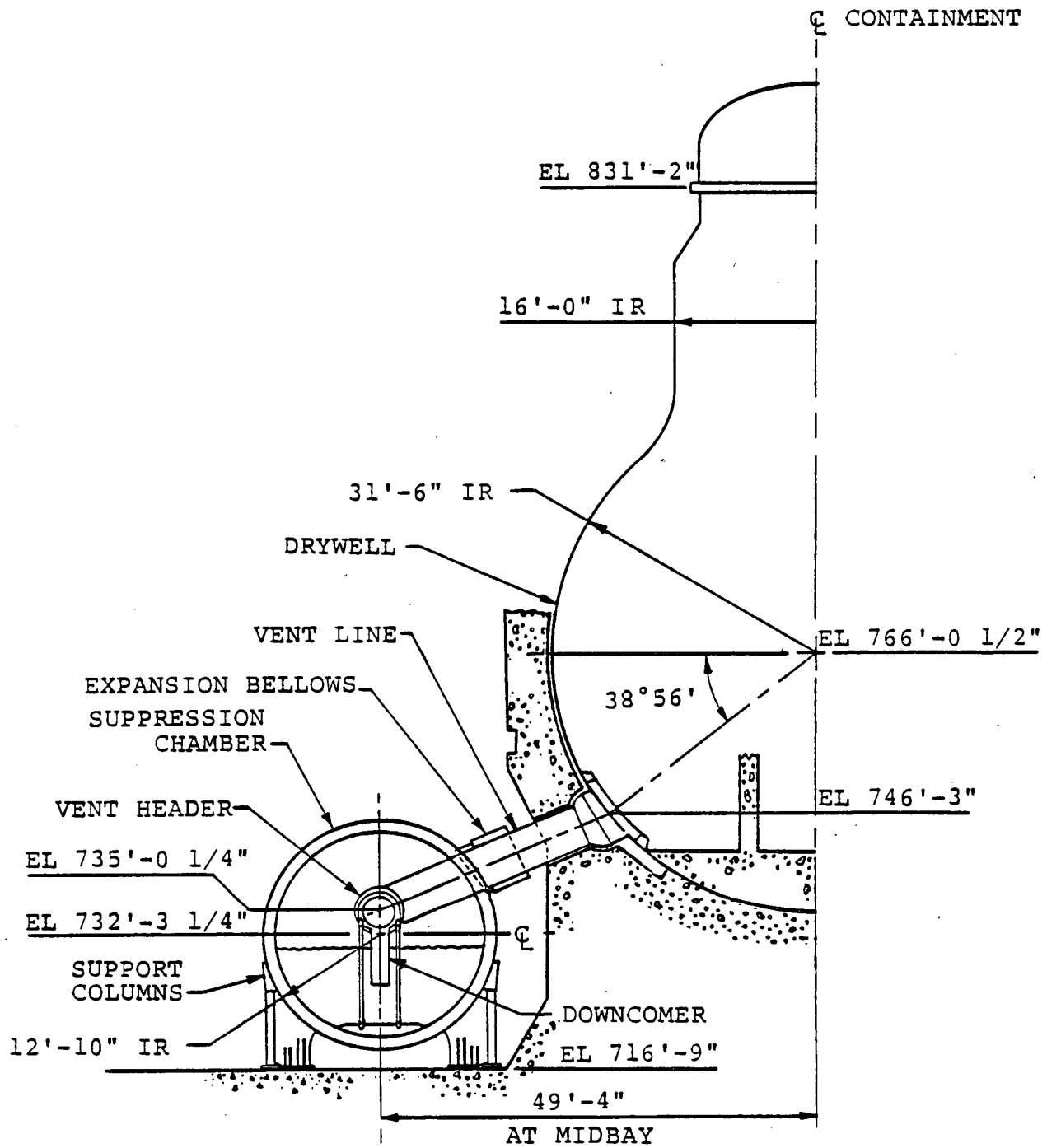


Figure 2-2.1-2

ELEVATION VIEW OF CONTAINMENT

IOW-40-199-2
Revision 0.

2-2.10

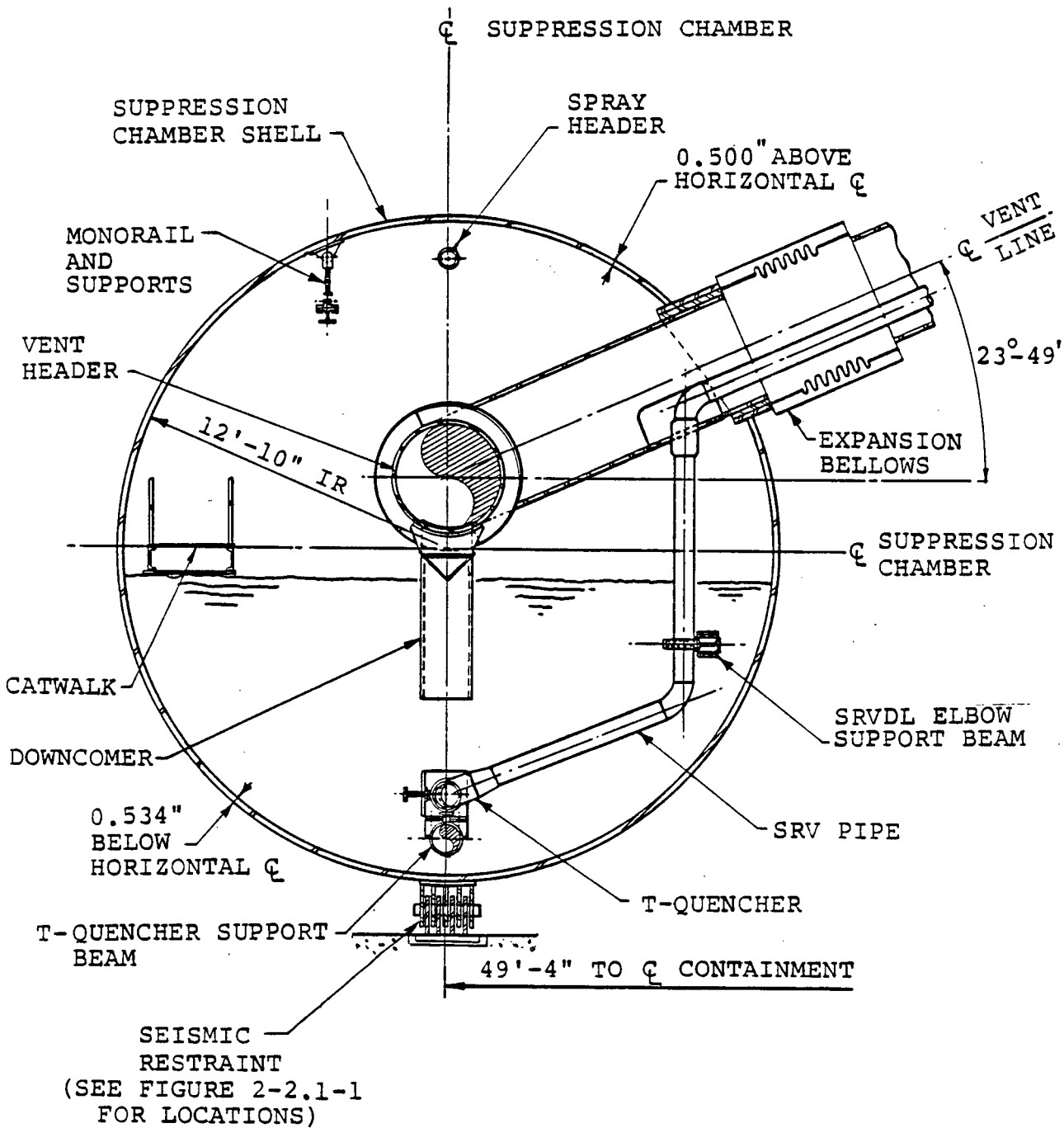
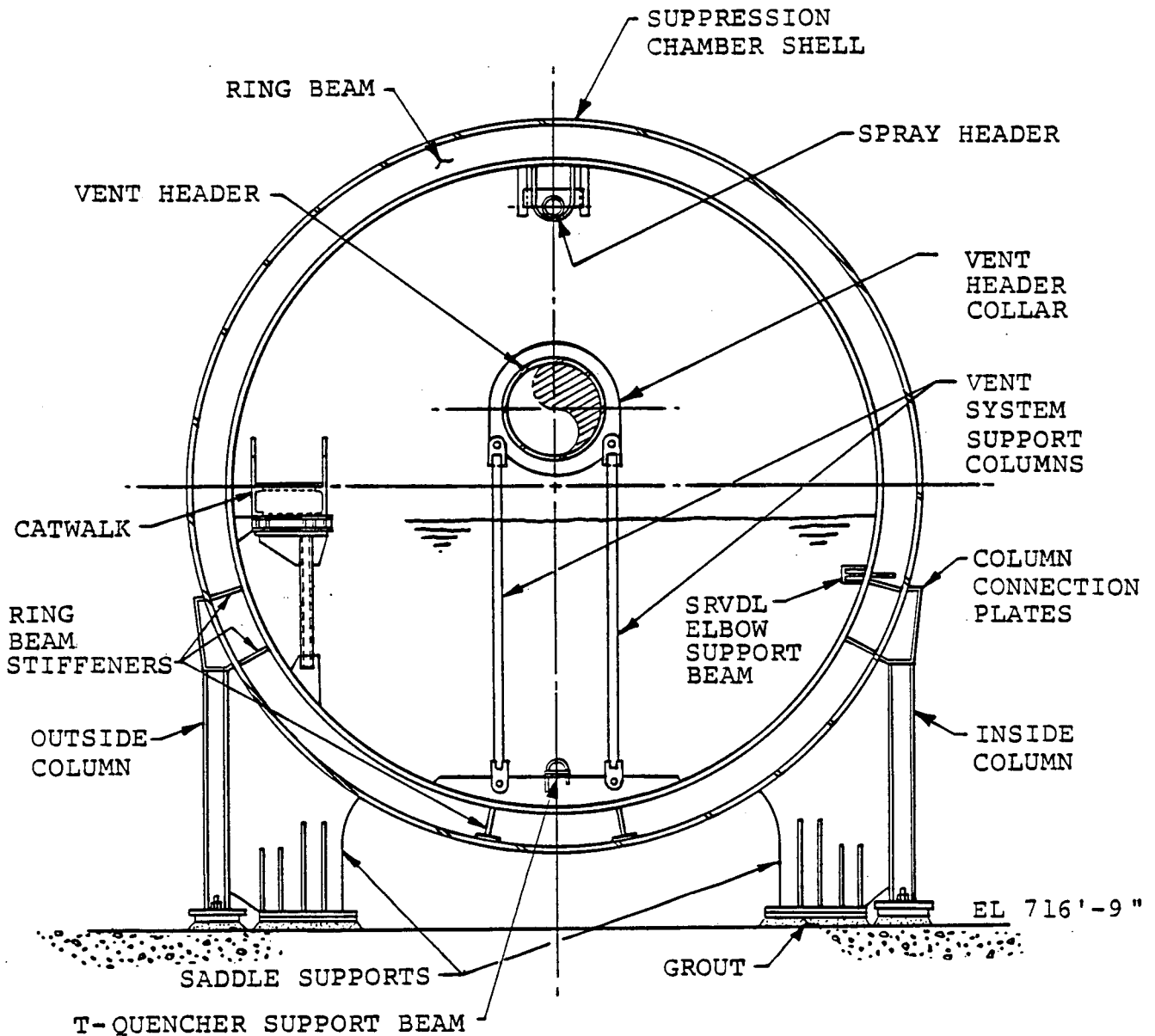


Figure 2-2.1-3

SUPPRESSION CHAMBER SECTION-
MIDBAY - VENT BAY

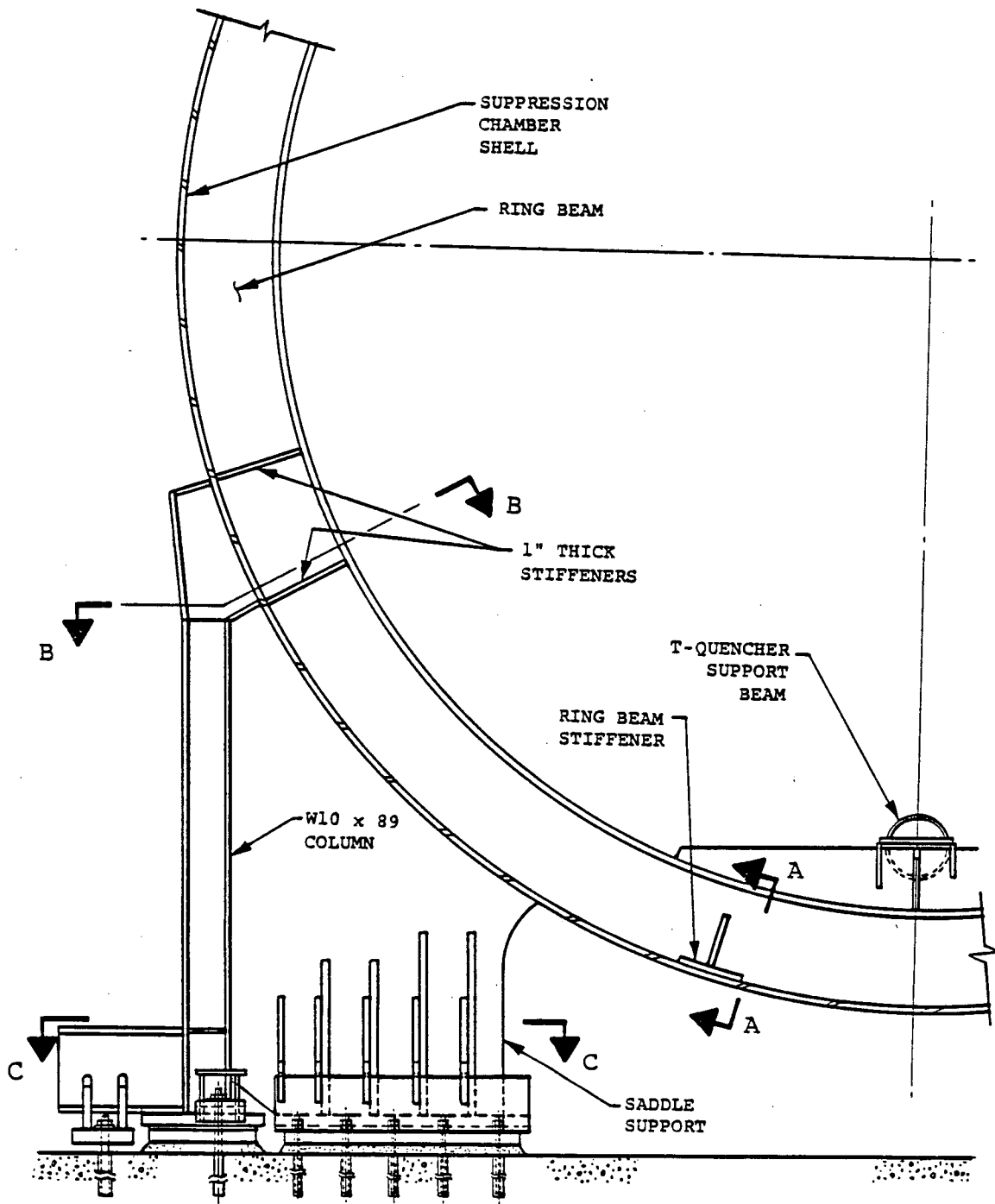
IOW-40-199-2
Revision 0

2-2.11



1. ADDITIONAL ANCHORAGE NOT SHOWN FOR CLARITY.

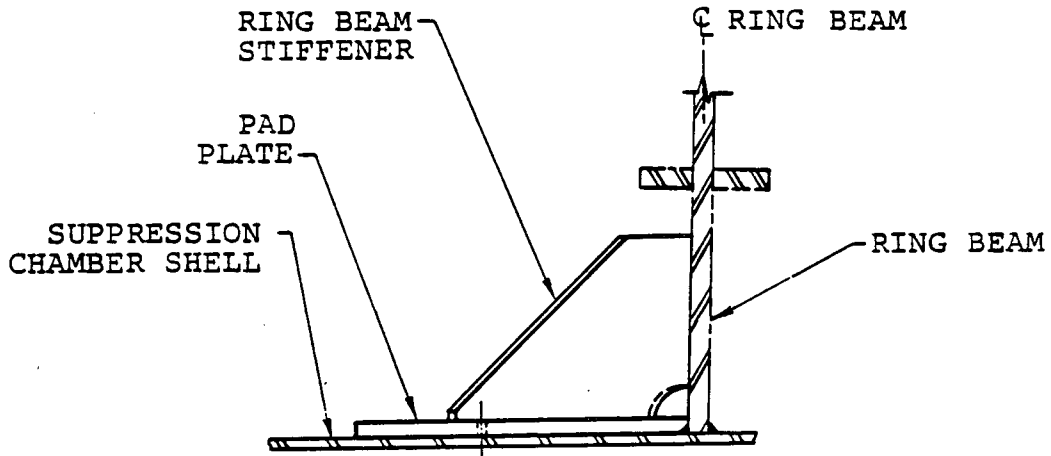
Figure 2-2.1-4
SUPPRESSION CHAMBER SECTION -
MITER JOINT



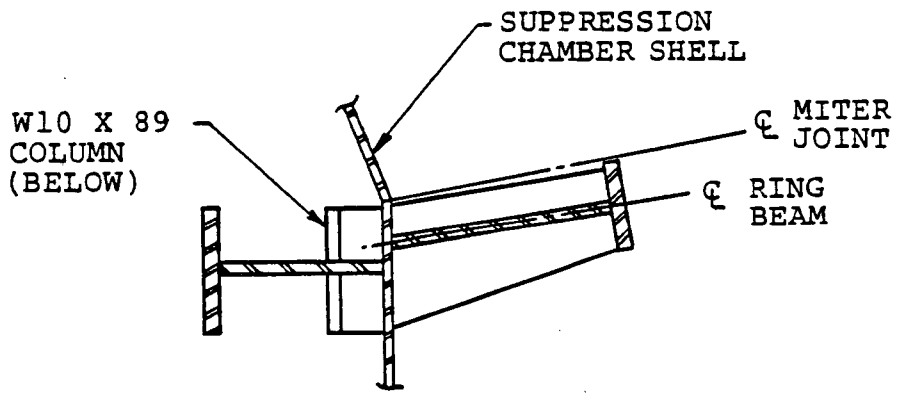
1. SEE FIGURE 2-2.1-6 FOR SECTION A-A AND B-B;
SEE FIGURE 2-2.1-7 FOR SECTION C-C

Figure 2-2.1-5

SUPPRESSION CHAMBER RING BEAM AND VERTICAL SUPPORTS
- PARTIAL ELEVATION VIEW

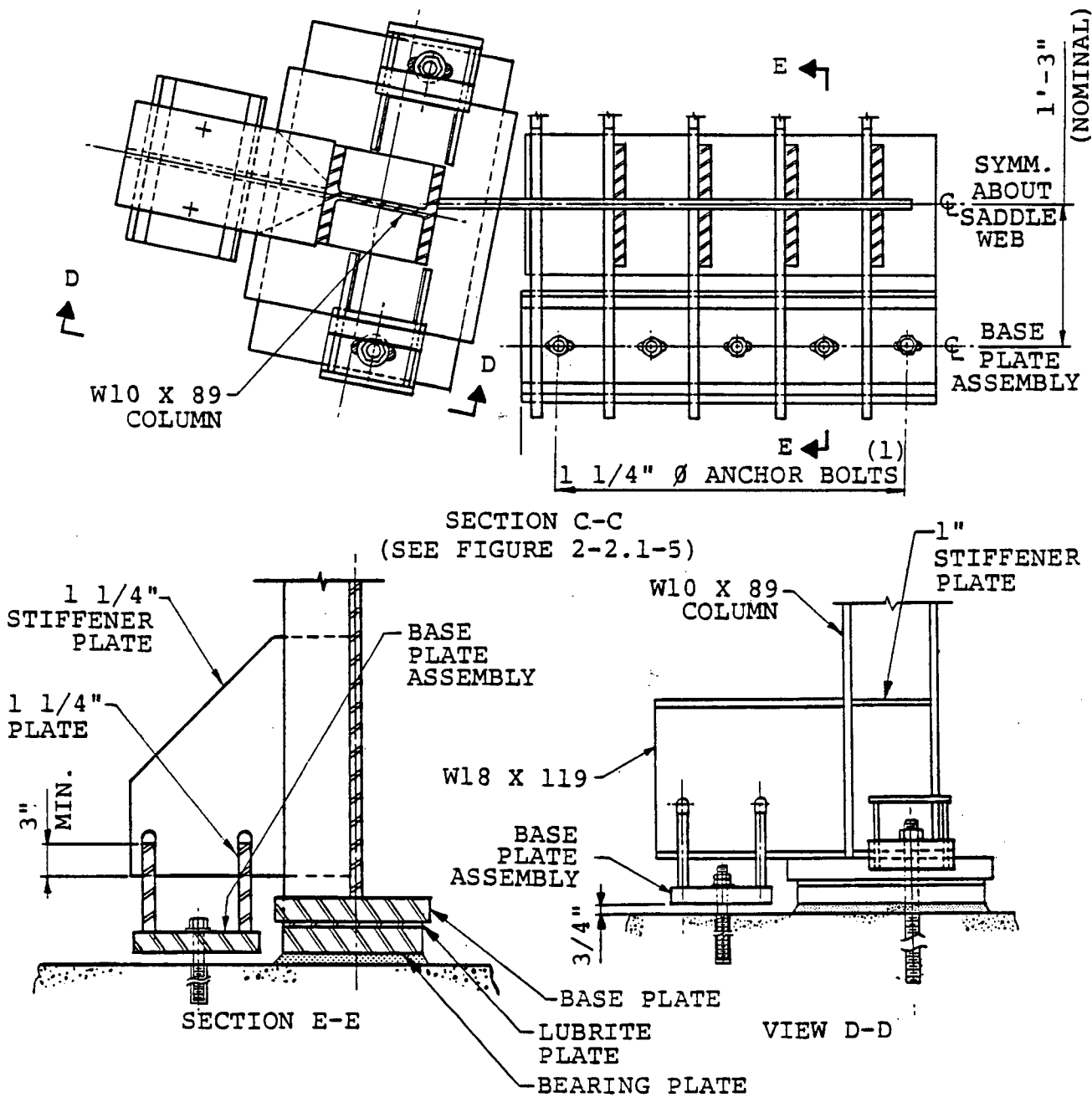


SECTION A-A
(SEE FIGURE 2-2.1-5)



SECTION B-B
(SEE FIGURE 2-2.1-5)

Figure 2-2.1-6
SUPPRESSION CHAMBER RING BEAM STIFFENER DETAILS



(1) NUMBER OF ANCHOR BOLTS VARIES FROM 3 TO 5 DEPENDING ON LOCATION.

Figure 2-2.1-7

SUPPRESSION CHAMBER VERTICAL SUPPORT
BASE PLATES - PARTIAL PLAN VIEW AND DETAILS

IOW-40-199-2
Revision 0

2-2.15

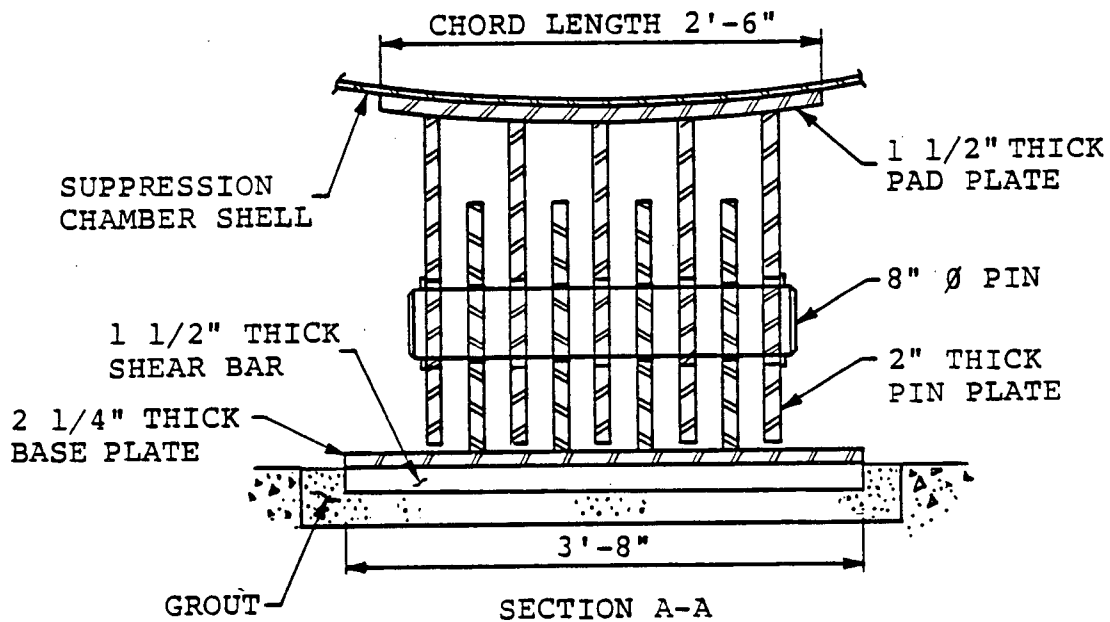
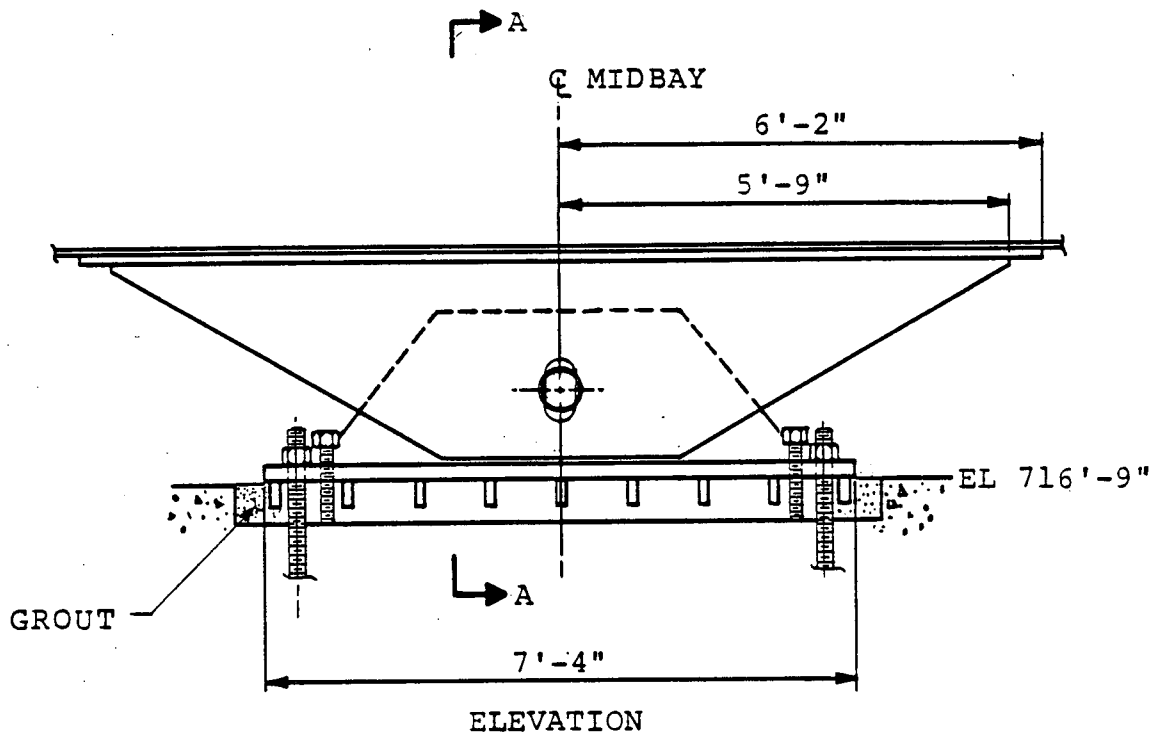
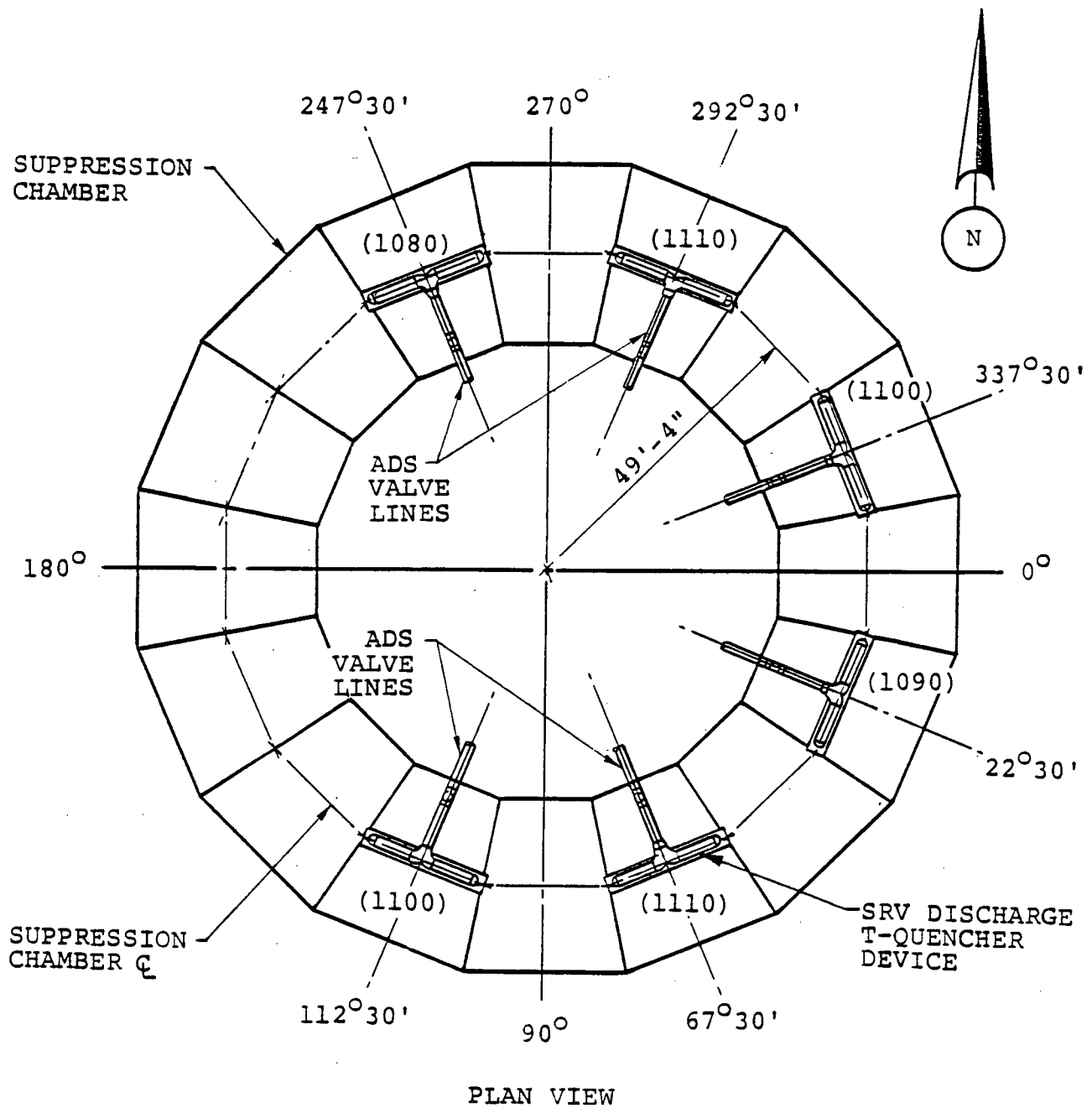


Figure 2-2.1-8
SUPPRESSION CHAMBER SEISMIC RESTRAINT

IOW-40-199-2
 Revision 0

2-2.16



1. SET POINT PRESSURE IN psi ARE DESIGNATED BY ().

Figure 2-2.1-9
LOCATIONS OF T-QUENCHERS

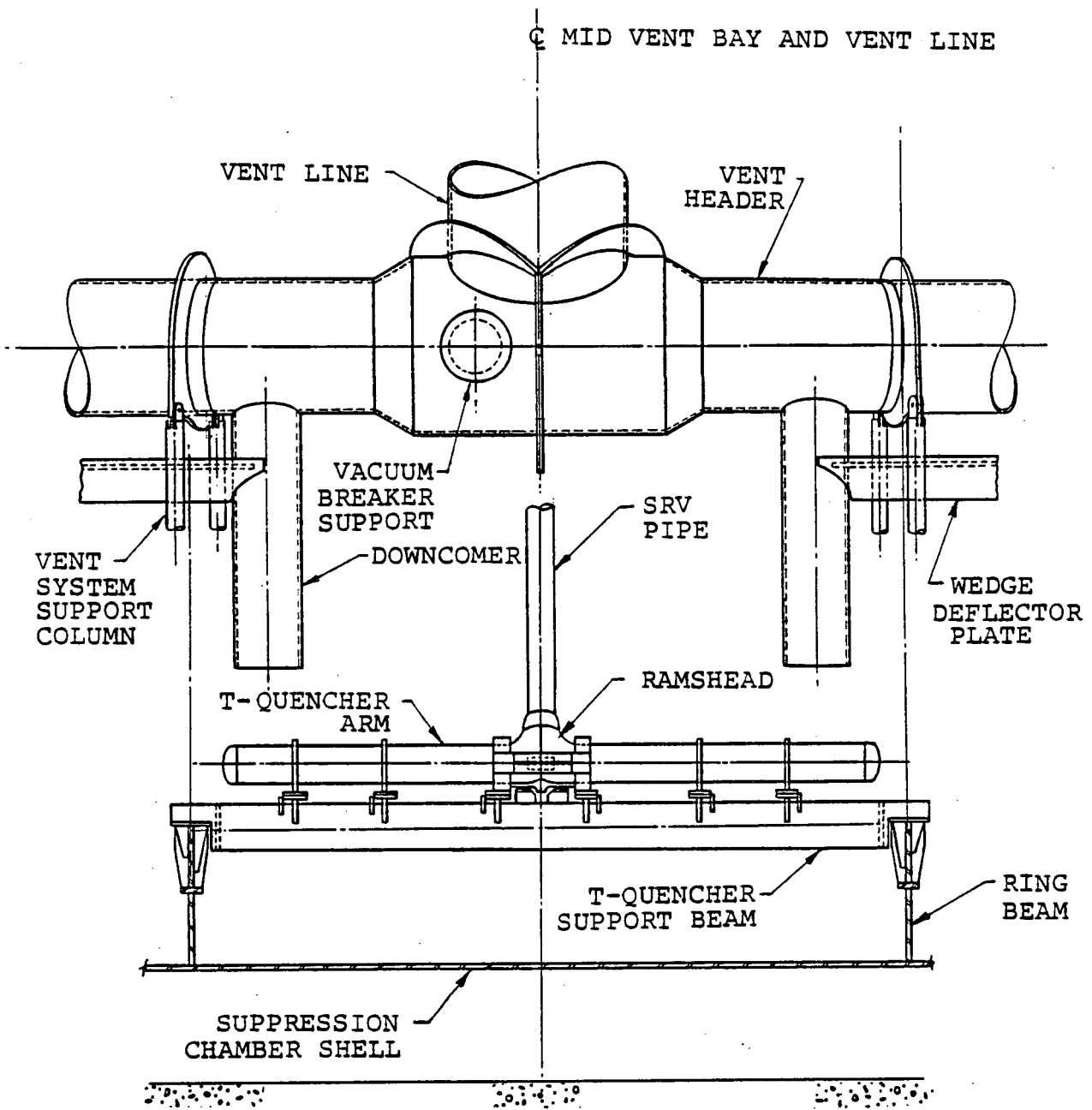


Figure 2-2.1-10

DEVELOPED VIEW OF SUPPRESSION CHAMBER SEGMENT

IOW-40-199-2
Revision 0

2-2.18

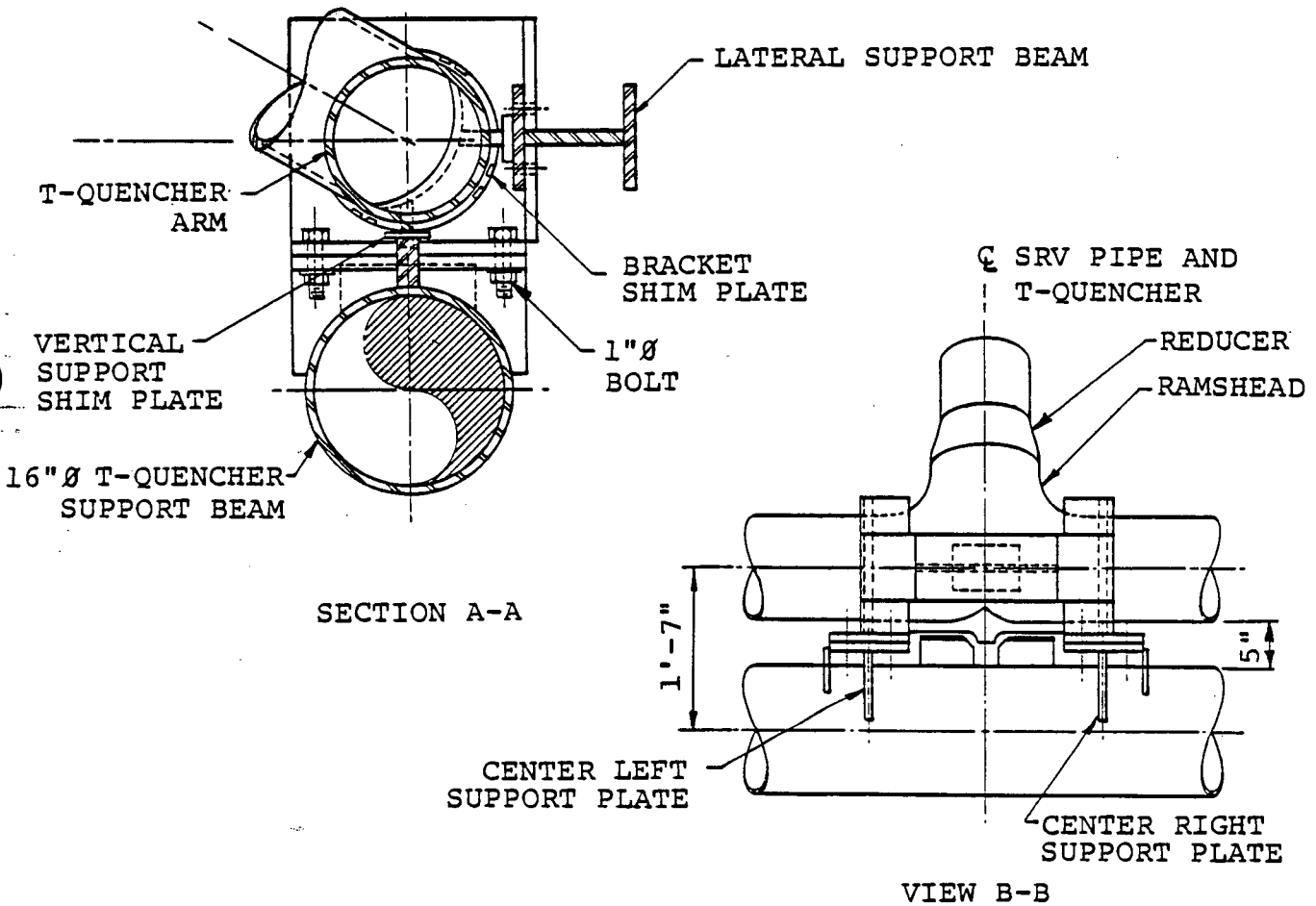
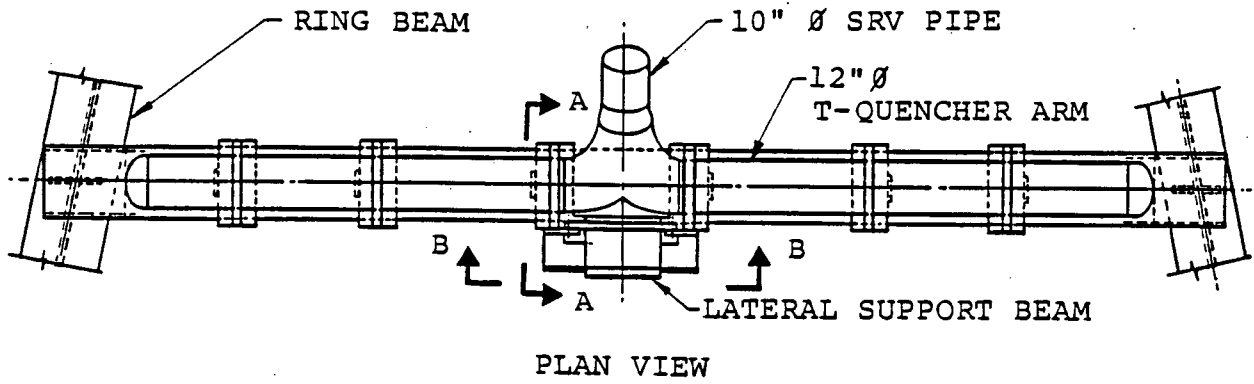


Figure 2-2.1-11

T-QUENCHER AND T-QUENCHER SUPPORTS-PLAN VIEW AND DETAILS

IOW-40-199-2
Revision 0

2-2.19

2-2.2 Loads and Load Combinations

The loads for which the DAEC suppression chamber is evaluated are defined in NUREG-0661 on a generic basis for all Mark I plants. The methodology used to develop plant unique suppression chamber loads for each load defined in NUREG-0661 is discussed in Section 1-4.0. The results of applying the methodology to develop specific values for each of the governing loads which act on the suppression chamber are discussed and presented in Section 2-2.2.1.

The controlling load combinations which affect the suppression chamber are formulated using the event combinations and event sequencing defined in NUREG-0661 and discussed in Sections 1-3.2 and 1-4.3. The controlling suppression chamber load combinations are discussed and presented in Section 2-2.2.2.

2-2.2.1 Loads

The loads acting on the suppression chamber are categorized as follows.

1. Dead Loads
2. Seismic Loads
3. Pressure and Temperature Loads
4. Pool Swell Loads
5. Condensation Oscillation Loads
6. Chugging Loads
7. Safety Relief Valve Discharge Loads
8. Containment Interaction Loads

Loads in categories 1 through 3 were considered in the original containment design as documented in the plant's FSAR. Additional category 3 pressure and temperature loads result from postulated LOCA and SRV discharge events. Loads in categories 4 through 6 result from postulated LOCA events; loads in category 7 result from SRV discharge events; loads in category 8 are reactions which result from loads acting on other containment structures attached to the suppression chamber.

Not all of the loads defined in NUREG-0661 are evaluated in detail, since some are enveloped by others or have a negligible effect on the suppression chamber. Only those loads which maximize the suppression chamber response and lead to controlling stresses are fully evaluated. In subsequent discussions, these loads are referred to as governing loads.

Table 2-2.2-1 shows the specific suppression chamber components affected by each of the loadings defined in NUREG-0661. The table also lists the section in the PUAR which discusses the methodology for developing values for each loading. The magnitudes and characteristics of each governing suppression chamber load in each load category are identified and presented in the following paragraphs.

1. Dead Loads

- a. Weight of Steel: The weight of steel used to construct the as-modified suppression chamber and its supports is considered. The nominal component dimensions and a density of steel of 490 lb/ft^3 are used in this calculation.

- b. Weight of Water: The weight of water contained in the suppression chamber is considered. A volume of water of 61,500 ft³, corresponding to a water level of 2.42 feet below the suppression chamber horizontal centerline, and a water density of 62.4 lb/ft³ are used in this calculation. This water volume is the maximum expected during normal operating conditions.

2. Seismic Loads

- a. OBE: The suppression chamber is subjected to horizontal and vertical accelerations during an Operating Basis Earthquake (OBE). This loading is taken from the original design basis for the containment documented in the plant's FSAR. The OBE loads are based on a horizontal acceleration of 0.12g and a vertical acceleration of 0.053g.
- b. SSE: The suppression chamber is subjected to horizontal and vertical accelerations during a Safe Shutdown Earthquake (SSE). This loading is taken from the original design basis for

the containment documented in the plant's FSAR, where it was termed Design Basis Earthquake (DBE). The SSE loads are based on a horizontal acceleration of 0.24g and a vertical acceleration of 0.106g.

3. Pressure and Temperature Loads

- a. Normal Operating Internal Pressure: The suppression chamber shell is subjected to internal pressure loads during normal operating conditions. This loading is taken from the original design basis for the containment documented in the plant's FSAR. The range of normal operating internal pressures specified is -2.0 to 2.0 psi.

- b. LOCA Internal Pressure: The suppression chamber shell is subjected to internal pressure during a small break accident (SBA), an intermediate break accident (IBA), or a design basis accident (DBA) event. The procedure used to develop LOCA internal pressures for the containment is discussed in Section 1-4.1.1. Figures 2-2.2-1 through 2-2.2-3

present the resulting suppression chamber internal pressure transients and pressure magnitudes at key times during the SBA, IBA, and DBA events.

The pressures specified for each event are assumed to act uniformly over the suppression chamber shell surface, except during the early portion of a DBA event. The effects of internal pressure on the suppression chamber for the initial portion of a DBA event are included in the pool swell suppression chamber shell loads discussed in load case 4a. The corresponding suppression chamber external or secondary containment pressure for all events is assumed to be zero.

- c. Normal Operating Temperature: The suppression chamber is subjected to the thermal expansion load associated with normal operating conditions. This loading is taken from the original design basis for the containment documented in the plant's FSAR. The range of normal operating temperatures for the suppression chamber is 50° to 100°F.

For specific conditions of normal operation, the suppression chamber temperatures are taken from the suppression pool temperature response analysis. The resulting temperatures are summarized in Table 2-2.2-2.

- d. LOCA Temperature: The suppression chamber is subjected to thermal expansion loads associated with the SBA, IBA, and DBA events. The procedure used to develop LOCA containment temperatures is discussed in Section 1-4.1.1. Figures 2-2.2-4 through 2-2.2-6 present the resulting suppression chamber temperature transients and temperature magnitudes at key times during the SBA, IBA, and DBA events.

For specific conditions of the SBA event, the suppression chamber temperatures are taken from the suppression pool temperature response analysis. The resulting suppression chamber temperatures are summarized in Table 2-2.2-2. The greater of the temperatures specified in Figure 2-2.2-4 and Table 2-2.2-2 is used in evaluating the effects of SBA event temperatures.

The temperatures specified for each event are assumed to be representative of pool temperatures, airspace temperatures, and suppression chamber shell metal temperatures throughout the suppression chamber. The ambient temperature for all events is assumed to be equal to the arithmetic mean of the minimum and maximum suppression chamber operating temperatures, which is 75°F. As the temperature of the suppression chamber shell begins to increase, the temperature difference between the suppression chamber shell and the suppression chamber vertical supports will result in differential thermal expansion effects.

4. Pool Swell Loads

- a. Pool Swell Suppression Chamber Shell: During the initial phase of a DBA event, transient pressures are postulated to act on the suppression chamber shell above and below the suppression pool surface. The procedure used to develop local suppression chamber shell pressures due to pool swell is discussed in Section 1-4.1.3. Figures 2-2.2-7 and 2-2.2-8

show the resulting pressure time-histories at selected locations on the suppression chamber shell. Table 2-2.2-3 shows a sampling of pool swell suppression chamber shell pressures at various locations and key times during the event.

These results are based on plant unique QSTF test data contained in the PULD (Reference 3) and include the effects of the generic spatial distribution factors and the conservatism factors on the peak upward and downward loads. Pool swell suppression chamber shell loads consist of a pseudo-static internal pressure component and a dynamic pressure component and include the effects of the DBA internal pressure discussed in load case 3a. Pool swell loads do not occur during SBA and IBA events.

- b. LOCA Air Clearing, Submerged Structures: Transient drag pressures are postulated to act on the submerged portions of the suppression chamber components during the air clearing phase of a DBA event. The components affected

are the ring beams. The procedure used to develop the transient forces and spatial distribution of LOCA air clearing drag loads on the ring beam is discussed in Section 1-4.1.6.

Table 2-2.2-4 shows the resulting magnitudes and distribution of drag pressures acting on the ring beams for the controlling LOCA air clearing load case. These results include the effects of velocity drag, acceleration drag, interference effects, and wall effects. The LOCA air clearing submerged structure loads which occur during an SBA or IBA event have a negligible effect on the suppression chamber.

5. Condensation Oscillation Loads

- a. DBA Condensation Oscillation, Suppression Chamber Shell: Harmonic pressures are postulated to act on the submerged portion of the suppression chamber shell during the condensation oscillation phase of a DBA event. The procedure used to develop DBA condensation oscillation suppression chamber

shell pressures is discussed in Section 1-4.1.7. Figure 2-2.2-9 shows the resulting normalized spatial distribution of pressures on a typical suppression chamber shell cross-section. Table 2-2.2-5 shows the amplitudes for each of the 50 harmonics for four DBA condensation oscillation load case alternates.

The results of each harmonic in the DBA condensation oscillation loading are combined using the methodology discussed in Section 1-4.1.7. To account for the difference in the ratio of pool area to the downcomer area between the FSTF and DAEC, a factor of 0.825 is also applied to the results.

- b. IBA Condensation Oscillation, Suppression Chamber Shell: Harmonic pressures are postulated to act on the submerged portion of the suppression chamber shell during an IBA event. In accordance with NUREG-0661, the suppression chamber shell loads specified for pre-chug are used in lieu of IBA condensation oscillation suppression chamber shell loads. Pre-chug suppression chamber shell loads are

discussed under load case 6a. Condensation oscillation loads do not occur during an SBA event.

- c. DBA Condensation Oscillation, Submerged Structures: Harmonic drag pressures are postulated to act on the submerged portions of the suppression chamber components during the condensation oscillation phase of a DBA event. The components affected are the ring beams. The procedure used to develop the harmonic forces and spatial distribution of DBA condensation oscillation drag loads on the ring beam is discussed in Section 1-4.1.7.

Loads are developed for the case with the maximum source strength at all downcomers and for the case with twice the maximum source strength at the nearest downcomer. The results of these two cases are evaluated to determine the controlling loads. Table 2-2.2-6 shows the resulting magnitudes and distribution of drag pressures acting on the ring beam for the controlling DBA condensation oscillation load case.

These results include the effects of velocity drag, acceleration drag, suppression chamber shell FSI acceleration drag, interference effects, wall effects, and acceleration drag volumes. Figure 2-2.2-10 shows a typical pool acceleration profile from which the FSI accelerations are derived. The results of each harmonic in the DBA condensation oscillation loading are combined using the methodology discussed in Section 1-4.1.7.

- d. IBA Condensation Oscillation, Submerged Structures: Harmonic pressures are postulated to act on the submerged portions of the suppression chamber during the condensation oscillation phase of an IBA event. In accordance with NUREG-0661, the submerged structure loads specified for pre-chug are used in lieu of IBA condensation oscillation submerged structure loads. Pre-chug submerged structure loads are discussed under load case 6c. Condensation oscillation loads do not occur during an SBA event.

6. Chugging Loads

- a. Pre-Chug, Suppression Chamber Shell: During the chugging phase of an SBA, IBA, or DBA event, harmonic pressures associated with the pre-chug portion of a chugging cycle are postulated to act on the submerged portion of the suppression chamber shell. The procedure used to develop pre-chug suppression chamber shell loads is discussed in Section 1-4.1.8.

The loading consists of a single harmonic with a specified frequency range and can act either symmetrically or asymmetrically with respect to the vertical centerline of the containment. Figure 2-2.2-11 shows the circumferential pressure distribution on a typical suppression chamber cross-section for both symmetric and asymmetric pre-chug. Figure 2-2.2-12 shows the longitudinal pressure distribution for asymmetric pre-chug. The symmetric pre-chug load results in vertical loads on the suppression chamber while the asymmetric pre-chug load results in both vertical and lateral loads on the suppression chamber.

b. Post-Chug, Suppression Chamber Shell: During the chugging phase of an SBA, IBA, or DBA event, harmonic pressures associated with the post-chug portion of a chugging cycle are postulated to act on the submerged portion of the suppression chamber shell. The procedure used to develop post-chug suppression chamber shell loads is defined in Section 1-4.1.8. Figure 2-2.2-9 shows the resulting normalized spatial distribution of pressure on a typical suppression chamber cross-section. Table 2-2.2-7 shows the pressure amplitudes for each of the 50 harmonics for the post-chug loading. The results of each harmonic in the post-chug loading are combined using the methodology discussed in Section 1-4.1.8.

c. Pre-Chug, Submerged Structures: During the chugging phase of an SBA, IBA, or DBA event, harmonic drag pressures associated with the pre-chug portion of a chugging cycle are postulated to act on the submerged portions of the suppression chamber components. The components affected are the ring beams. The procedure used to develop the harmonic forces

and spatial distribution of pre-chug drag loads on the ring beam is discussed in Section 1-4.1.8.

Loads are developed for the case with the average source strength at all downcomers and the case with twice the average source strength at the nearest downcomer. The results of these two cases are evaluated to determine the controlling loads. Table 2-2.2-8 shows the resulting magnitudes and distribution of drag pressures acting on the ring beams for the controlling pre-chug drag load case.

These results include the effects of velocity drag, acceleration drag, suppression chamber shell FSI acceleration drag, interference effects, wall effects, and acceleration drag volumes. Figure 2-2.2-10 shows a typical pool acceleration profile from which the FSI accelerations are derived.

- d. Post-Chug, Submerged Structures: During the chugging phase of an SBA, IBA, or DBA event,

harmonic drag pressures associated with the post-chug portion of a chugging cycle are postulated to act on the submerged portion of the suppression chamber components. The components affected are the ring beams. The procedure used to develop the harmonic forces and spatial distribution of post-chug drag loads on the ring beam is discussed in Section 1-4.1.8.

Loads are developed for the case with the maximum source strength at the nearest two downcomers acting both in-phase and out-of-phase. The results of these cases are evaluated to determine the controlling loads. Table 2-2.2-9 shows the resulting magnitudes and distribution of post-chug drag pressures acting on the ring beams for the controlling post-chug drag load case.

These results include the effects of velocity drag, acceleration drag, suppression chamber shell FSI acceleration drag, interference effects, wall effects, and acceleration drag volumes. Figure 2-2.2-10 shows a typical pool

acceleration profile from which the FSI accelerations are derived. The results of each harmonic in the post-chug loading are combined using the methodology discussed in Section 1-4.1.8.

7. Safety Relief Valve Discharge Loads

a-c. SRV Discharge, Suppression Chamber Shell: Transient pressures are postulated to act on the submerged portion of the suppression chamber shell during the air clearing phase of an SRV discharge event. The procedure used to develop SRV discharge suppression chamber shell loads is discussed in Section 1-4.2.3. The maximum suppression chamber shell pressures and characteristics of the SRV discharge pressure transients are developed using an attenuated bubble model. Pressure transients include the load mitigation effects of the 12" diameter T-quenchers.

The SRV actuation cases considered are discussed in Section 1-4.2.1. Figure 2-2.1-9 shows the location of each T-quencher and the

corresponding SRV set point pressure. The cases which result in controlling load or load combination effects for which suppression chamber shell pressures are developed include the single valve actuation case with normal operating initial conditions (7a-Case A1.1/A1.3 for the quencher location which results in the highest shell pressures), the multiple valve actuation (MVA) case with elevated drywell pressures and temperatures (7b-Case A1.2/C3.2 with pressures from all six valves acting in phase), and the ADS valve actuation case with elevated drywell pressures and temperatures (7c-Case A2.2 with pressures from all four ADS valves acting in phase).

The multiple valve actuation case with normal operating initial conditions (Case A1.1/C3.1 with pressures from all six valves acting in phase) is enveloped by 7b-Case A1.2/C3.2 and is therefore not evaluated. Figure 2-2.1-9 shows the SRVDL's with ADS valves. Consideration of a six-valve actuation case conservatively exceeds the requirements of the plant's operating procedures.

Figures 2-2.2-13 and 2-2.2-14 show the resulting SRV discharge suppression chamber shell loads for the single valve Case 7a and multiple valve Case 7b, respectively. The results shown include the effects of applying the LDR (Reference 2) pressure attenuation algorithm to obtain the spatial distribution of suppression chamber shell pressures, the absolute summation of multiple valve effects with application of the bubble pressure cutoff criteria, use of first actuation pressures with subsequent actuation frequencies, and application of the $\pm 25\%$ and $\pm 40\%$ margins to the first and subsequent actuation frequencies, respectively. This methodology is in accordance with the conservative criteria contained in NUREG-0661. Since the number of ADS valves (4) is close to the total number of SRV valves (6), a separate analysis for ADS valve actuation is not required; the results from the multiple valve case will envelop those from ADS valves.

The distribution of SRV discharge suppression chamber shell pressures is either symmetric or asymmetric with respect to the vertical centerline of the containment, depending on the number and location of the valves considered to be actuating. The symmetric pressure distribution, which results in the maximum total vertical load on the suppression chamber, occurs for the multiple valve Case 7b (Figure 2-2.2-14). The asymmetric pressure distribution which results in the maximum total horizontal load on the suppression chamber also occurs for the multiple valve Case 7b.

- d. SRV Discharge Air Clearing, Submerged Structures: Transient drag pressures are postulated to act on the submerged portions of the suppression chamber components during the air clearing phase of an SRV discharge event. The components affected are the ring beams. The procedure used to develop the transient forces and spatial distribution of the SRV discharge air clearing drag loads on the ring beams is discussed in Section 1-4.2.4.

Loads are developed for the following load cases: four bubbles (from each quencher) in a bay acting in phase; two bubbles on the outside of one quencher acting in phase; and two bubbles on diagonally opposite sides of one quencher acting in phase. The results are evaluated to determine the controlling loads. Table 2-2.2-10 shows the resulting magnitudes and distribution of drag pressures acting on the ring beams for the controlling SRV discharge drag load case. The results include the effects of velocity drag, acceleration drag, interference effects, wall effects, acceleration drag volumes, and the load mitigation effects of the 12" diameter T-quenchers.

8. Suppression Chamber Interaction Loads

- a. Suppression Chamber Internal Structure Reactions: Loads acting on the suppression chamber, vent system, T-quencher and T-quencher supports, catwalk, SRV discharge line, and monorail cause interaction effects between these structures. These interaction

effects result in reaction loads on the suppression chamber shell and ring beam at the attachments of these structures to the suppression chamber. The effects of these reaction loads on the suppression chamber are considered in the suppression chamber analysis.

The interaction effects of TAP loads on the suppression chamber shell in combination with other loads will be discussed in Volume 6 of this report.

The values of the loads presented in the preceding paragraphs envelop those which could occur during the LOCA or SRV discharge events postulated. An evaluation for the effects of these loads results in conservative estimates of the suppression chamber responses and leads to bounding values of suppression chamber stresses.

Table 2-2.2-1

SUPPRESSION CHAMBER COMPONENT LOADING IDENTIFICATION

VOLUME 2 LOAD DESIGNATION			PUAN SECTION REFERENCE	COMPONENT LOADED					REMARKS
CATEGORY	LOAD TYPE	CASE NUMBER		SUPPRESSION CHAMBER SHELL	RING BEAM	COLUMNS	COLUMN CONNECTIONS	SADDLES	
DEAD LOADS	DEAD WEIGHT STEEL	1a	1-3.0	X	X	X	X	X	AS-MODIFIED GEOMETRY
	DEAD WEIGHT WATER	1b	1-3.0	X					61,500 FT ³ WATER (MAX)
SEISMIC LOADS	OBE SEISMIC LOADS	2a	1-3.0	X	X	X	X	X	0.12g HORIZONTAL, 0.053g VERTICAL
	SSE SEISMIC LOADS	2b	1-3.0	X	X	X	X	X	0.24g HORIZONTAL, 0.106g VERTICAL
PRESSURE AND TEMPERATURE LOADS	NORMAL OPERATING INTERNAL PRESSURE	3a	1-3.0	X					-2.0 TO 2.0 PSI
	LOCA INTERNAL PRESSURE	3b	1-4.1.1	X					SBA, IBA, & DBA PRESSURES
	NORMAL OPERATING TEMPERATURE LOADS	3c	1-3.1	X	X	X	X	X	50 TO 100° F
	LOCA TEMPERATURE LOADS	3d	1-4.1.1	X	X	X	X	X	SBA, IBA, & DBA TEMPERATURES
POOL SWELL LOADS	POOL SWELL TORUS SHELL LOADS	4a	1-4.1.3	X					INCLUDES DBA INTERNAL PRESSURES
	LOCA WATER CLEANING SUBMERGED STRUCTURE LOADS	N/A	1-4.1.5		X				EFFECTS NEGLIGIBLE
	LOCA AIR CLEANING SUBMERGED STRUCTURE LOADS	4b	1-4.1.6		X				PRIMARILY LOCAL EFFECTS
CONDENSATION OSCILLATION LOADS	DBA CO TORUS SHELL LOADS	5a	1-4.1.7.1	X					FOUR LOADING ALTERNATES
	IBA CO TORUS SHELL LOADS	5b	1-4.1.7.1	X					ENVELOPED BY LOAD CASE 6a
	DBA CO SUBMERGED STRUCTURE LOADS	5c	1-4.1.7.3		X				PRIMARILY LOCAL EFFECTS
	IBA CO SUBMERGED STRUCTURE LOADS	5d	1-4.1.7.3		X				ENVELOPED BY LOAD CASE 6c
CHUGGING LOADS	PRE-CHUG TORUS SHELL LOADS	6a	1-4.1.8.1	X					SYMMETRIC & ASYMMETRIC LOADINGS
	POST-CHUG TORUS SHELL LOADS	6b	1-4.1.8.1	X					SYMMETRIC LOADING
	PRE-CHUG SUBMERGED STRUCTURE LOADS	6c	1-4.1.8.3		X				PRIMARILY LOCAL EFFECTS
	POST-CHUG SUBMERGED STRUCTURE LOADS	6d	1-4.1.8.3		X				PRIMARILY LOCAL EFFECTS
SRV DISCHARGE LOADS	SRV DISCHARGE TORUS SHELL LOADS	7a-7c	1-4.2.3	X					SINGLE, MULTIPLE, & ADS VALVE CASES
	SRV DISCHARGE WATER CLEANING SUBMERGED STRUCTURE LOADS	N/A	1-4.2.4		X				EFFECTS NEGLIGIBLE
	SRV DISCHARGE AIR CLEANING SUBMERGED STRUCTURE LOADS	7d	1-4.2.4		X				PRIMARILY LOCAL EFFECTS
SUPPRESSION CHAMBER INTERACTION LOADS	SUPPRESSION CHAMBER REACTION LOADS	8a	Vol. 3-5	X	X				SUPPORTED STRUCTURES REACTIONS

IOW-40-199-2
Revision 0

2-2.43

Table 2-2.2-2

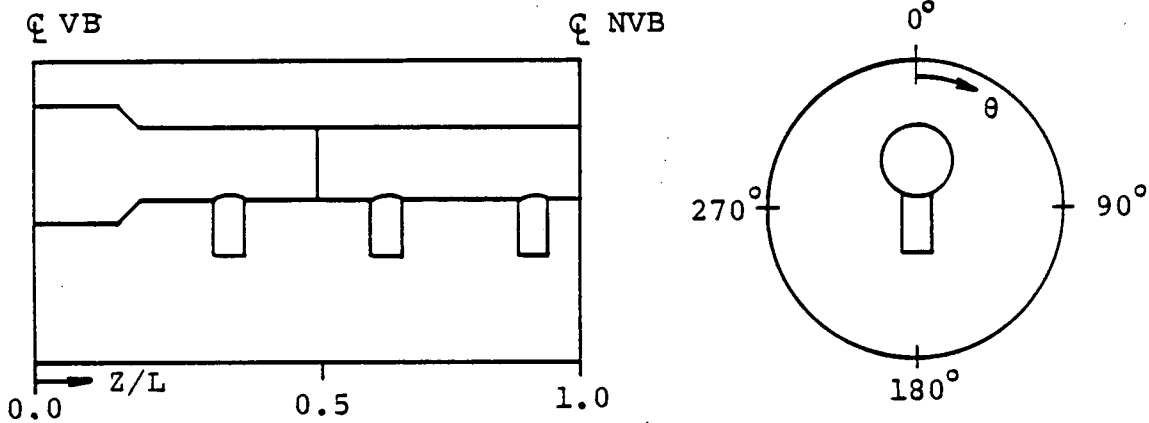
SUPPRESSION POOL
TEMPERATURE RESPONSE ANALYSIS
RESULTS-MAXIMUM TEMPERATURES

CONDITION	CASE (1) NUMBER	NUMBER OF SRV's ACTUATED	MAXIMUM BULK POOL TEMPERATURE (°F)
NORMAL OPERATING	1a	0	156.0
	1b	0	181.0
	2a	4	173.0
	2b	0	166.0
	2c	4	177.0
SBA EVENT	3a	4 (ADS)	160.0
	3b	4	177.0

(1) SEE SECTION 1-5.1 FOR DESCRIPTION OF SRV DISCHARGE EVENTS CONSIDERED.

Table 2-2.2-3

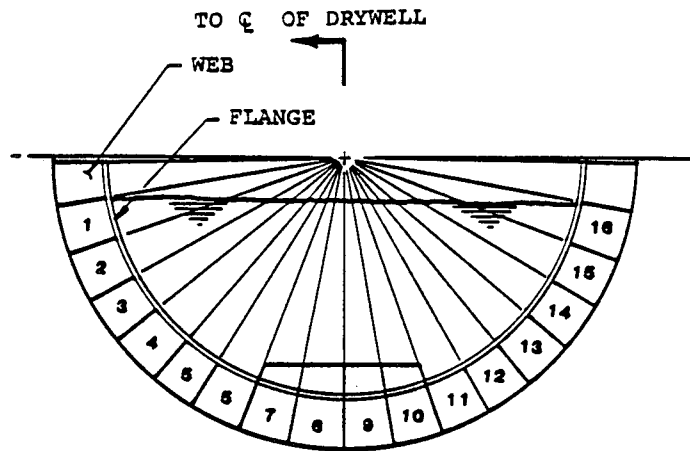
TORUS SHELL PRESSURES DUE TO POOL SWELL AT KEY
TIMES AND SELECTED LOCATIONS



LONGITUDINAL LOCATION (z/L)		CIRCUMFERENTIAL LOCATION (θ) (DEG)	TORUS SHELL PRESSURE (PSI)	
LONGITUDINAL FACTOR LOCATION	APPLICABLE RANGE		PEAK DOWNLOAD (t=0.322 sec)	PEAK UPLOAD (t=0.564 sec)
0.0	0.000 - .181	180	6.74	3.66
	0.000 - .181	165,195	6.69	3.76
	0.000 - .181	150,210	6.05	3.78
	0.000 - .181	135,225	4.97	4.12
	0.000 - .181	120,240	3.57	4.77
	0.000 - .181	0-90,270-0	0.44	6.50
0.361	0.181 - .500	180	7.31	3.27
	0.181 - .500	165,195	7.26	3.37
	0.181 - .500	150,210	6.57	3.39
	0.181 - .500	135,225	5.40	3.68
	0.181 - .500	120,240	3.87	4.27
	0.181 - .500	0-90,270-0	0.44	6.50
0.552	0.500 - .640	180	8.22	3.28
	0.500 - .640	165,195	8.17	3.38
	0.500 - .640	150,210	7.39	3.40
	0.500 - .640	135,225	6.07	3.70
	0.500 - .640	120,240	4.35	4.29
	0.500 - .640	0-90,270-0	0.44	6.50
FACTOR INTERPOLATED AT 0.724	0.640 - .810	180	8.59	3.20
	0.640 - .810	165,195	8.54	3.30
	0.640 - .810	150,210	7.72	3.31
	0.640 - .810	135,225	6.34	3.61
	0.640 - .810	120,240	4.55	4.18
	0.640 - .810	0-90,270-0	0.44	6.50
0.895	0.810 - 1.0	180	8.97	3.11
	0.810 - 1.0	165,195	8.91	3.21
	0.810 - 1.0	150,210	8.06	3.22
	0.810 - 1.0	135,225	6.61	3.51
	0.810 - 1.0	120,240	4.75	4.07
	0.810 - 1.0	0-90,270-0	0.44	6.50

Table 2-2.2-4

RING BEAM LOCA AIR CLEARING SUBMERGED STRUCTURE
LOAD DISTRIBUTION



RING BEAM

KEY DIAGRAM

ITEM	SEGMENT NUMBER	WEB PRESSURE (psi)	FLANGE PRESSURE (psi)
RING BEAM	1	0.07	0.60
	2	0.17	0.64
	3	0.27	0.38
	4	0.39	0.06
	5	0.51	0.56
	6	0.63	0.97
	7	1.65	2.15
	8	1.65	1.96
	9	1.44	1.73
	10	1.17	1.57
	11	0.37	0.70
	12	0.27	0.37
	13	0.20	0.01
	14	0.12	0.32
	15	0.10	0.55
	16	0.02	0.47

1. LOADS SHOWN INCLUDE DLF's.

Table 2-2.2-5

DBA CONDENSATION OSCILLATION TORUS
SHELL PRESSURE AMPLITUDES

FREQUENCY INTERVAL (Hz)	MAXIMUM PRESSURE AMPLITUDE (psi) (1)			
	ALTERNATE 1	ALTERNATE 2	ALTERNATE 3	ALTERNATE 4
0 - 1	0.29	0.29	0.29	0.25
1 - 2	0.25	0.25	0.25	0.28
2 - 3	0.32	0.32	0.32	0.33
3 - 4	0.48	0.48	0.48	0.56
4 - 5	1.86	1.20	0.24	2.71
5 - 6	1.05	2.73	0.48	1.17
6 - 7	0.49	0.42	0.99	0.97
7 - 8	0.59	0.38	0.30	0.47
8 - 9	0.59	0.38	0.30	0.34
9 - 10	0.59	0.38	0.30	0.47
10 - 11	0.34	0.79	0.18	0.49
11 - 12	0.15	0.45	0.12	0.38
12 - 13	0.17	0.12	0.11	0.20
13 - 14	0.12	0.08	0.08	0.10
14 - 15	0.06	0.07	0.03	0.11
15 - 16	0.10	0.10	0.02	0.08
16 - 17	0.04	0.04	0.04	0.04
17 - 18	0.04	0.04	0.04	0.05
18 - 19	0.04	0.04	0.04	0.03
19 - 20	0.27	0.27	0.27	0.34
20 - 21	0.20	0.20	0.20	0.23
21 - 22	0.30	0.30	0.30	0.49
22 - 23	0.34	0.34	0.34	0.37
23 - 24	0.33	0.33	0.33	0.31
24 - 25	0.16	0.16	0.16	0.22

Table 2-2.2-5

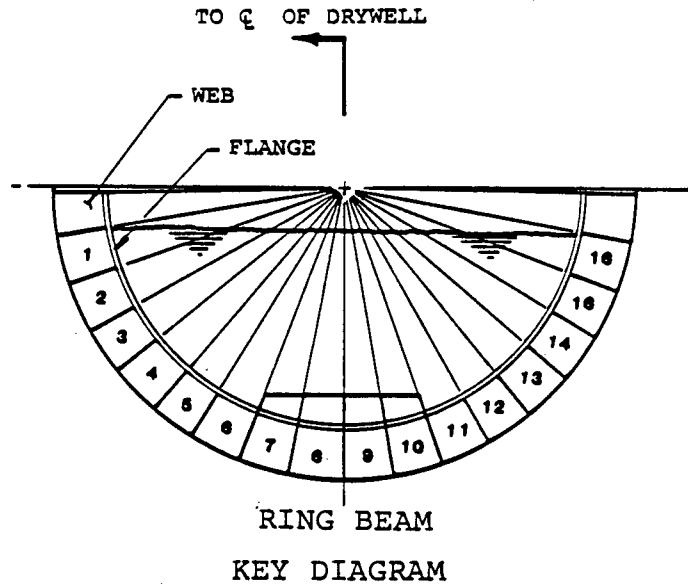
DBA CONDENSATION OSCILLATION TORUS
SHELL PRESSURE AMPLITUDES
 (Concluded)

FREQUENCY INTERVAL (Hz)	MAXIMUM PRESSURE AMPLITUDE (psi) (1)			
	ALTERNATE 1	ALTERNATE 2	ALTERNATE 3	ALTERNATE 4
25 - 26	0.25	0.25	0.25	0.50
26 - 27	0.58	0.58	0.58	0.51
27 - 28	0.13	0.13	0.13	0.39
28 - 29	0.19	0.19	0.19	0.27
29 - 30	0.14	0.14	0.14	0.09
30 - 31	0.08	0.08	0.08	0.08
31 - 32	0.03	0.03	0.03	0.07
32 - 33	0.03	0.03	0.03	0.05
33 - 34	0.03	0.03	0.03	0.04
34 - 35	0.05	0.05	0.05	0.04
35 - 36	0.08	0.08	0.08	0.07
36 - 37	0.10	0.10	0.10	0.11
37 - 38	0.07	0.07	0.07	0.06
38 - 39	0.06	0.06	0.06	0.05
39 - 40	0.09	0.09	0.09	0.03
40 - 41	0.33	0.33	0.33	0.08
41 - 42	0.33	0.33	0.33	0.19
42 - 43	0.33	0.33	0.33	0.19
43 - 44	0.33	0.33	0.33	0.13
44 - 45	0.33	0.33	0.33	0.18
45 - 46	0.33	0.33	0.33	0.30
46 - 47	0.33	0.33	0.33	0.18
47 - 48	0.33	0.33	0.33	0.19
48 - 49	0.33	0.33	0.33	0.17
49 - 50	0.33	0.33	0.33	0.21

(1) SEE FIGURE 2-2.2-9 FOR SPATIAL DISTRIBUTION OF PRESSURES.

Table 2-2.2-6

RING BEAM DBA CONDENSATION OSCILLATION SUBMERGED
STRUCTURE LOAD DISTRIBUTION



ITEM	SEGMENT NUMBER	WEB PRESSURE (psi)			FLANGE PRESSURE (psi)		
		APPLIED LOAD	FSI	TOTAL	APPLIED LOAD	FSI	TOTAL
RING BEAM	1	0.10	2.95	3.05	0.18	1.80	1.98
	2	0.34	2.66	3.00	0.14	1.79	1.93
	3	0.61	1.78	2.39	0.03	1.66	1.69
	4	0.98	1.12	2.10	0.27	1.54	1.81
	5	1.49	0.73	2.22	0.52	1.36	1.88
	6	2.20	0.68	2.88	0.67	1.73	2.40
	7	7.88	1.69	9.57	1.44	3.97	5.41
	8	9.05	0.48	9.53	1.28	4.44	5.72
	9	8.36	1.00	9.36	1.17	4.22	5.39
	10	6.36	1.79	8.15	1.12	3.27	4.39
	11	1.63	0.49	2.12	0.50	1.03	1.53
	12	1.07	0.34	1.41	0.35	0.71	1.06
	13	0.68	0.44	1.12	0.16	1.03	1.19
	14	0.41	0.85	1.26	0.01	1.73	1.74
	15	0.24	1.46	1.70	0.14	2.44	2.58
	16	0.07	1.44	1.51	0.15	2.54	2.69

1. LOADS SHOWN INCLUDE DLF's.

Table 2-2.2-7

POST-CHUG TORUS SHELL PRESSURE AMPLITUDES

FREQUENCY INTERVAL (Hz)	MAXIMUM PRESSURE AMPLITUDE (psi) (1)
0 - 1	0.04
1 - 2	0.04
2 - 3	0.05
3 - 4	0.05
4 - 5	0.06
5 - 6	0.05
6 - 7	0.10
7 - 8	0.10
8 - 9	0.10
9 - 10	0.10
10 - 11	0.06
11 - 12	0.05
12 - 13	0.03
13 - 14	0.03
14 - 15	0.02
15 - 16	0.02
16 - 17	0.01
17 - 18	0.01
18 - 19	0.01
19 - 20	0.04
20 - 21	0.03
21 - 22	0.05
22 - 23	0.05
23 - 24	0.05
24 - 25	0.04

Table 2-2.2-7

POST-CHUG TORUS SHELL PRESSURE AMPLITUDES

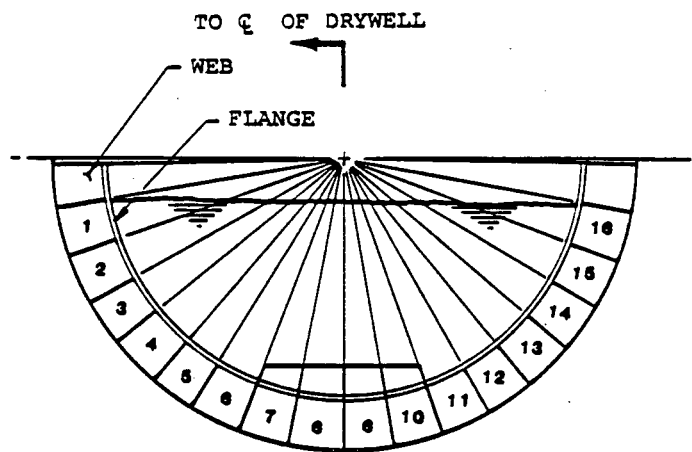
(Concluded)

FREQUENCY INTERVAL (Hz)	MAXIMUM (1) PRESSURE AMPLITUDE (psi)
25 - 26	0.04
26 - 27	0.28
27 - 28	0.18
28 - 29	0.12
29 - 30	0.09
30 - 31	0.03
31 - 32	0.02
32 - 33	0.02
33 - 34	0.02
34 - 35	0.02
35 - 36	0.03
36 - 37	0.05
37 - 38	0.03
38 - 39	0.04
39 - 40	0.04
40 - 41	0.15
41 - 42	0.15
42 - 43	0.15
43 - 44	0.15
44 - 45	0.15
45 - 46	0.15
46 - 47	0.15
47 - 48	0.15
48 - 49	0.15
49 - 50	0.15

(1) SEE FIGURE 2-2.2-9 FOR SPATIAL DISTRIBUTION OF PRESSURES.

Table 2-2.2-8

RING BEAM PRE-CHUG SUBMERGED STRUCTURE
LOAD DISTRIBUTION



RING BEAM

KEY DIAGRAM

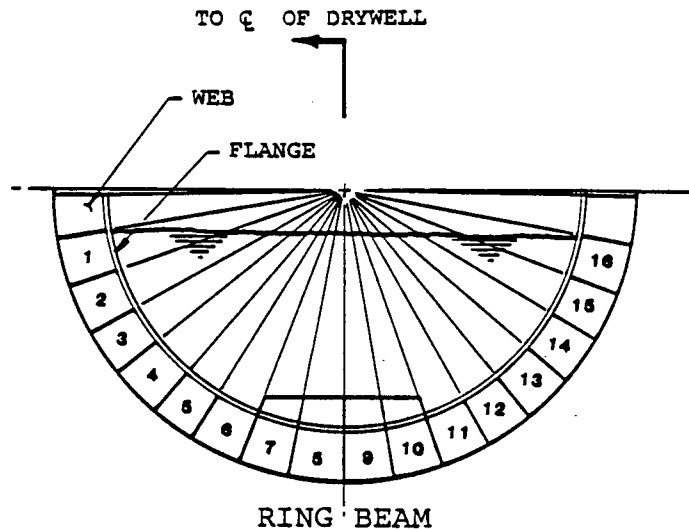
ITEM	SEGMENT NUMBER	WEB PRESSURE (psi)			FLANGE PRESSURE (psi)		
		APPLIED LOAD	FSI	TOTAL	APPLIED LOAD	FSI	TOTAL
RING BEAM	1	0.012	0.005	0.017	0.075	0.015	0.090
	2	0.034	0.002	0.036	0.080	0.011	0.090
	3	0.054	0.002	0.056	0.050	0.014	0.060
	4	0.076	0.002	0.078	0.004	0.016	0.020
	5	0.100	0.000	0.100	0.055	0.005	0.060
	6	0.122	0.000	0.122	0.090	0.020	0.110
	7	0.310	0.000	0.310	0.180	0.090	0.270
	8	0.310	0.003	0.313	0.160	0.130	0.290
	9	0.299	0.010	0.309	0.160	0.150	0.310
	10	0.227	0.014	0.241	0.170	0.140	0.310
	11	0.071	0.010	0.081	0.080	0.050	0.130
	12	0.051	0.002	0.053	0.050	0.030	0.080
	13	0.037	0.007	0.044	0.010	0.040	0.050
	14	0.024	0.005	0.029	0.030	0.070	0.100
	15	0.017	0.007	0.024	0.060	0.070	0.130
	16	0.007	0.000	0.007	0.050	0.010	0.060

1. LOADS SHOWN INCLUDE DLF's.

Table 2-2.2-9

RING BEAM POST-CHUG SUBMERGED STRUCTURE

LOAD DISTRIBUTION



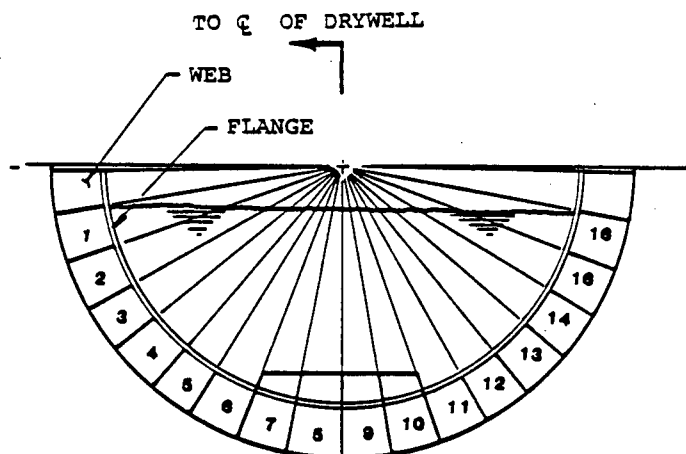
RING BEAM
KEY DIAGRAM

ITEM	SEGMENT NUMBER	WEB PRESSURE (psi)			FLANGE PRESSURE (psi)		
		APPLIED LOAD	FSI	TOTAL	APPLIED LOAD	FSI	TOTAL
RING BEAM	1	0.68	1.27	1.95	0.50	0.60	1.10
	2	2.12	1.15	3.27	0.38	0.56	0.94
	3	3.83	0.68	4.51	0.05	0.48	0.53
	4	6.05	0.39	6.44	0.66	0.43	1.09
	5	9.20	0.24	9.44	1.28	0.40	1.68
	6	13.32	0.24	13.56	1.65	0.54	2.19
	7	46.89	0.69	47.58	3.41	1.29	4.70
	8	53.39	0.21	53.60	2.99	1.46	4.45
	9	49.43	0.41	49.84	2.73	1.37	4.10
	10	37.91	0.72	38.63	2.68	1.05	3.73
	11	9.96	0.20	10.16	1.23	0.34	1.57
	12	6.51	0.12	6.63	0.88	0.22	1.10
	13	4.17	0.17	4.34	0.40	0.34	0.74
	14	2.61	0.34	2.95	0.05	0.56	0.61
	15	1.59	0.63	2.22	0.38	0.80	1.18
	16	0.49	0.63	1.12	0.42	0.86	1.28

1. LOADS SHOWN INCLUDE DLF'S.

Table 2-2.2-10

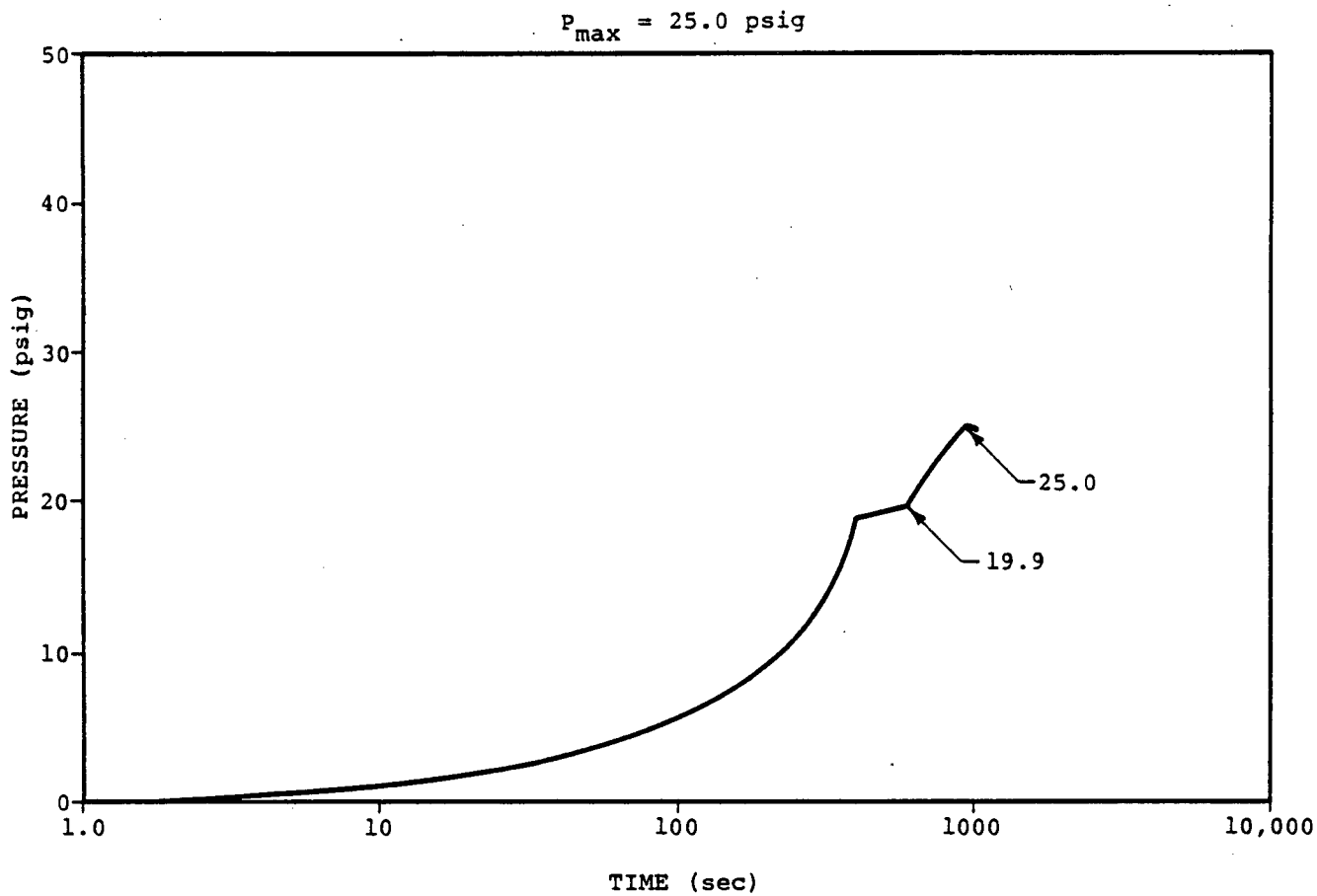
RING BEAM SRV SUBMERGED STRUCTURE
LOAD DISTRIBUTION



RING BEAM
KEY DIAGRAM

ITEM	SEGMENT NUMBER	WEB PRESSURE (psi)	FLANGE PRESSURE (psi)
RING BEAM	1	0.73	3.57
	2	1.46	2.98
	3	2.27	0.92
	4	4.22	3.14
	5	9.30	9.57
	6	15.40	12.62
	7	15.42	4.01
	8	11.62	1.20
	9	14.04	1.32
	10	20.77	1.95
	11	13.71	2.29
	12	9.88	1.64
	13	5.64	0.65
	14	3.12	0.69
	15	1.78	3.41
	16	0.34	3.06

1. LOADS SHOWN INCLUDE DLF's.



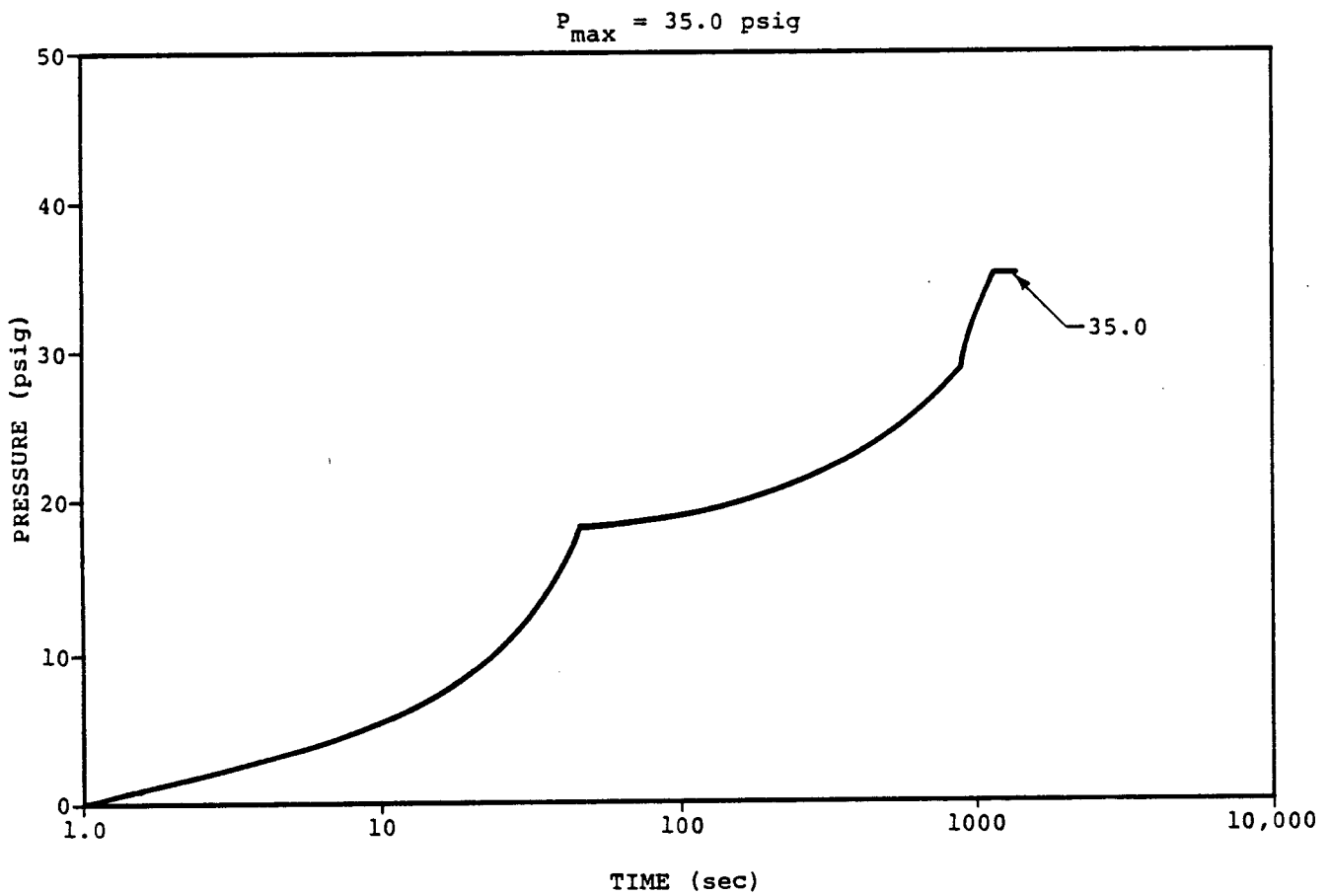
EVENT DESCRIPTION	PRESSURE DESIGNATION	TIME (sec)		PRESSURE (psig)	
		t_{min}	t_{max}	P_{min}	P_{max}
INSTANT OF BREAK TO ONSET OF CHUGGING	P_1	0	300	0.59	13.0
ONSET OF CHUGGING TO INITIATION OF ADS	P_2	300	600	13.0	19.9
INITIATION OF ADS TO RPV DEPRESSURIZATION	P_3	600	1200	19.9	25.0

Figure 2-2.2-1

SUPPRESSION CHAMBER INTERNAL PRESSURES FOR SBA EVENT

IOW-40-199-2
Revision 0

2-2.55



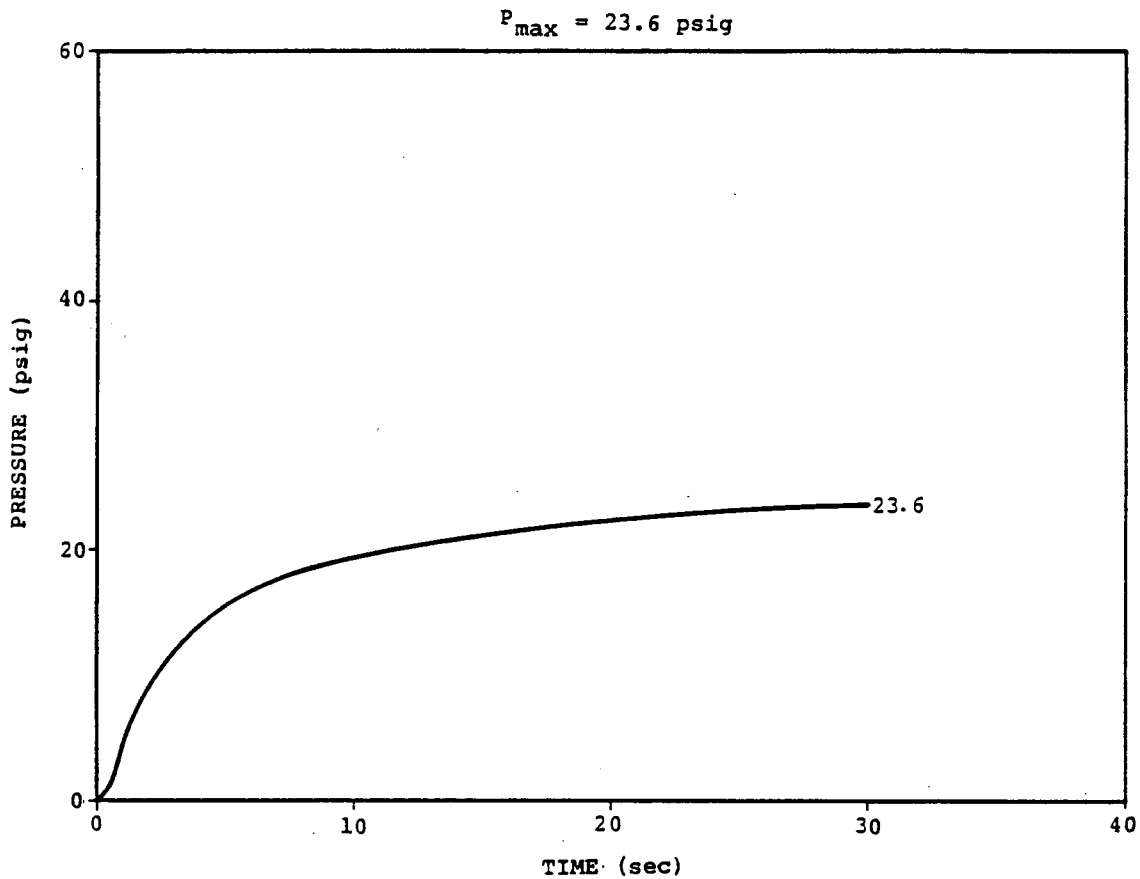
EVENT DESCRIPTION	PRESSURE DESIGNATION	TIME (sec)		PRESSURE (psig)	
		t_{min}	t_{max}	P_{min}	P_{max}
INSTANT OF BREAK TO ONSET OF CO AND CHUGGING	P_1	0	5	0.59	3.5
ONSET OF CO AND CHUGGING TO INITIATION OF ADS	P_2	5	900	3.5	28.2
INITIATION OF ADS TO RPV DEPRESSURIZATION	P_3	900	1100	28.2	35.0

Figure 2-2.2-2

SUPPRESSION CHAMBER INTERNAL PRESSURES FOR IBA EVENT

IOW-40-199-2
Revision 0

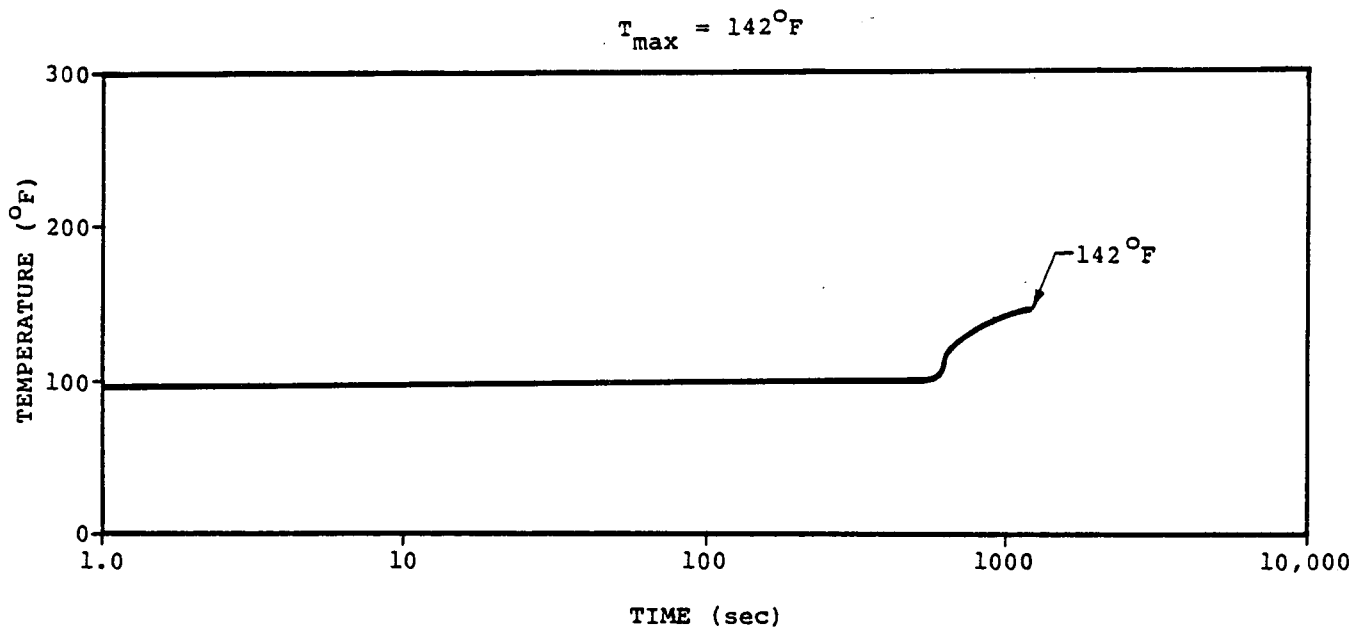
2-2.56



EVENT DESCRIPTION	PRESSURE DESIGNATION	TIME (sec)		PRESSURE (psig)	
		t_{min}	t_{max}	P_{min}	P_{max}
INSTANT OF BREAK TO TERMINATION OF POOL SWELL	P_1	0.0	1.5	0.59	7.0
TERMINATION OF POOL SWELL TO ONSET OF CO	P_2	1.5	5.0	7.0	16.00
ONSET OF CO TO ONSET OF CHUGGING	P_3	5.0	35.0	16.00	23.6
ONSET OF CHUGGING TO RPV DEPRESSURIZATION	P_4	35.0	65.0	23.6	23.6

Figure 2-2.2-3

SUPPRESSION CHAMBER INTERNAL PRESSURES FOR DBA EVENT



EVENT DESCRIPTION	TEMPERATURE DESIGNATION	TIME (sec)		TEMPERATURE (F°)	
		t_{min}	t_{max}	T_{min}	T_{max}
INSTANT OF BREAK TO ONSET OF CHUGGING	T_1 (1)	0	300	95.0	101.0
ONSET OF CHUGGING TO INITIATION OF ADS	T_2 (1)	300	600	101.0	107.0
INITIATION OF ADS TO RPV DEPRESSURIZATION	T_3 (2)	600	1200	107.0	142.0

- (1) THE TEMPERATURE FOR CASE 3B IN TABLE 2-2.2-2 IS USED IN LIEU OF THESE TEMPERATURES.
- (2) THE TEMPERATURE FOR CASE 3A IN TABLE 2-2.2-2 IS USED IN LIEU OF THESE TEMPERATURES.

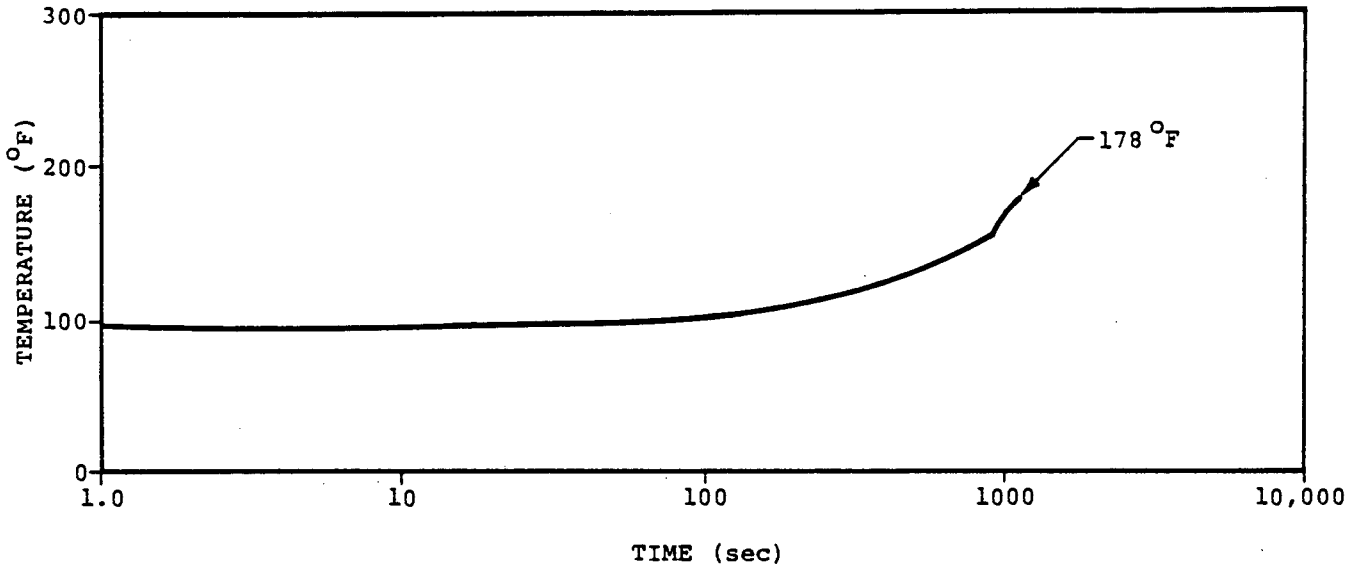
Figure 2-2.2-4

SUPPRESSION CHAMBER TEMPERATURES FOR SBA EVENT

IOW-40-199-2
Revision 0

2-2.58

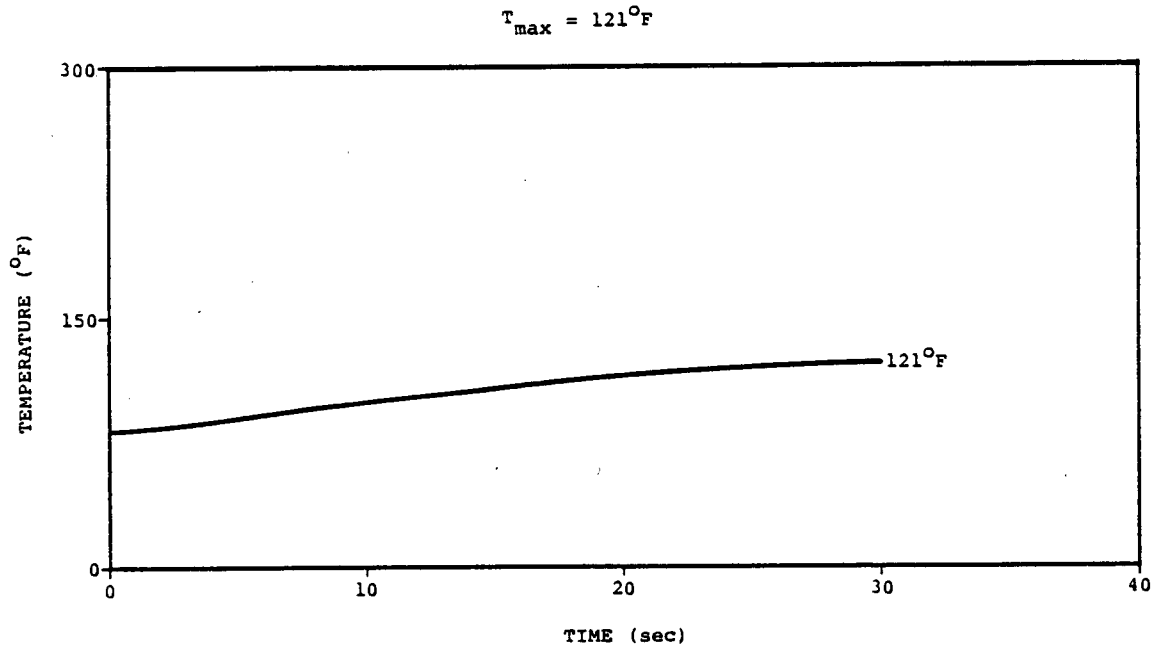
$T_{\max} = 178^{\circ}\text{F}$



EVENT DESCRIPTION	TEMPERATURE DESIGNATION	TIME (sec)		TEMPERATURE (°F)	
		t_{\min}	t_{\max}	T_{\min}	T_{\max}
INSTANT OF BREAK TO ONSET OF CO AND CHUGGING	T_1	0	5	95.0	95.0
ONSET OF CO AND CHUGGING TO INITIATION OF ADS	T_2	5	900	95.0	154.0
INITIATION OF ADS TO RPV DEPRESSURIZATION	T_3	900	1100	154.0	178.0

Figure 2-2.2-5

SUPPRESSION CHAMBER TEMPERATURES FOR IBA EVENT



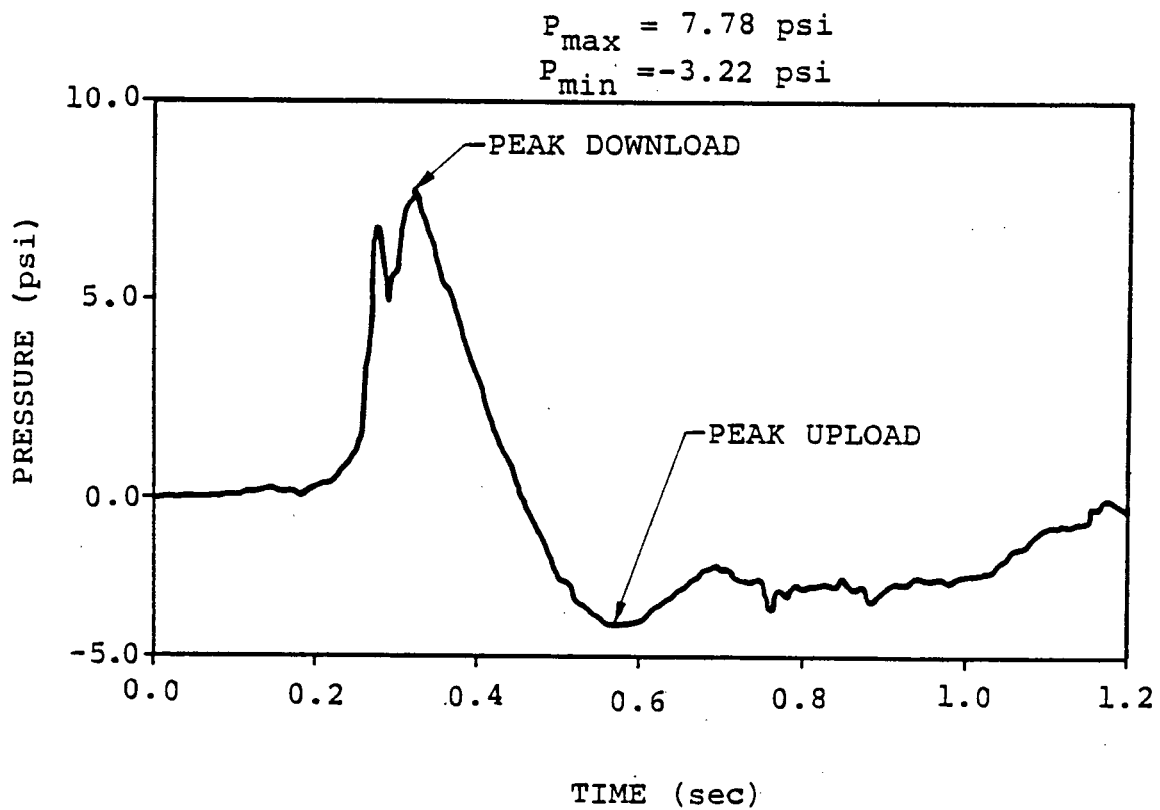
EVENT DESCRIPTION	TEMPERATURE DESIGNATION	TIME (sec)		TEMPERATURE ($^{\circ}\text{F}$)	
		t_{\min}	t_{\max}	T_{\min}	T_{\max}
INSTANT OF BREAK TO TERMINATION OF POOL SWELL	T_1	0.0	1.5	81.0	83.0
TERMINATION OF POOL SWELL TO ONSET OF CO	T_2	1.5	5.0	83.0	90.0
ONSET OF CO TO ONSET OF CHUGGING	T_3	5.0	35.0	90.0	121.0
ONSET OF CHUGGING TO RPV DEPRESSURIZATION	T_4	35.0	65.0	121.0	121.0

Figure 2-2.2-6

SUPPRESSION CHAMBER TEMPERATURES FOR DBA EVENT

IOW-40-199-2
Revision 0

2-2.60



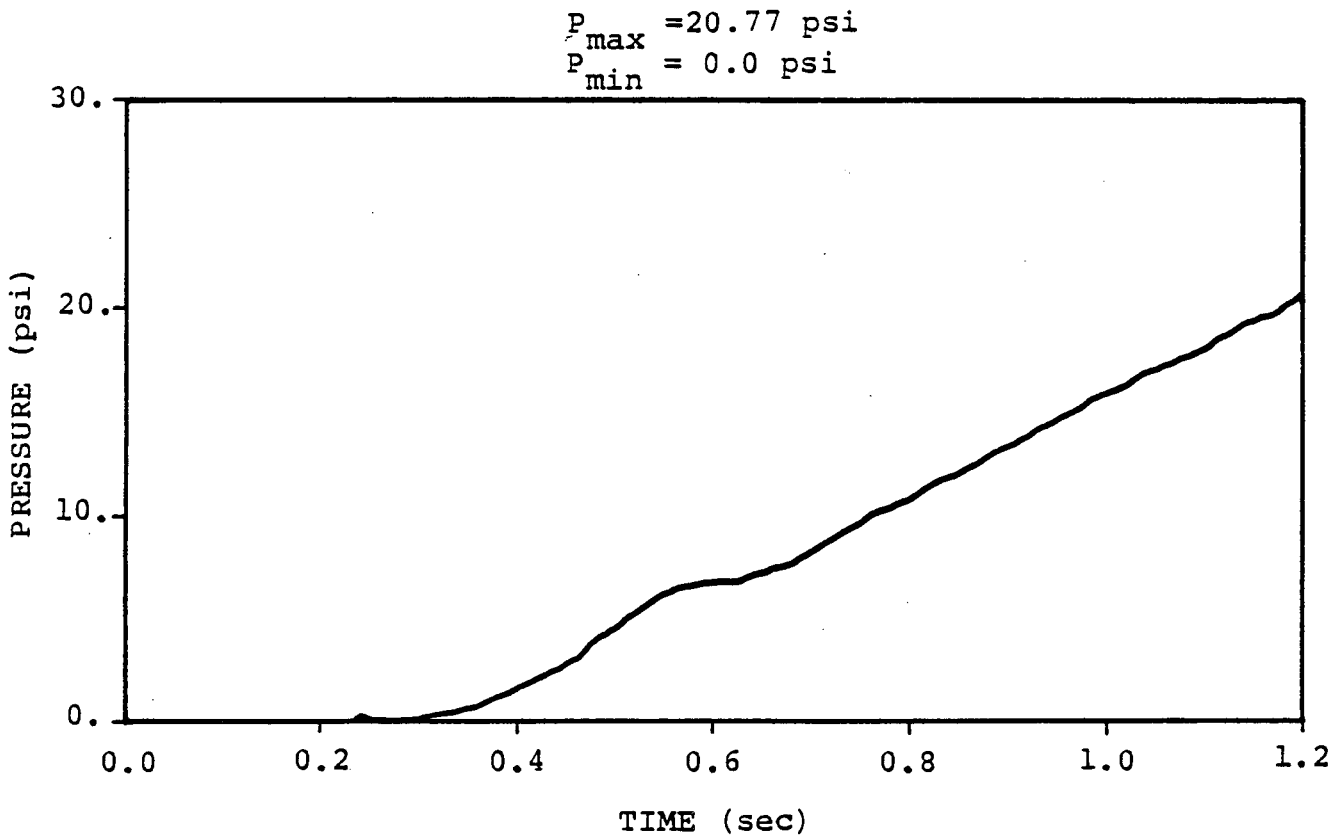
1. PRESSURES SHOWN DO NOT INCLUDE DBA INTERNAL PRESSURE.

Figure 2-2.2-7

POOL SWELL TORUS SHELL PRESSURE TRANSIENT
AT SUPPRESSION CHAMBER MITER JOINT - BOTTOM
DEAD CENTER LOCATION

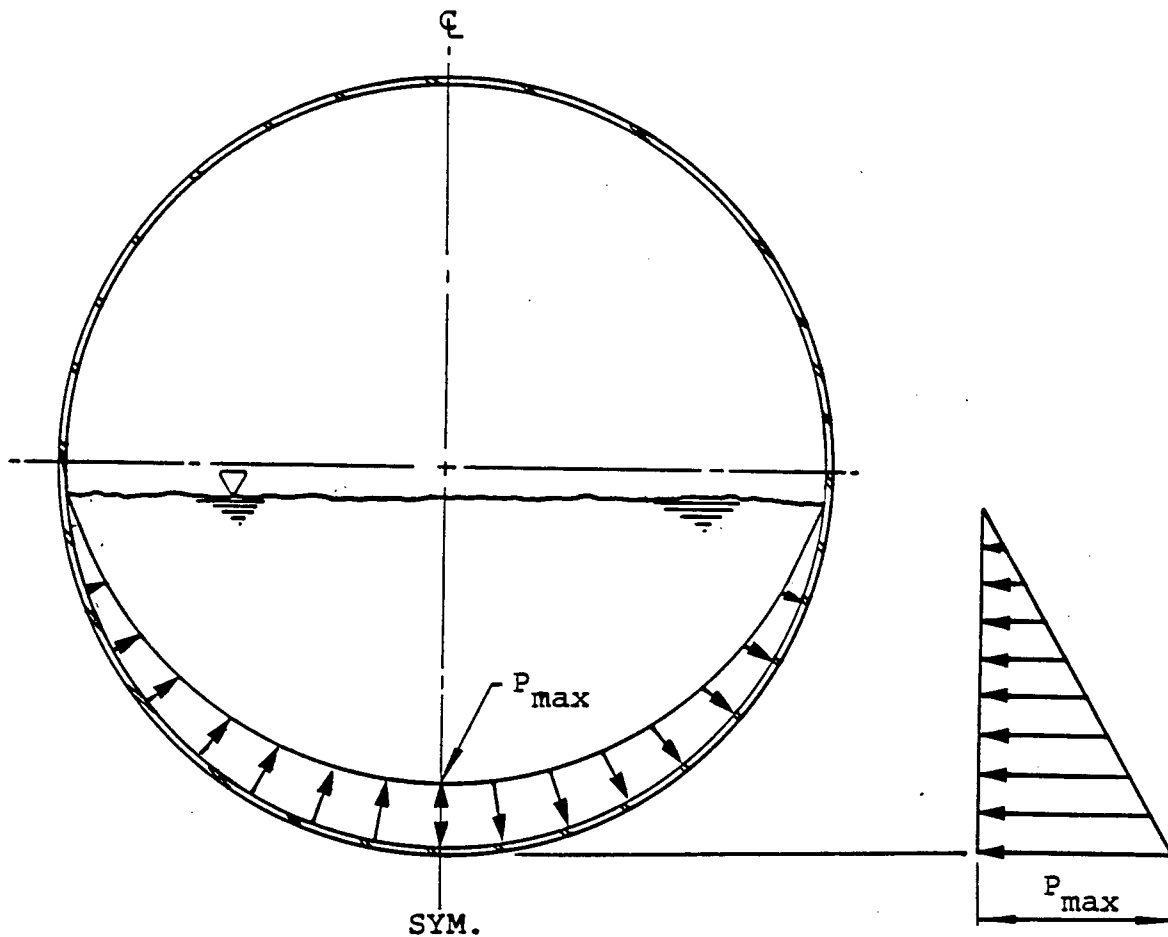
IOW-40-199-2
Revision 0

2-2.61



1. PRESSURES SHOWN INCLUDE THE EFFECTS OF DBA INTERNAL PRESSURE IN FIGURE 2-2.2-3.

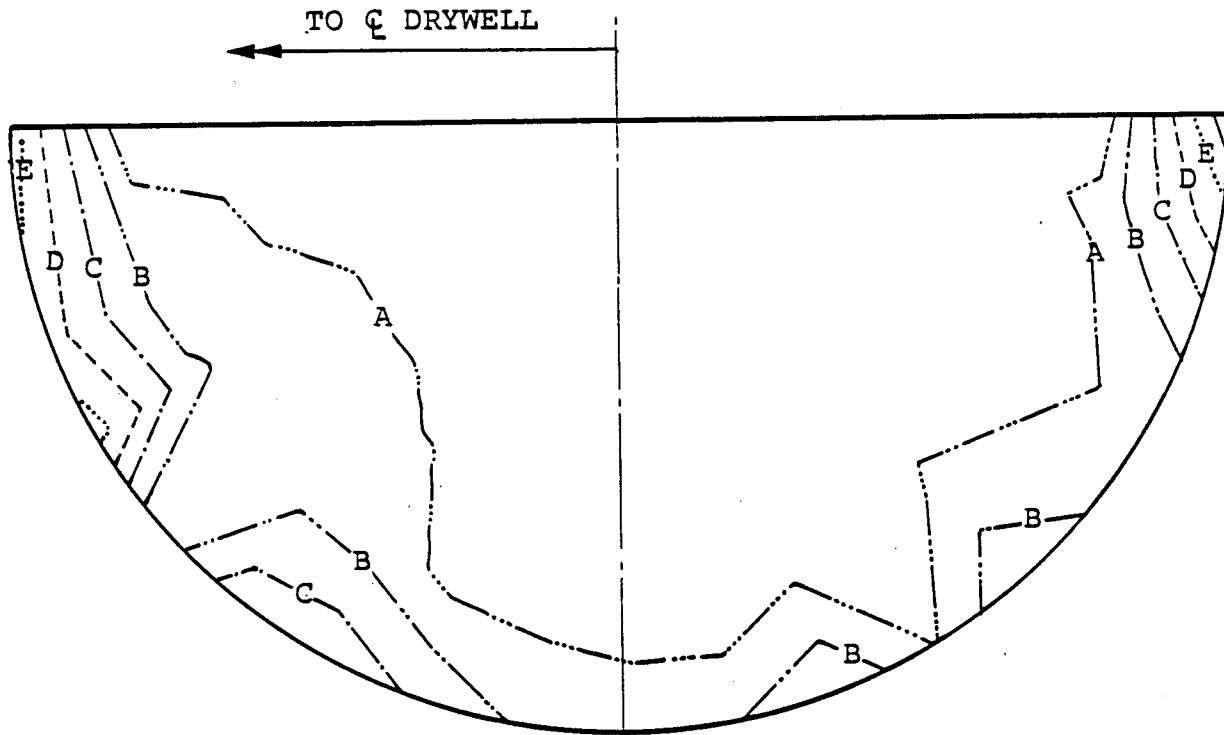
Figure 2-2.2-8
POOL SWELL TORUS SHELL PRESSURE TRANSIENT
FOR SUPPRESSION CHAMBER AIRSPACE



1. PRESSURE AMPLITUDES FOR DBA CONDENSATION OSCILLATION LOADS SHOWN IN TABLE 2-2.2-5
2. PRESSURE AMPLITUDES FOR POST-CHUG LOADS SHOWN IN TABLE 2-2.2-7.

Figure 2-2.2-9

NORMALIZED TORUS SHELL PRESSURE DISTRIBUTION
FOR DBA CONDENSATION OSCILLATION AND POST-CHUG LOADINGS



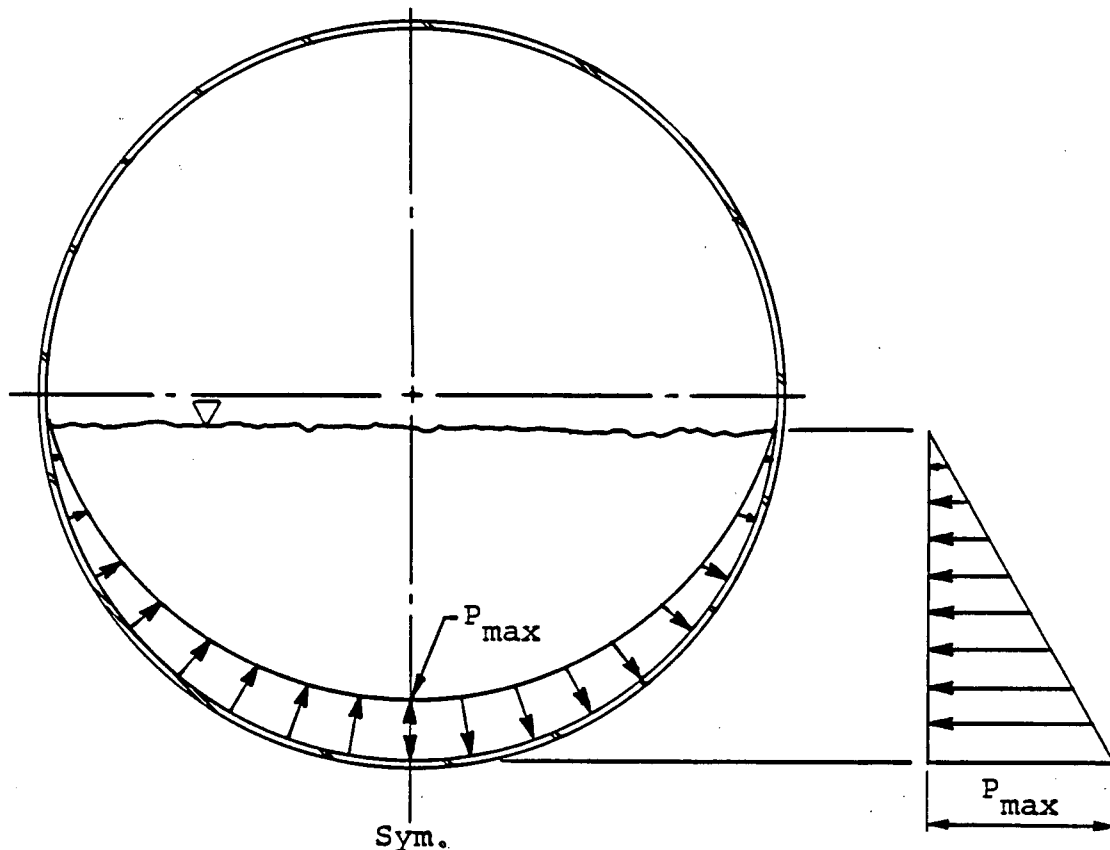
KEY DIAGRAM

NORMALIZED POOL ACCELERATIONS	
PROFILE	POOL ACCELERATION (ft/sec ²)
A	100.0
B	200.0
C	300.0
D	400.0
E	500.0
F	600.0

POOL ACCELERATIONS DUE TO HARMONIC APPLICATION OF TORUS SHELL PRESSURES (FIGURE 2-2.2-9) AT A SUPPRESSION CHAMBER FREQUENCY OF 20.98Hz.

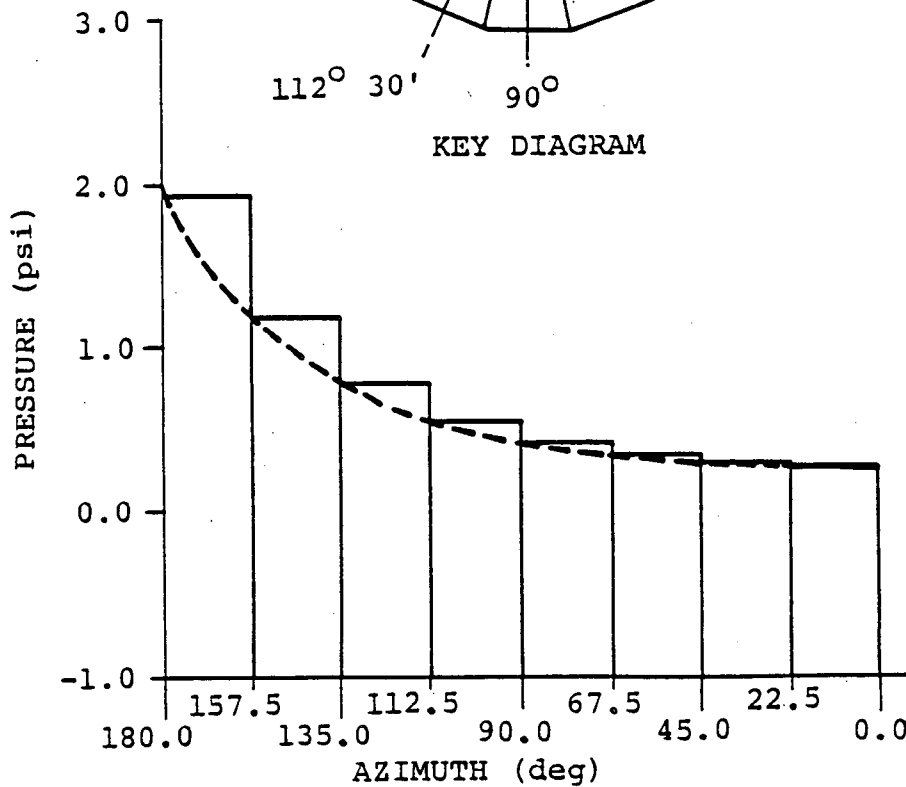
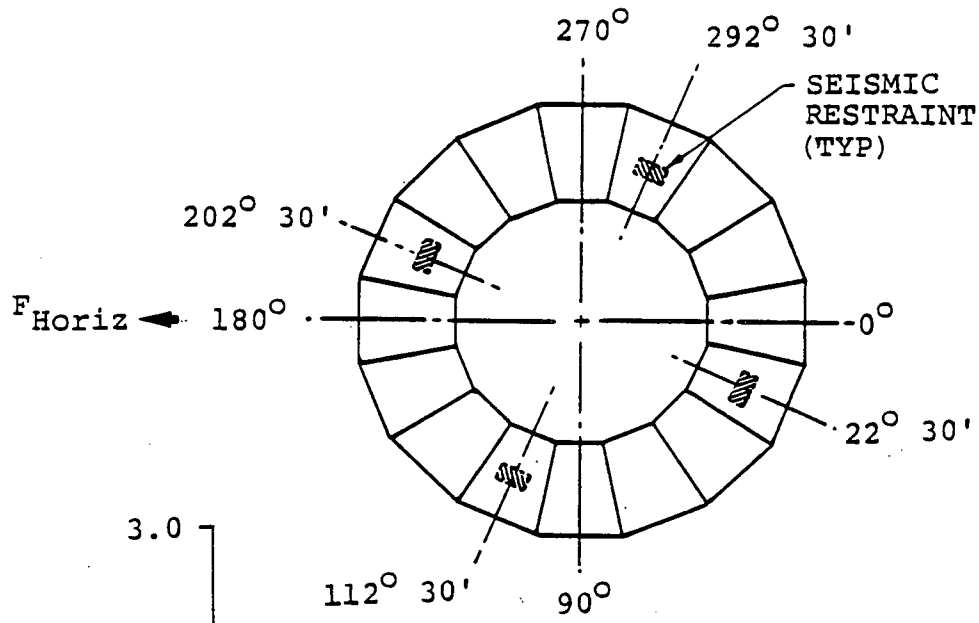
Figure 2-2.2-10

FSI POOL ACCELERATION PROFILE FOR DOMINANT SUPPRESSION CHAMBER FREQUENCY AT MIDBAY LOCATION



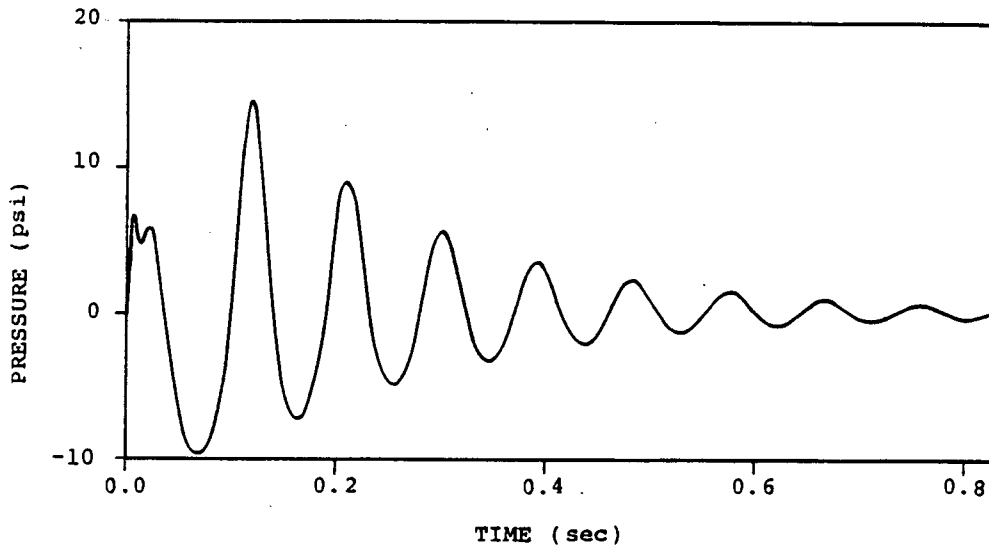
LOADING CHARACTERISTICS	
<u>SYMMETRIC DISTRIBUTION:</u>	
P_{max}	= ± 2.0 psi AT ALL BOTTOM DEAD CENTER LOCATIONS
<u>ASYMMETRIC DISTRIBUTION:</u>	
P_{max}	= ± 2.0 psi IN ONE BAY WITH LONGITUDINAL ATTENUATION SHOWN IN FIGURE 2-2.2-12
<u>FREQUENCY:</u>	
SINGLE HARMONIC IN 6.9 TO 9.5 Hz RANGE, RESULTING IN MAXIMUM RESPONSE	
<u>TOTAL INTEGRATED LOAD:</u>	
SYM DIST:	$F_{vert} = 292.80$ kips PER MITERED CYL.
ASYM DIST:	$F_{horiz} = 21.45$ kips TOTAL HORIZONTAL

Figure 2-2.2-11
CIRCUMFERENTIAL TORUS SHELL PRESSURE DISTRIBUTION FOR SYMMETRIC AND ASYMMETRIC PRE-CHUG LOADINGS

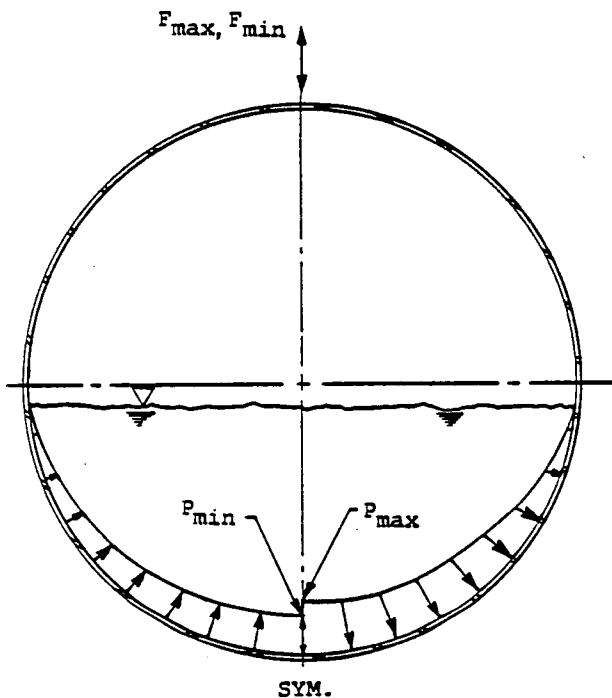


1. SEE FIGURE 2-2.2-11 FOR CIRCUMFERENTIAL TORUS SHELL PRESSURE DISTRIBUTION.

Figure 2-2.2-12
LONGITUDINAL TORUS SHELL PRESSURE
DISTRIBUTION FOR ASYMMETRIC PRE-CHUG LOADINGS



SHELL PRESSURE FORCING FUNCTION



LOADING CHARACTERISTICS	
<u>7a - CASE A1.1/A1.3(SINGLE VALVE)</u>	
<u>PRESSURE (psi):</u> LONGEST SRVDL BUBBLE:	
P_{max}	P_{min}
17.28	-11.54
SHELL:	
P_{max}	P_{min}
14.54	-9.72
<u>TOTAL APPLIED LOAD (kips):</u>	
VERTICAL PER MITERED CYLINDER:	
DOWNWARD:	F_{max}
735.8	
UPWARD:	F_{min}
650.0	
<u>LOAD FREQUENCY (Hz):</u>	
RANGE:	
$4.03 \leq f_L \leq 10.72$	

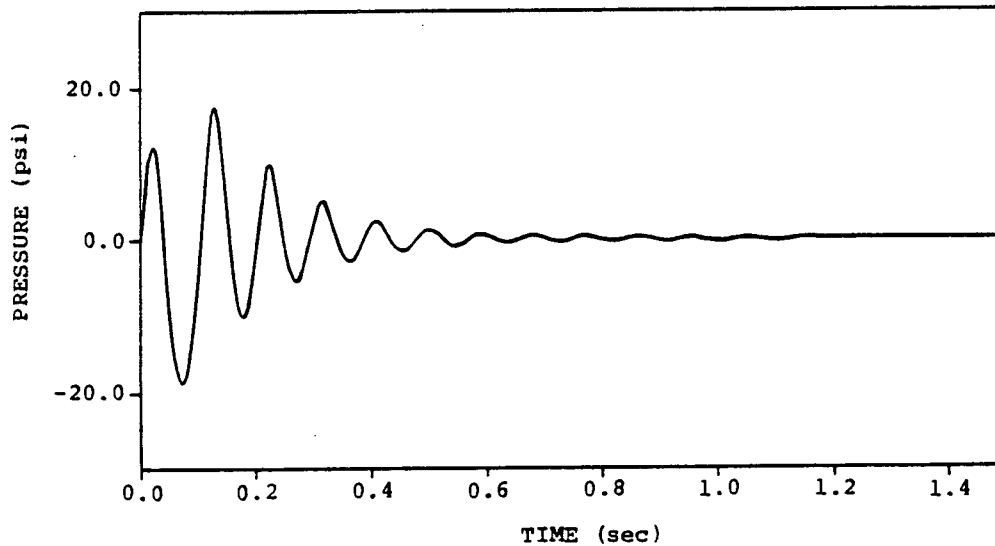
MITER JOINT SPATIAL DISTRIBUTION

Figure 2-2.2-13

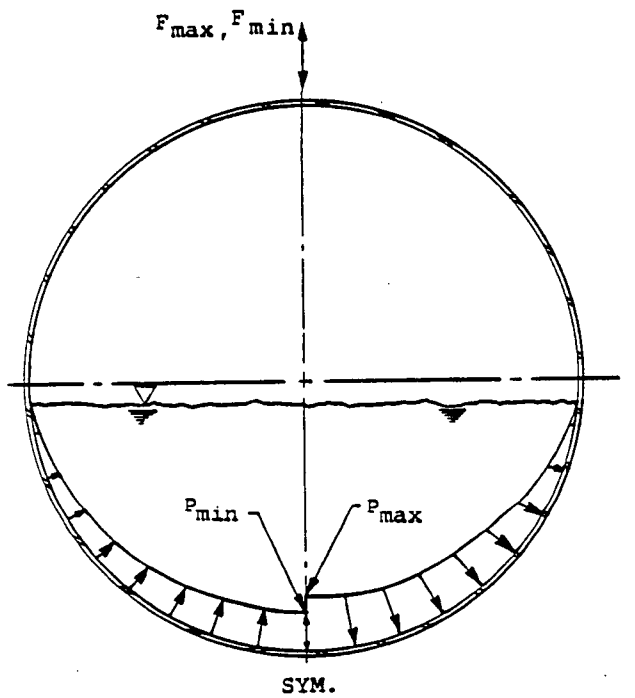
SRV DISCHARGE TORUS SHELL LOADS FOR CASE A1.1/A1.3-
SINGLE VALVE ACTUATION

IOW-40-199-2
Revision 0

2-2.67



SHELL PRESSURE FORCING FUNCTION



MITER JOINT SPATIAL DISTRIBUTION

LOADING CHARACTERISTICS
<u>7b - CASE A1.2/C3.2 (MULTIPLE VALVE)</u>
PRESSURE (psi): SHORTEST SRVDL BUBBLE:
$P_{max} = 20.03, P_{min} = -22.84$
SHELL: ONE VALVE
$P_{max} = 17.71, P_{min} = -18.84$
SHELL: ALL VALVES
$P_{max} = 20.03, P_{min} = -22.84$
<u>TOTAL APPLIED LOAD (kips):</u>
VERTICAL PER MITERED CYLINDER:
DOWNWARD: $F_{max} = 1218.84$
UPWARD: $F_{min} = 1291.92$
<u>LOAD FREQUENCY (Hz):</u>
RANGE:
$7.66 \leq f_L \leq 17.88$

Figure 2-2.2-14

SRV DISCHARGE TORUS SHELL LOADS FOR CASE A1.2/C3.2-
MULTIPLE VALVE ACTUATION

2-2.2.2 Load Combinations

The load categories and associated load cases for which the suppression chamber is evaluated are presented in Section 2-2.2.1. Table 2-2.2-11 presents the NUREG-0661 criteria for grouping the respective loads and load categories into event combinations.

The 27 general event combinations shown in Table 2-2.2-11 are expanded to form 107 specific suppression chamber load combinations for the Normal Operating, SBA, IBA, and DBA events. The specific load combinations reflect a greater level of detail than is contained in the general event combinations, including distinctions between SBA and IBA, distinctions between pre-chug and post-chug, distinctions between SRV actuation cases, and consideration of multiple cases of particular loadings. The total number of suppression chamber load combinations consists of 5 for the normal operating event, 36 for the SBA event, 42 for the IBA event, and 24 for the DBA event. Several different service level limits and corresponding sets of allowable stresses are associated with these load combinations.

Not all the possible suppression chamber load combinations are evaluated, as many are enveloped by others and do not lead to controlling suppression chamber stresses. The enveloping load combinations are determined by examining the possible suppression chamber load combinations and comparing the respective load cases and allowable stresses. Table 2-2.2-12 shows the results of this examination. In this table, a number is assigned to each enveloping load combination for ease of identification.

The enveloping load combinations are reduced further by examining relative load magnitudes and individual load characteristics to determine which load combinations lead to controlling suppression chamber stresses. The load combinations which have been found to produce controlling suppression chamber stresses are separated into three groups: the IBA III, IBA IV, DBA II, and DBA III combinations are used to evaluate the suppression chamber vertical support system since these combinations result in the maximum vertical loads on the suppression chamber; the IBA III, IBA IV, DBA II, and DBA III combinations are used to evaluate stresses in the suppression chamber shell and ring beams since these combinations result in maximum pressures on the

suppression chamber shell; and the IBA III and IBA V combinations are used to evaluate the effects of lateral loads on the suppression chamber near the seismic restraints. Selection of these controlling suppression chamber load combinations is explained in the following paragraphs. Table 2-2.2-13 summarizes the controlling load combinations and identifies which load combinations are enveloped by each of the controlling combinations.

Many of the general event combinations (Table 2-2.2-11) have the same allowable stresses and are enveloped by others which contain the same or additional load cases. There is no distinction between load combinations with Service Level A and Service Level B conditions for the suppression chamber since the Service Level A and B allowable stress values are the same.

Except for seismic loads, many pairs of load combinations contain identical load cases. One of the load combinations in the pair contains OBE loads and has Service Level A or B allowables, while the other contains SSE loads with Service Level C allowables. Examination of the load magnitudes presented in Section 2-2.2.1 shows that both the OBE and SSE vertical accelerations are small compared to gravity. As a

result, suppression chamber stresses and vertical support reactions due to vertical seismic loads are small compared to those caused by other loads in the load combination. Except at the seismic restraints, which provide lateral support for the suppression chamber, the horizontal seismic loads for OBE and SSE are less than 50% of gravity and result in small suppression chamber stresses compared with those caused by other loads in the load combinations. The Service Level C primary stress allowables for the load combinations containing SSE loads are more than 75% higher than the Service Level B allowables for the corresponding load combination containing OBE loads. Therefore, the controlling load combinations for evaluating suppression chamber stresses and vertical support reactions are those containing OBE loads and Service Level B allowables.

Because seismic loading is the largest contributor to lateral loads acting on the suppression chamber, the evaluation of both OBE and SSE load combinations is necessary since either may result in controlling suppression chamber stresses near the seismic restraints.

By applying the above reasoning to the total number of suppression chamber load combinations, a reduced number of enveloping load combinations for each event is obtained. Table 2-2.2-12 shows the resulting suppression chamber load combinations for the normal operating, SBA, IBA, and DBA events, along with the associated service level assignments. For ease of identification, each load combination in each event is assigned a number. The reduced number of enveloping load combinations (Table 2-2.2-12) consists of two for normal operating conditions, five for the SBA event, five for the IBA event, and six for the DBA event. The load case designations for the loads which compose the combinations are the same as those presented in Section 2-2.2.1.

Examination of Table 2-2.2-12 reveals that further reductions are possible in the number of suppression chamber load combinations requiring evaluation. Any of the SBA or IBA combinations envelop the NOC I and II combinations since they contain the same loadings as the NOC I and II combinations and, in addition, contain condensation oscillation or chugging loads. The effects of the NOC I and II combinations are considered in the suppression chamber fatigue evaluation.

The remaining suppression chamber load combinations can be separated into those which result in maximum vertical reaction loads, those which result in maximum shell pressures, and those which result in maximum horizontal reaction loads. The loading combinations which result in maximum vertical reaction loads are discussed first.

Since SRV discharge 7b-Case A1.2/C3.2 has been considered conservatively in lieu of SRV discharge 7c-Case A2.2 in all SBA and IBA load combinations, the IBA IV combination envelops the SBA IV and IBA III combinations. This is due to the IBA IV pressure and temperature loadings being higher than SBA pressure and temperature loadings, which results in slightly higher net vertical loads in the suppression chamber. It also follows from the reasoning presented earlier for OBE and SSE loads that the IBA IV combination envelops the DBA VI combination for the effects of vertical reaction loads.

Since pre-chug loads are specified in lieu of IBA condensation oscillation loads, the IBA I combination is the same as the SBA I combination. Thus the SBA I combination can be eliminated from further consideration for combinations affecting vertical reaction loads. The

IBA II combination also envelops the IBA I combination since the internal pressures for IBA II are higher than those for IBA I. There are differences among some loads in the SBA I, IBA I, and IBA II combinations, but these loadings do not affect net vertical loads on the suppression chamber. By the same reasoning, the IBA III combination envelops the SBA II and IBA II combination. From the reasoning presented earlier for OBE and SSE loads, it also follows that the IBA III combination envelops the SBA V and IBA V combinations for the effects of vertical loads. Similarly, it can be shown that the IBA III combination envelops the DBA V combination.

The IBA and SBA load combinations which result in the maximum total pressures on the suppression chamber shell include the SBA II, SBA IV, SBA V, IBA II, IBA III, IBA IV, and IBA V combinations. These combinations contain the maximum internal pressures which occur during the SBA and IBA events and SRV Discharge 7b-Case A1.2/C3.2 loads. The combined effect of these loadings results in the maximum pressure loads on the suppression chamber shell.

The IBA III combination envelops the SBA II combination for the effects of maximum pressure loads since the internal pressures for IBA III are larger than those of SBA II. Since pre-chug loads are specified in lieu of IBA condensation oscillation loads, the IBA III combination is the same as the IBA II combination. Thus the IBA II combination can be eliminated from further consideration for combinations which result in maximum pressure loads. It also follows from the reasoning presented earlier for OBE and SSE loads that the IBA III combination envelops the SBA V and the IBA V combinations. The IBA IV combination envelops the SBA IV for consideration of maximum pressure loads since the internal pressures for IBA IV are larger than those for SBA IV.

The DBA III combination envelops the DBA I combination for the effects of vertical reaction loads and pressure loads since it contains the same loadings as the DBA I combination and, in addition, contains SRV discharge loads. The DBA I combination has Service Level B limits with allowances for increased allowable stresses which, when applied, result in allowable stresses which are about the same as the Service Level C allowable stresses for the DBA III combination.

The DBA II combination envelops the DBA IV combination for the effects of vertical reaction loads and pressure loads since SRV discharge loads which occur late in the DBA event have a negligible effect on the suppression chamber. The DBA II combination also has more restrictive allowables than the DBA IV combination.

The load combinations which result in maximum horizontal reaction loads on the suppression chamber are the SBA II, SBA V, IBA III, and IBA V combinations. All of these combinations contain asymmetric pre-chug loads, SRV discharge 7c-Case A2.2, and either OBE or SSE loads. The symmetric arrangement of ADS valves with respect to the suppression chamber axis (Figure 2-2.1-9) results in the horizontal reaction load on the seismic restraints being zero from SRV discharge 7c-Case A2.2. This load is therefore replaced by SRV discharge 7b-Case A1.2/C3.2 in the load combinations referred to above for evaluation of seismic restraints. The combined effect of this load with pre-chug, OBE and SSE loads results in the maximum possible lateral load on the suppression chamber. The IBA III and SBA II combinations are the same except for differences in internal pressure and temperature loads which do not affect lateral loads on the suppression chamber. The same can be said for the IBA V and SBA V combinations.

The controlling suppression chamber load combinations evaluated in the remaining sections can now be summarized. The IBA III, IBA IV, DBA II, and DBA III combinations are evaluated when examining the effects of vertical reaction loads on the suppression chamber vertical support system and the effects of pressure loads on the suppression chamber shell and ring beams. The IBA III and IBA V combinations are evaluated when examining the effects of lateral loads on the suppression chamber near the seismic restraints.

To ensure that fatigue in the suppression chamber is not a concern over the life of the plant, the combined effects of fatigue due to normal operating plus SBA and normal operating plus IBA events are evaluated. Figures 2-2.2-15, 2-2.2-16, and 2-2.2-17 show the relative sequencing and timing of each loading in the SBA, IBA, and DBA events used in this evaluation. The fatigue effects for normal operating plus DBA events are enveloped by the normal operating plus SBA or IBA events since combined effects of SRV discharge loads and other loads for the SBA and IBA events are more severe than those of DBA. The bottom of Table 2-2.2-12 summarizes additional information used in the suppression chamber fatigue evaluation.

The load combinations and event sequencing described in the preceding paragraphs envelop those postulated to occur during an actual LOCA or SRV discharge event. An evaluation of the above load combinations results in a conservative estimate of the suppression chamber responses and leads to bounding values of suppression chamber stresses and fatigue effects.

Table 2-2.2-11

MARK I CONTAINMENT EVENT COMBINATIONS

EARTHQUAKE TYPE	SRV		SRV + EQ		SBA IBA		SBA + EQ IBA + EQ				SBA+SRV IBA+SRV		SBA+SRV+EQ IBA+SRV+EQ				DBA		DBA + EQ				DBA+SRV		DBA+SRV+EQ			
	1	2	3	4	5	6	7	8	9	10	11	12	13	14	15	16	17	18	19	20	21	22	23	24	25	26	27	
NORMAL	X	X	X	X	X	X	X	X	X	X	X	X	X	X	X	X	X	X	X	X	X	X	X	X	X	X	X	
EARTHQUAKE		X	X			X	X	X	X			X	X	X	X			X	X	X	X			X	X	X	X	
SRV DISCHARGE	X	X	X							X	X	X	X	X								X	X	X	X	X	X	
LOCA THERMAL				X	X	X	X	X	X	X	X	X	X	X	X	X	X	X	X	X	X	X	X	X	X	X	X	
LOCA REACTIONS				X	X	X	X	X	X	X	X	X	X	X	X	X	X	X	X	X	X	X	X	X	X	X	X	
LOCA QUASI-STATIC PRESSURE				X	X	X	X	X	X	X	X	X	X	X	X	X	X	X	X	X	X	X	X	X	X	X	X	
LOCA POOL SWELL															X		X	X					X	X				
LOCA CONDENSATION OSCILLATIONS					X			X	X		X			X	X		X			X	X	X	X			X	X	
LOCA CHUGGING					X			X	X		X			X	X		X			X	X	X	X			X	X	

- SEE SECTION 1-3.2 FOR ADDITIONAL EVENT COMBINATION INFORMATION.

IOW-40-199-2
Revision 0

2-2.80

Table 2-2.2-12

CONTROLLING SUPPRESSION CHAMBER LOAD COMBINATIONS

SECTION 2-2.2.1 LOAD DESIGNATION	CONDITION/EVENT	NOC		SBA					IBA					DBA					
	VOLUME 2 LOAD COMBINATION NUMBER	I	II	I	II	III	IV	V	I	II	III	IV	V	I	II	III	IV	V	VI
	TABLE 2-2.2-11 LOAD COMBINATION NUMBER	2	2	14	14	14	14	15	14	14	14	14	15	18	20	25	27	27	27
1) DEAD		1a, 1b	←																→ 1a, 1b
2) SEISMIC	OBE	2a	←					→ 2a	2a	←			→ 2a	2a	2a				
	SSE							2b					2b			2b	←		→ 2b
3) PRESSURE (1)		P (2)	P (2)	P ₂	P ₃	P	P ₃	P ₃	P ₂	P ₃	P ₃	P ₃	P ₃	P ₁	P ₃	P ₁	P ₃	P ₄	P ₄
3) TEMPERATURE (3)		T (4)	T (4)	T ₂	T ₃	T	T ₃	T ₃	T ₂	T ₃	T ₃	T ₃	T ₃	T ₁	T ₃	T ₁	T ₃	T ₄	T ₄
4) POOL SWELL														4a, 4b		4a, 4b			
5) CONDENSATION OSCILLATION									5b, 5d	5b, 5d					5a, 5c		5a, 5c		
6) CHUGGING	PRE-CHUG			6a, 6c	6a, 6c			6a, 6c			6a, 6c		6a, 6c					6a, 6c	
	POST-CHUG					6b, 6d	6b, 6d					6b, 6d							6b, 6d
7) SRV DISCHARGE	SINGLE	7a, 7d														7a, 7d	(5)		(5)
	MULTIPLE		7b, 7d	7b, 7d		7b, 7d			7b, 7d								7a, 7d		7a, 7d
	ADS				7c, 7d		7c, 7d	7c, 7d		7c, 7d	←		→ 7c, 7d						
8) CONTAINMENT INTERACTION		8a	←																→ 8a
SERVICE LEVEL		B	B	B	B	B	B	C	B	B	B	B	C	B (6)	B	C	C	C	C
NUMBER OF EVENT OCCURENCES (7)		150	150	1	←														→ 1
NUMBER OF SRV ACTUATIONS (8)		740	60	50	2	50	2	2	25	2	2	2	2	0	0	1	1	1	1

IOM-40-199-2
Revision 0

2-2.81

NOTES TO TABLE 2-2.2-12

- (1) SEE FIGURES 2-2.2-1 THROUGH 2-2.2-3 FOR SBA, IBA, AND DBA INTERNAL PRESSURE VALUES.
- (2) THE RANGE OF NORMAL OPERATING INTERNAL PRESSURES IS -2.0 TO 2.0 psi AS SPECIFIED BY THE FSAR.
- (3) SEE FIGURES 2-2.2-4 THROUGH 2-2.2-6 FOR SBA, IBA, AND DBA TEMPERATURE VALUES.
- (4) THE RANGE OF NORMAL OPERATING TEMPERATURES IS 50.0° TO 100.0° F AS SPECIFIED BY THE FSAR. SEE TABLE 2-2.2-2 FOR ADDITIONAL NORMAL OPERATING TEMPERATURES.
- (5) THE SRV DISCHARGE LOADS WHICH OCCUR DURING THIS PHASE OF THE DBA EVENT HAVE A NEGLIGIBLE EFFECT ON THE SUPPRESSION CHAMBER.
- (6) EVALUATION OF SECONDARY STRESS RANGE OR FATIGUE IS NOT REQUIRED. WHEN EVALUATING TORUS SHELL STRESSES, THE VALUE OF S_{mc} MAY BE INCREASED BY THE DYNAMIC LOAD FACTOR DERIVED FROM THE ANALYTICAL MODEL.
- (7) THE NUMBER OF SEISMIC LOAD CYCLES USED FOR FATIGUE IS 600.
- (8) THE VALUES SHOWN ARE CONSERVATIVE ESTIMATES OF THE NUMBER OF ACTUATIONS EXPECTED FOR DAEC.

Table 2-2.2-13

ENVELOPING LOGIC FOR CONTROLLING SUPPRESSION
CHAMBER LOAD COMBINATIONS

CONDITION / EVENT		NOC		SBA					IBA					DBA						
TABLE 2-2.2-11 LOAD COMBINATION NUMBER		2	2	14	14	14	14	15	14	14	14	14	15	18	20	25	27	27	27	
TABLE 2-2.2-11 LOAD COMBINATIONS ENVELOPED		1	1	4-6, 8, 10-12	4-6, 8, 10-12	4-6, 8, 10-12	4-6, 8, 10-12	3,7, 9,13	4-6, 8, 10-12	4-6, 8, 10-12	4-6, 8, 10-12	4-6, 8, 10-12	3,7, 9,13	16	17	19, 22, 24	21, 23, 26	21, 23, 26	21, 23, 26	
SECTION 2-2.2-1 LOAD COMBINATION DESIGNATION		I	II	I	II	III	IV	V	I	II	III	IV	V	I	II	III	IV	V	VI	
CONTROLLING LOAD COMBINATIONS EVALUATED	VERTICAL SUPPORT LOADS	SBA III	X	X				X				X							X	
		IBA I	X	X	X	X			X		X	X		X					X	
		DBA II																X		
		DBA III													X					
	TORUS SHELL PRESSURES	IBA III	X	X	X	X	X		X	X	X			X						X
		IBA IV	X	X				X												X
		DBA II																X		
		DBA III													X					
	LATERAL LOADS	IBA III	X	X	X	X	X	X		X	X		X	X						
		IBA V							X							X	X	X	X	X

SECTION 2-2.1.1 LOAD DESIGNATION

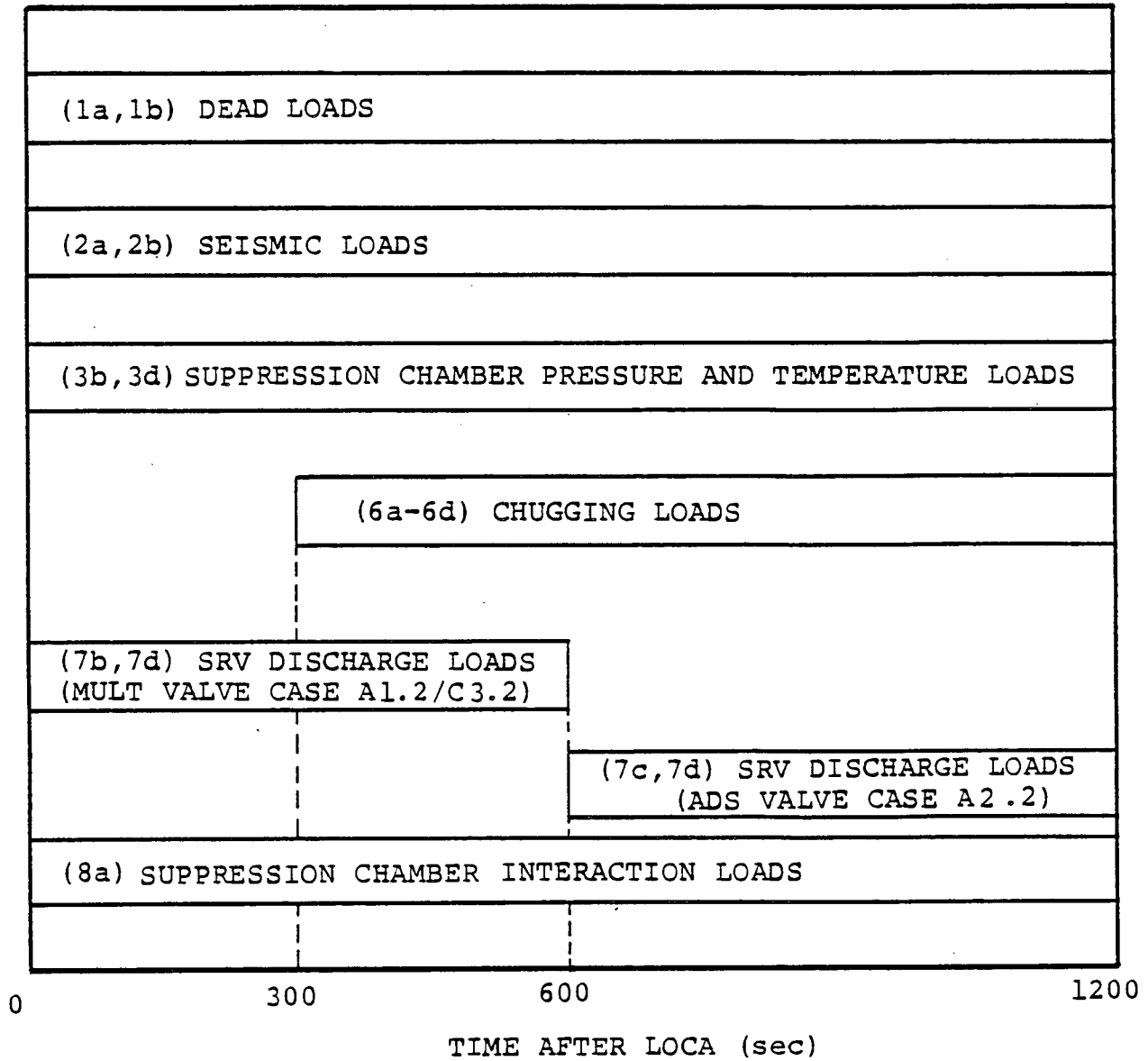


Figure 2-2.2-15
SUPPRESSION CHAMBER SBA EVENT SEQUENCE

SECTION 2-2.1.1 LOAD DESIGNATION

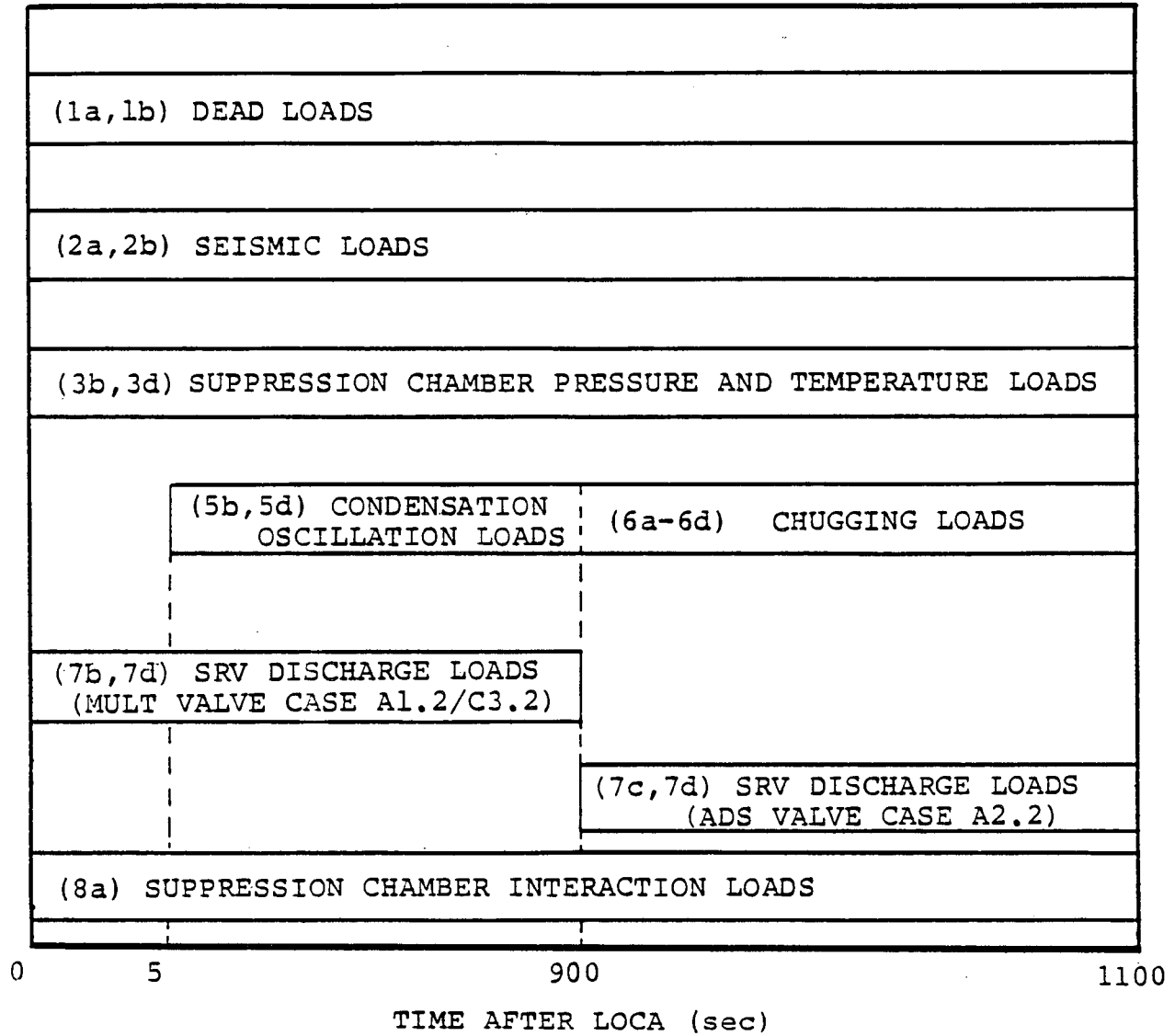


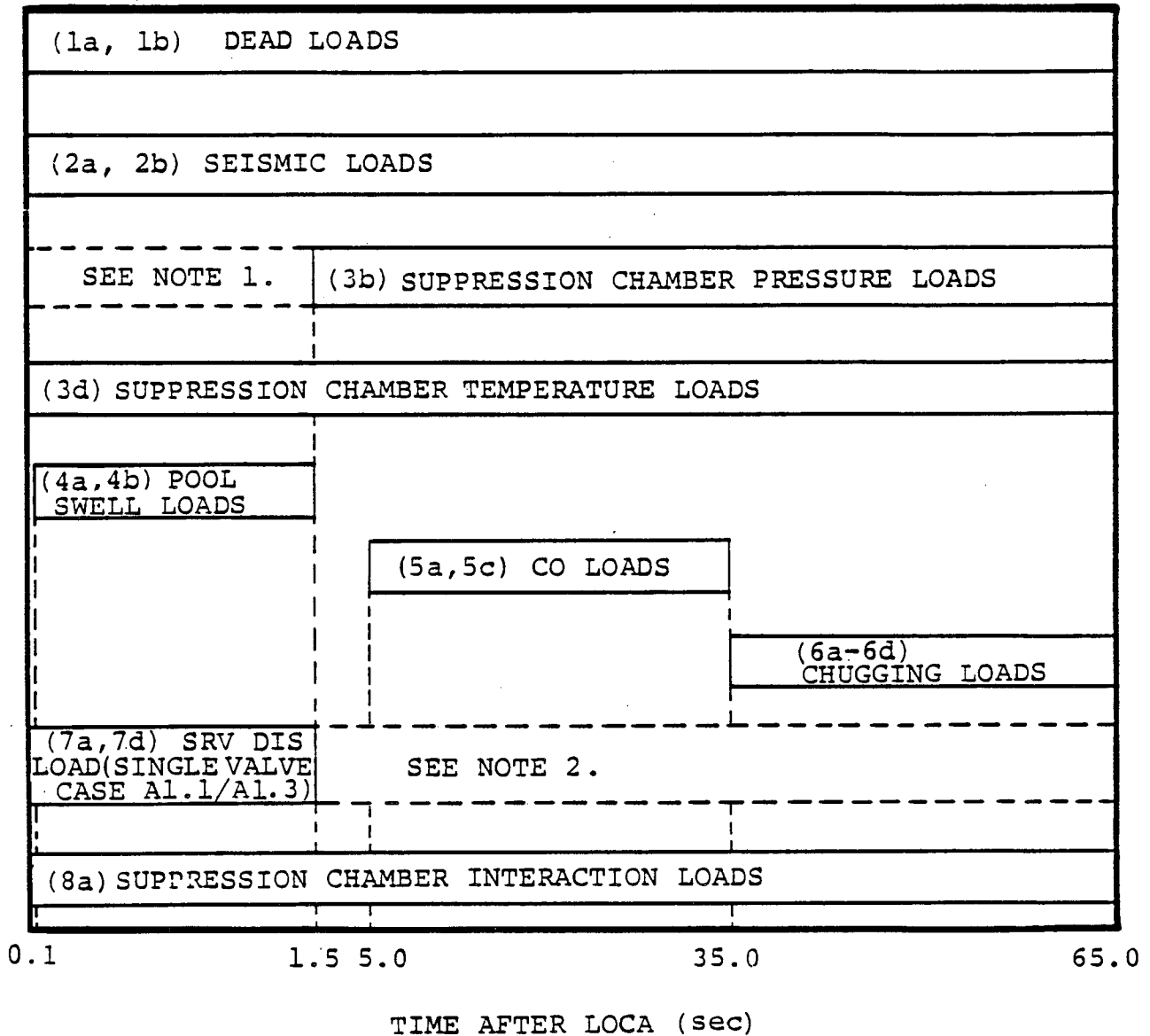
Figure 2-2.2-16

SUPPRESSION CHAMBER IBA EVENT SEQUENCE

IOW-40-199-2
Revision 0

2-2.85

SECTION 2-2.2.1 LOAD DESIGNATION



1. THE EFFECTS OF INTERNAL PRESSURE LOADS ARE INCLUDED IN POOL SWELL TORUS SHELL LOADS.
2. THE SRV DISCHARGE LOADS WHICH OCCUR DURING THIS PHASE OF THE DBA EVENT ARE NEGLIGIBLE.

Figure 2-2.2-17
SUPPRESSION CHAMBER DBA EVENT SEQUENCE

2-2.3 Analysis Acceptance Criteria

The NUREG-0661 acceptance criteria on which the DAEC suppression chamber analysis is based are discussed in Section 1-3.2. In general, the acceptance criteria follow the rules contained in the ASME Code, Section III, Division 1, 1977 Edition with Addenda up to and including Winter 1978 for Class MC components and component supports (Reference 6). The corresponding service limit assignments, jurisdictional boundaries, allowable stresses, and fatigue requirements are consistent with those contained in the applicable subsections of the ASME Code and the "Mark I Containment Program Structural Acceptance Criteria Plant Unique Analysis Application Guide" (PUAAG) (Reference 5). The acceptance criteria used in the analysis of the suppression chamber are summarized in the following paragraphs.

The items examined in the analysis of the suppression chamber include the suppression chamber shell, ring beams, and suppression chamber horizontal and vertical support systems. Figures 2-2.1-1 through 2-2.1-8 identify the specific components associated with each of these items.

The suppression chamber shell and ring beams are evaluated in accordance with the requirements for Class MC components contained in Subsection NE of the ASME Code. Fillet welds and partial penetration welds in which one or both of the joined parts includes the suppression chamber shell and ring beams are also evaluated in accordance with the requirements for Class MC component attachment welds contained in Subsection NE of the ASME Code.

The suppression chamber columns, column connections, saddle supports, and associated components and welds are evaluated in accordance with the requirements for Class MC component supports contained in Subsection NF of the ASME Code.

Table 2-2.2-12 indicates that the SBA III, IBA I, IBA III, IBA IV, and DBA II combinations all have Service Level B limits while the IBA V and DBA III combinations both have Service Level C limits. Since these load combinations have somewhat different maximum temperatures, the allowable stresses for the two load combination groups with Service Level B and C limits are conservatively determined at the highest temperature in each load combination group unless indicated otherwise.

The allowable stresses for each component of the suppression chamber and the vertical support system are determined at the maximum IBA temperature of 178°F. Table 2-2.3-1 shows the resulting allowable stresses for the load combinations with Service Level B and C limits.

The 1-1/4" diameter bolts provided to transfer uplift loads from the suppression chamber columns and saddle supports are embedded 33" into the basemat concrete. The allowable uplift load per bolt is 85 kips, in accordance with the requirements of the ACI Code (Reference 7).

The bearing stresses in the grout and reactor building basemat in the vicinity of the column and saddle base plates are evaluated in accordance with the requirements of the ACI Code.

The allowable load capacities for the suppression chamber vertical support system are determined using an analytical model of the column and saddle base plate assemblies. Downward reaction load capacity is determined by adding support reactions for hydrostatic loads applied on a unit load basis. The support reactions thus obtained are used to ratio the stresses

from the analysis to obtain Code allowable capacities. Upward load capacity (uplift) is determined by the allowable tension in the anchor bolts. Table 2-2.3-2 summarizes the resulting allowable load capacities for the suppression chamber vertical supports.

The allowable stresses in each component of the suppression chamber seismic restraints are taken from the FSAR, and are shown in Table 2-2.5-8. This is permitted by NUREG-0661 in cases where the analysis technique used in the evaluation is the same as that contained in the plant's FSAR. The suppression chamber shell, in the vicinity of the seismic restraints, is evaluated in accordance with the requirements for Class MC components previously discussed.

The acceptance criteria described in the preceding paragraphs result in conservative estimates of the existing margins of safety and ensure that the original suppression chamber design margins are restored.

Table 2-2.3-1

ALLOWABLE STRESSES FOR SUPPRESSION CHAMBER
COMPONENTS AND SUPPORTS

ITEM	MATERIAL	MATERIAL (1) PROPERTIES (ksi)	STRESS TYPE	ALLOWABLE STRESS (ksi)	
				SERVICE (2) LEVEL B	SERVICE (3) LEVEL C
C O M P O N E N T S					
SHELL	SA-516 GR. 70	$S_{mc} = 19.30$	PRIMARY MEMBRANE	19.30	35.52
		$S_{ml} = 23.15$	LOCAL PRIMARY MEMBRANE	28.95	53.28
		$S_y = 35.52$	PRIMARY + (4) SECONDARY STRESS RANGE	69.45	N/A
RING BEAM	SA-516 GR. 70	$S_{mc} = 19.30$	PRIMARY MEMBRANE	19.30	35.52
		$S_{ml} = 23.15$	LOCAL PRIMARY MEMBRANE	28.95	53.28
		$S_y = 35.52$	PRIMARY + (4) SECONDARY STRESS RANGE	69.45	N/A
C O M P O N E N T S U P P O R T S					
COLUMN (5) CONNECTION	SA-516 GR. 70	$S_y = 35.52$	MEMBRANE	21.31	28.42
			EXTREME FIBER	26.64	35.52
SADDLE (5)	SA-516 GR. 70	$S_y = 35.52$	MEMBRANE	21.31	28.42
			EXTREME FIBER	26.64	35.52

Table 2-2.3-1

ALLOWABLE STRESSES FOR SUPPRESSION CHAMBER
COMPONENTS AND SUPPORTS

(Concluded)

ITEM	MATERIAL	MATERIAL (1) PROPERTIES (ksi)	STRESS TYPE	ALLOWABLE STRESS (ksi)	
				SERVICE (2) LEVEL B	SERVICE (3) LEVEL C
W E L D S					
RING BEAM TO SHELL	SA-516 GR. 70	$S_{mc} = 19.30$ $S_{m1} = 23.15$ $S_y = 35.52$	PRIMARY	22.52 ⁽⁶⁾	41.45
			SECONDARY	54.03 ⁽⁷⁾	N/A
COLUMN CONNECTION TO SHELL	SA-516 GR. 70	$S_{mc} = 19.30$ $S_{m1} = 23.15$ $S_y = 35.52$	PRIMARY	19.30	35.52
			SECONDARY	69.45 ⁽⁷⁾	N/A
SADDLE TO SHELL	SA-516 GR. 70	$S_{mc} = 19.30$ $S_{m1} = 23.15$ $S_y = 35.52$	PRIMARY	19.30	35.52
			SECONDARY	69.45 ⁽⁷⁾	N/A

- (1) MATERIAL PROPERTIES ARE TAKEN AT MAXIMUM EVENT TEMPERATURES.
- (2) SERVICE LEVEL B ALLOWABLES ARE USED WHEN EVALUATING IBA III, IBA IV, AND DBA II LOAD COMBINATION RESULTS.
- (3) SERVICE LEVEL C ALLOWABLES ARE USED WHEN EVALUATING IBA V AND DBA III LOAD COMBINATION RESULTS.
- (4) THERMAL BENDING STRESSES MAY BE EXCLUDED WHEN COMPARING PRIMARY-PLUS-SECONDARY STRESS RANGE VALUES TO ALLOWABLES.
- (5) STRESSES DUE TO THERMAL LOADS MAY BE EXCLUDED WHEN EVALUATING COMPONENT SUPPORTS.
- (6) STRESS INCLUDES PRIMARY MEMBRANE PLUS BENDING.
- (7) SECONDARY STRESS RANGE IS USED.

IOW-40-199-2
Revision 0

2-2.92

Table 2-2.3-2

SUPPRESSION CHAMBER VERTICAL SUPPORT
SYSTEM ALLOWABLE LOADS

SUPPORT COMPONENT		LOAD CAPACITY (kips)	
		(2)(3) UPWARD	(1) DOWNWARD
COLUMN	INSIDE	148 (148)	485
	OUTSIDE	318 (148)	485
SADDLE	INSIDE	680 (510)	1200
	OUTSIDE	850 (510)	1200
TOTAL PER MITERED CYLINDER		1996 (1316)	3370

- (1) CAPACITIES SHOWN ARE BASED ON SERVICE LEVEL B ALLOWABLES. FOR SERVICE LEVEL C ALLOWABLES, INCREASE VALUES SHOWN BY ONE-THIRD.
- (2) CAPACITY IS CONTROLLED BY THE ALLOWABLE TENSION IN ANCHOR BOLTS IN ACCORDANCE WITH ACI CODE (REFERENCE 7).
- (3) FIGURES IN PARENTHESES ARE ALLOWABLE UPLIFT LOADS FOR BAYS WITHOUT T-QUENCHERS.

2-2.4 Methods of Analysis

The governing loads for which the DAEC suppression chamber is evaluated are presented in Section 2-2.2.1. The methodology used to evaluate the suppression chamber for the effects of all loads, except those which result in lateral loads on the suppression chamber, is discussed in Section 2-2.4.1. The methodology used to evaluate the suppression chamber for the effects of lateral loads is discussed in Section 2-2.4.2.

The methodology used to formulate results for the controlling load combinations, examine fatigue effects, and evaluate the analysis results for comparison with the applicable acceptance limits is discussed in Section 2-2.4.3.

2-2.4.1 Analysis for Major Loads.

The repetitive nature of the suppression chamber geometry is such that the suppression chamber can be divided into 16 identical segments which extend from midbay of the vent bay to midbay of the non-vent bay (Figure 2-2.1-1). The suppression chamber can be further divided into 32 identical segments extending from the miter joint to midbay, provided the offset ring beam and vertical supports are assumed to lie in the plane of the miter joint. The effects of the ring beam and vertical supports offset have been evaluated and found to have a negligible effect on the suppression chamber response. The analysis of the suppression chamber, therefore, is performed for a typical 1/32 segment.

A finite element model of a 1/32 segment of the suppression chamber (Figure 2-2.4-1) is used to obtain the suppression chamber response to all loads except those resulting in lateral loads on the suppression chamber. The analytical model includes the suppression chamber shell, the ring beam, the column connections and associated column members, the saddle support and associated base plates, and miscellaneous internal and external stiffener plates.

The analytical model is composed of 736 nodes, 186 beam elements, and 946 plate bending and stretching elements. The suppression chamber shell has a circumferential node spacing of 8° at midbay with additional mesh refinement near discontinuities to facilitate examination of local stresses. Additional refinement is included in modeling of the column connections and saddle support at locations where locally higher stresses occur. The ring beam is modeled as beam elements located at the center of gravity of the ring beam. These beam elements are connected to the suppression chamber shell nodes by offset rigid links. The stiffness and mass properties used in the model are based on the nominal dimensions and densities of the materials used to construct the suppression chamber (Figures 2-2.1-1 through 2-2.1-8). Small displacement linear-elastic behavior is assumed throughout.

The boundary conditions used in the analytical model are both physical and mathematical in nature. The physical boundary conditions consist of vertical restraints at each column and saddle base plate location. As previously discussed, the vertical support system base plates permit movement of the suppression chamber in the radial direction. The mathematical boundary conditions

consist of either symmetry, anti-symmetry, or a combination of both at the miter joint and midbay planes, depending on the characteristics of the load being evaluated.

A separate finite element model of the ring beam, which includes a finite length of the suppression chamber on either side of the miter joint, is used for analysis of submerged structure loads on the ring beam. The analytical model contains 1,435 nodes, 288 beam elements, and 1,940 plate elements.

When computing the response of the suppression chamber to dynamic loadings, the fluid-structure interaction effects of the suppression chamber shell and contained fluid (water) are considered. This is accomplished using a finite element model of the fluid (Figure 2-2.4-2). The analytical fluid model is used to develop a coupled mass matrix which is added to the submerged nodes of the suppression chamber analytical model to represent the fluid. A water volume corresponding to a water level 2.42 feet below the suppression chamber horizontal centerline is used in this calculation. This is the maximum water volume expected during normal operating conditions. Additional fluid mass is lumped

along the length of the ring beam to account for the effective mass of water which acts with the ring beam during dynamic loadings.

Using the suppression chamber analytical model, a frequency analysis is performed in which all structural modes in the range of 0 to 50.75 Hz are extracted. Table 2-2.4-1 shows the resulting frequencies and vertical mass participation factors. The dominant suppression chamber frequencies are in the range of 16.33 to 20.98 Hz.

A dynamic analysis is performed for each of the hydrodynamic suppression chamber shell load cases specified in Section 2-2.2.1 using the analytical model of the suppression chamber. The analysis consists of either a transient or a harmonic analysis, depending on the characteristics of the suppression chamber shell load being considered. The modal superposition technique with 2% damping as per Regulatory Guide 1.61 (Reference 8) is utilized in both transient and harmonic analyses.

The remaining suppression chamber load cases specified in Section 2-2.2.1 involve either static loads or dynamic loads which are evaluated using an equivalent

static approach. For the latter, conservative dynamic amplification factors are developed and applied to the maximum spatial distributions of the individual dynamic loadings.

The specific treatment of each load in the load categories identified in Section 2-2.2.1 is discussed in the following paragraphs.

1. Dead Loads

a. Weight of Steel: A static analysis is performed for a unit vertical acceleration applied to the weight of suppression chamber steel.

b. Weight of Water: A static analysis is performed for hydrostatic pressures applied to the submerged portion of the suppression chamber shell.

2. Seismic Loads

a. OBE: A static analysis is performed for a 0.053g vertical acceleration applied to the

combined weight of suppression chamber steel and water. The effects of horizontal OBE accelerations are evaluated in Section 2-2.4.2.

- b. SSE: A static analysis is performed for a 0.106g vertical acceleration applied to the combined weight of suppression chamber steel and water. The effects of horizontal SSE accelerations are evaluated in Section 2-2.4.2.

3. Containment Pressure and Temperature

- a. Normal Operating Internal Pressure: A static analysis is performed for a ± 2.0 psi internal pressure uniformly applied to the suppression chamber shell.
- b. LOCA Internal Pressure: A static analysis is performed for the SBA, IBA, and DBA internal pressures (Figures 2-2.2-1 through 2-2.2-3). These pressures are uniformly applied to the suppression chamber shell at selected times during each event.

- c. Normal Operating Temperature: A static analysis is performed for the appropriate temperature uniformly applied to the suppression chamber shell and ring beam.
- d. LOCA Temperature: A static analysis is performed for the SBA, IBA, and DBA temperatures, uniformly applied to the suppression chamber shell and ring beam. The SBA, IBA, and DBA event temperatures (Figures 2-2.2-4 through 2-2.2-6) are applied at selected times during each event.

4. Pool Swell Loads

- a. Pool Swell, Suppression Chamber Shell: A dynamic analysis is performed for the conservative non-vent bay pool swell loads (Figures 2-2.2-7 and 2-2.2-8, Table 2-2.2-3).
- b. LOCA Air Clearing, Submerged Structures: An equivalent static analysis is performed for the ring beam DBA air clearing submerged structure loads (Table 2-2.2-4). The values of the loads shown include dynamic amplifica-

tion factors which are computed using the dominant frequencies of the ring beam.

5. Condensation Oscillation Loads

- a. DBA Condensation Oscillation, Suppression Chamber Shell: A dynamic analysis is performed for the four condensation oscillation load alternates (Table 2-2.2-5). During harmonic summation, the amplitudes for each condensation oscillation load frequency interval are conservatively applied to the maximum response amplitudes obtained from the suppression chamber harmonic analysis results in the same frequency interval.
- b. IBA Condensation Oscillation, Suppression Chamber Shell: Pre-chug loads described in load case 6a are specified in lieu of IBA condensation oscillation loads.
- c. DBA Condensation Oscillation, Submerged Structures: An equivalent static analysis is performed for the ring beam DBA condensation oscillation submerged structure loads (Table

2-2.2-6). The values of the loads shown include dynamic amplification factors which are computed using the dominant frequencies of the ring beam.

- d. IBA Condensation Oscillation, Submerged Structures: Pre-chug loads described in load case 6c are specified in lieu of IBA condensation oscillation loads.

6. Chugging Loads

- a. Pre-Chug, Suppression Chamber Shell: A dynamic analysis is performed for the symmetric pre-chug loads (Figure 2-2.2-11). The maximum suppression chamber response in the 6.9 to 9.5 Hz range occurs at the maximum pre-chug load frequency of 9.5 Hz, which is close to the first mode frequency of 10.19 Hz of the suppression chamber.

An equivalent static analysis is performed for asymmetric pre-chug loads to evaluate the effects of unbalanced vertical loads across the suppression chamber miter joint. The

highest and next highest pressures (Figure 2-2.2-12) are assumed to act in two adjacent suppression chamber bays. A dynamic amplification factor, derived from the dynamic analysis results for symmetric pre-chug loads, is applied to the asymmetric pre-chug loads. The effects of lateral loads caused by asymmetric pre-chug are examined in Section 2-2.4.2.

- b. Post-Chug, Suppression Chamber Shell: A dynamic analysis is performed for the post-chug loads (Table 2-2.2-7) with a normalized spatial distribution of pressures (Figure 2-2.2-9). During harmonic summation, the amplitudes for each post-chug load frequency interval are conservatively applied to the maximum response amplitudes obtained from the suppression chamber harmonic analysis results in the same frequency interval.
- c. Pre-Chug, Submerged Structures: An equivalent static analysis is performed for the ring beam pre-chug submerged structure loads (Table 2-2.2-8). The values of the loads shown

include dynamic amplification factors which are computed using the dominant frequencies of the ring beam.

- d. Post-Chug, Submerged Structures: An equivalent static analysis is performed for the ring beam submerged structure loads (Table 2-2.2-9). The values of the loads shown include dynamic amplification factors which are computed using the dominant frequencies of the ring beam.

7. Safety Relief Valve Discharge Loads

- a-c. SRV Discharge, Suppression Chamber Shell: A dynamic analysis is performed for SRV Discharge 7a-Case A1.1/A1.3 and 7b-Case A1.2/C3.2 (Figures 2-2.2-13 and 2-2.2-14). Several frequencies within the range of the SRV discharge load frequencies specified for each case are evaluated to determine the maximum suppression chamber response. The effects of lateral loads on the suppression chamber caused by SRV Discharge 7b-Case A1.2/C3.2 are evaluated in Section 2-2.4.2.

The suppression chamber analytical model used in the analysis is calibrated using the methodology discussed in Section 1-4.2.3. The methodology involves use of modal correction factors which are applied to the response associated with each suppression chamber frequency. Figure 2-2.4-3 shows the resulting correction factors used in evaluating the effects of SRV discharge suppression chamber shell loads.

- d. SRV Discharge Air Clearing, Submerged Structures: An equivalent static analysis is performed for the ring beam SRV discharge drag loads. The values of the loads shown (Table 2-2.2-10) include dynamic amplification factors derived using the methodology discussed in Section 1-4.2.4. An equivalent static analysis for all submerged structure loads is performed using the special-purpose ring beam model referred to previously.

8. Suppression Chamber Interaction Loads

- a. Suppression Chamber Internal Structure Reactions: An equivalent static analysis is performed for the vent system support columns, T-quencher and T-quencher supports, catwalk, and monorail support reaction loads taken from the evaluations of these components as discussed in Volumes 3 through 5 of this report.

The methodology described in the preceding paragraphs results in a conservative evaluation of the suppression chamber response and associated stresses for the governing loads. Use of the analysis results obtained by applying this methodology leads to a conservative evaluation of the suppression chamber design margins.

Table 2-2.4-1

SUPPRESSION CHAMBER FREQUENCY ANALYSIS RESULTS

MODE NUMBER	FREQUENCY (Hz)	VERTICAL WEIGHT PARTICIPATION (lb)
1	10.19	41.45
2	10.35	132.58
3	12.45	1551.31
4	12.76	50.10
5	14.06	4441.66
6	14.81	1940.04
7	15.69	2629.03
8	16.33	23591.69
9	17.36	2660.78
10	17.88	11079.10
11	20.13	335.23
12	20.98	34706.92
13	23.00	11489.10
14	23.69	2443.36
15	24.64	12214.77
16	25.69	1168.32
17	26.45	0.37
18	26.71	61.57
19	28.10	2124.71
20	28.46	792.97
21	29.61	4864.36
22	30.99	228.62
23	31.21	24.22
24	31.73	14.43
25	32.22	5340.92

Table 2-2.4-1

SUPPRESSION CHAMBER FREQUENCY ANALYSIS RESULTS

(Continued)

MODE NUMBER	FREQUENCY (Hz)	VERTICAL WEIGHT PARTICIPATION (lb)
26	32.46	5506.17
27	33.27	2419.52
28	34.53	3.62
29	34.82	24.03
30	35.02	23.38
31	35.44	829.91
32	36.83	3.63
33	37.70	214.96
34	37.94	28.47
35	38.41	10.07
36	38.71	1529.21
37	39.70	6.26
38	39.78	485.80
39	40.53	150.07
40	40.74	47.40
41	40.83	540.35
42	41.27	90.29
43	41.69	1.40
44	42.74	4.22
45	42.89	181.12
46	44.24	10.00
47	45.12	1.31
48	45.29	0.33
49	45.79	107.20
50	45.91	19.89

Table 2-2.4-1

SUPPRESSION CHAMBER FREQUENCY ANALYSIS RESULTS
(Concluded)

MODE NUMBER	FREQUENCY (Hz)	VERTICAL WEIGHT PARTICIPATION (lb)
51	46.75	165.88
52	47.36	0.26
53	47.65	117.49
54	48.45	0.08
55	48.76	21.30
56	48.77	27.97
57	49.77	45.66
58	50.35	55.34
59	50.75	29.89

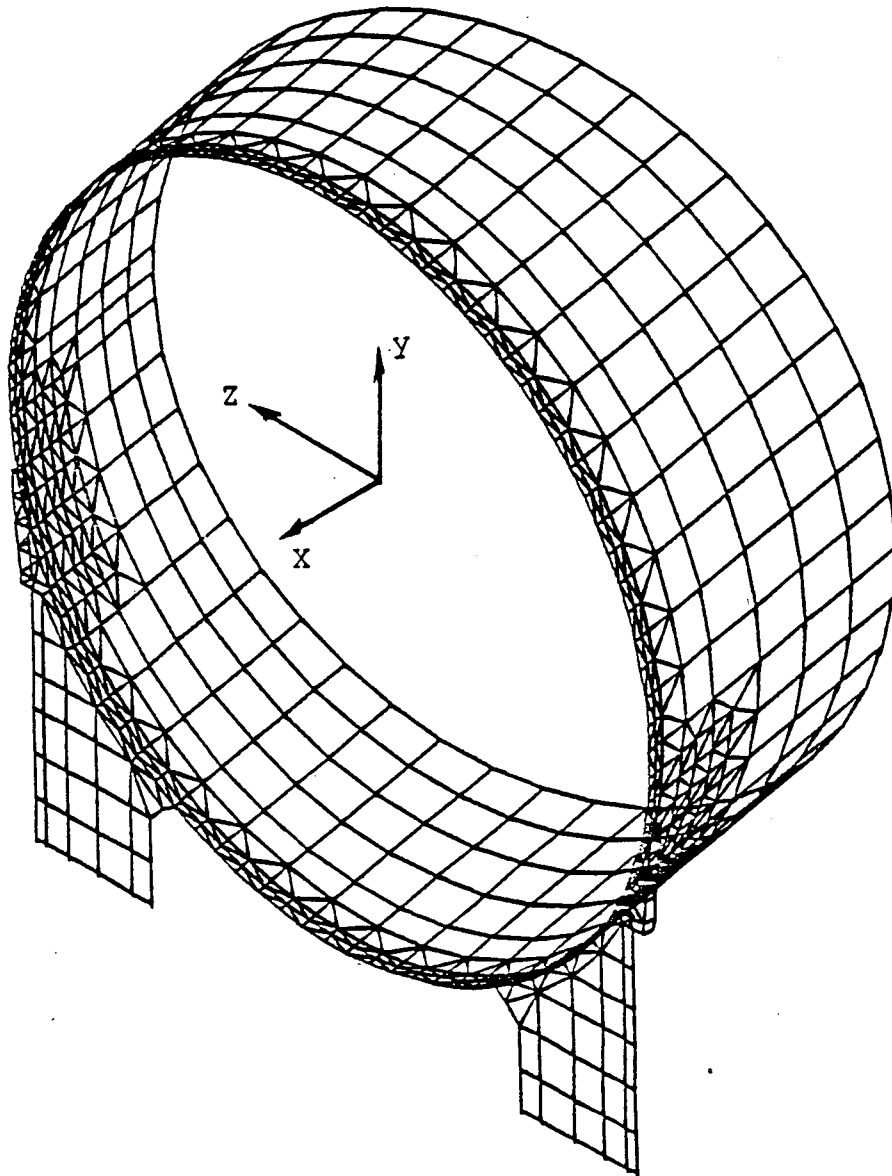


Figure 2-2.4-1

SUPPRESSION CHAMBER 1/32 SEGMENT FINITE
ELEMENT MODEL - ISOMETRIC VIEW

IOW-40-199-2
Revision 0

2-2.111

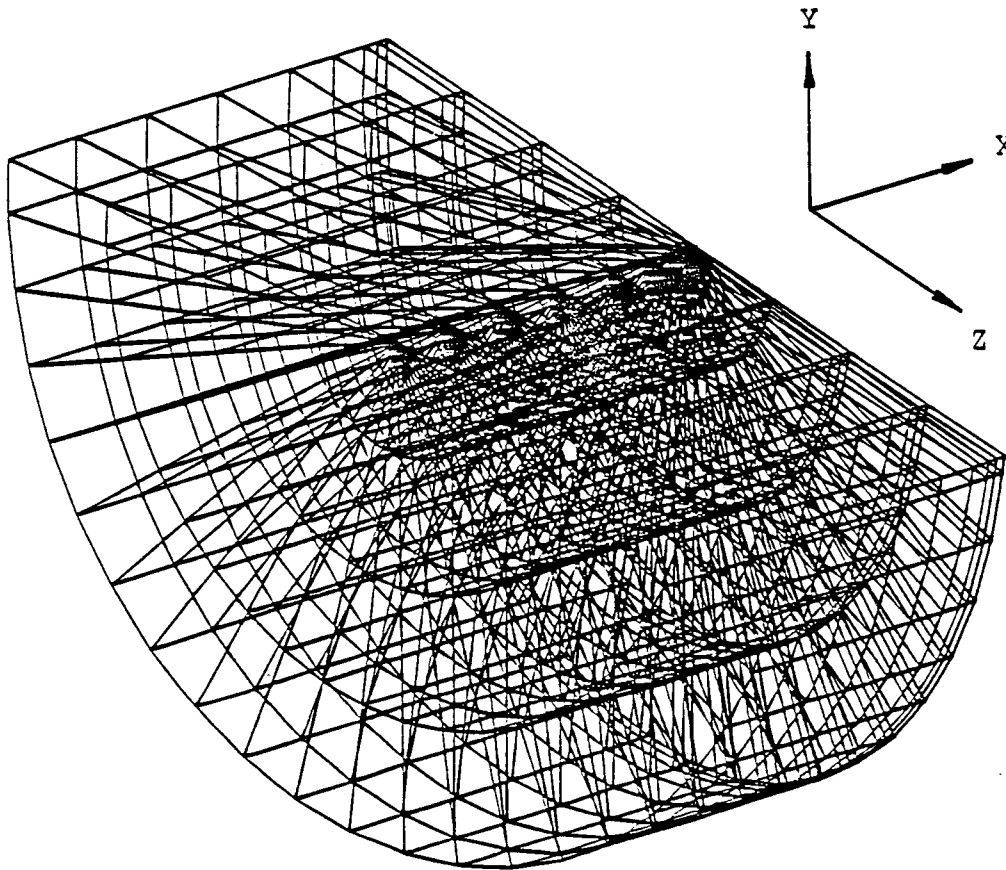
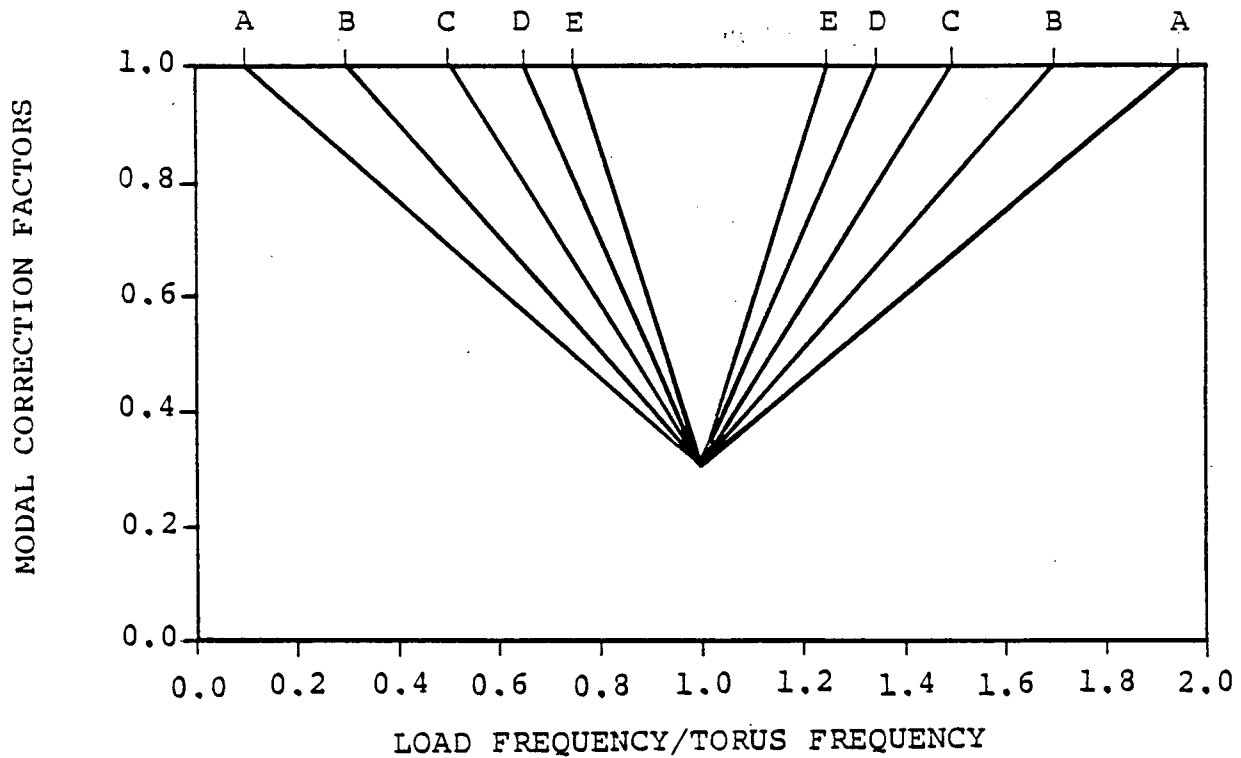


Figure 2-2.4-2

SUPPRESSION CHAMBER FLUID MODEL-ISOMETRIC VIEW

IOW-40-199-2
Revision 0

2-2.112



MODE NUMBER	FREQUENCY (Hz)	CORRECTION FACTOR	
		CASE A1.1/A1.3 ($f_L = 5.93$)	CASE A1.2/C3.2 ($f_L = 10.79$)
1	10.194	0.69	0.36
2	10.349	0.70	0.34
3	12.447	0.93	0.50
4	12.755	0.96	0.49
5	14.063	1.00	0.63
6	14.807	1.00	0.72
7	15.690	1.00	0.84
8	16.331	1.00	0.93
9-59	>17.356	1.00	1.00

LEGEND	
CURVE	TORUS FREQ. (Hz)
A	8
B	11
C	14
D	17-23
E	26-32

Figure 2-2.4-3

MODAL CORRECTION FACTORS USED FOR ANALYSIS OF
SRV DISCHARGE TORUS SHELL LOADS

2-2.4.2 Analysis for Lateral Loads

In addition to vertical loads, a few of the governing loads acting on the suppression chamber result in net lateral loads on the suppression chamber, as discussed in Section 2-2.2.1. These lateral loads are transferred to the reactor building basemat by the seismic restraints described in Section 2-2.1.

The general methodology used to evaluate the effects of lateral loads consists of establishing an upper bound value of the lateral load for each applicable load case. The results for each load case are then grouped in accordance with the controlling load combinations described in Section 2-2.2.2, and the maximum total lateral load acting on the suppression chamber is determined.

The maximum total lateral load is conservatively assumed to be aligned along an axis passing through two diametrically opposite seismic restraints and shared equally by the two restraints (Figure 2-2.1-1). Once the seismic restraint loads are known, the stresses in the various structural elements of the restraints, including welds connecting the pad plates to the suppression

chamber shell, are evaluated and compared with the allowable stresses.

Due to the eccentricity of the seismic restraint pin with respect to the shell middle surface, loads on the seismic restraints result in a shear force and bending moment acting on the suppression chamber shell. The effects of these shears and moments on the suppression chamber shell are evaluated using the analytical model of the suppression chamber described in Section 2-2.4.1. A distribution of forces which produces the desired shear and moment is applied to the suppression chamber shell at the perimeter of the seismic restraint pad plate (Figure 2-2.4-4). The resulting shell stresses are then combined with the other loads contained in the controlling load combination being evaluated, and the shell stresses in the vicinity of the seismic restraints are determined.

The magnitudes and characteristics of the governing loads which result in lateral loads on the suppression chamber are presented and discussed in Section 2-2.2.1. The specific treatment of each load which results in lateral loads on the suppression chamber is discussed in the following paragraphs.

2. Seismic Loads

- a. OBE: The total lateral load due to OBE loads is equal to the maximum horizontal acceleration of 0.12g applied to the weight of suppression chamber steel and the effective weight of suppression chamber water in the horizontal direction.

The effective weight of suppression chamber water in the horizontal direction is derived from generic small-scale tests performed on Mark I suppression chambers. These test results have been confirmed analytically using a model of the suppression chamber fluid (water) similar to the one shown in Figure 2-2.4-2.

The effective weight of suppression chamber water used in the evaluation is taken as 20% of the total weight of water contained in the suppression chamber. This value represents the amount of water acting with the suppression chamber as added mass during horizontal dynamic events. The effective weight of water

exhibits itself in reaction loads on the seismic restraints. The remaining 80% of suppression chamber water acts in sloshing modes at frequencies near zero. Only a portion of the total sloshing mass acting at considerably lower seismic accelerations results in reaction loads on the seismic restraints. The total sloshing mass is conservatively applied at the maximum OBE acceleration in the range of the sloshing frequencies.

- b. SSE: The total lateral load due to SSE loads is equal to the maximum horizontal acceleration of 0.24g applied to the weight of suppression chamber steel and the effective weight of suppression chamber water in the horizontal direction. The methodology used to evaluate horizontal SSE loads is discussed in load case 2a.

6. Chugging Loads

- a. Pre-Chug, Suppression Chamber Shell: The spatial distribution of asymmetric pre-chug

pressures is integrated, and the total lateral load is determined (Figures 2-2.2-11 and 2-2.2-12). A dynamic amplification factor is computed using first principles and characteristics of a chugging cycle transient (Figure 2-2.4-5). The maximum dynamic amplification factor possible, regardless of structural frequency, is conservatively used.

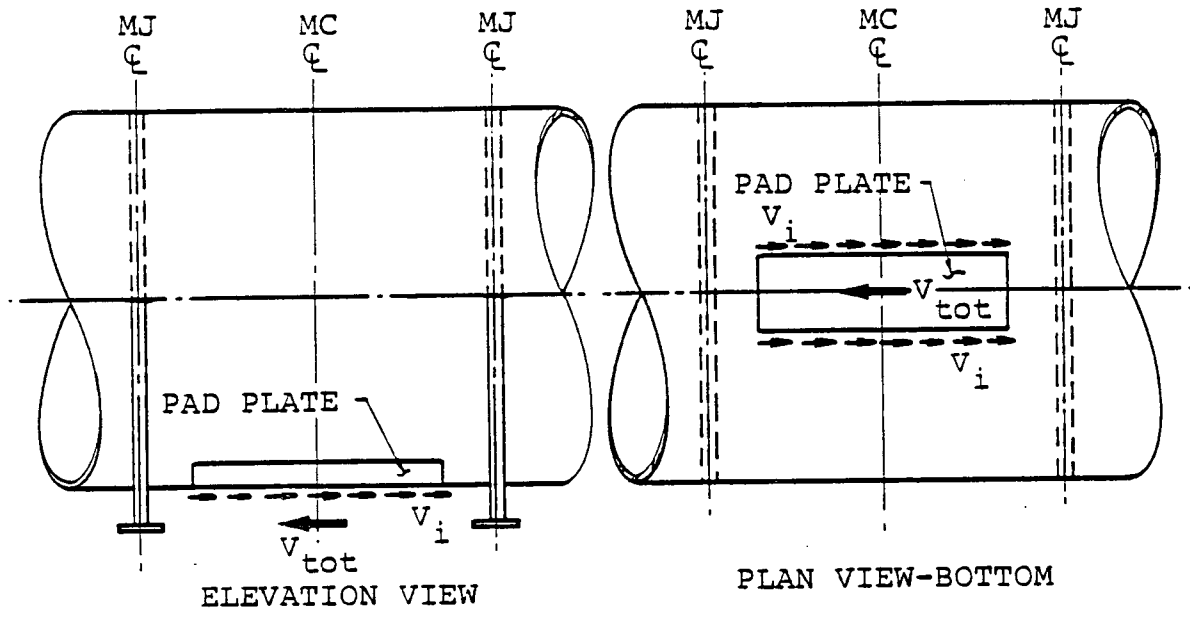
7. Safety Relief Valve Discharge Loads

- d. SRV Discharge, Suppression Chamber Shell: The spatial distribution of pressures for SRV discharge 7b-Case A1.2/C3.2 is integrated, and the total lateral load is determined (Figure 2-2.2-14). A dynamic amplification factor is computed, using the methodology discussed in Section 2-2.4.1, for SRV discharge suppression chamber shell loads analysis. The maximum dynamic amplification factor possible, regardless of structural frequency, is conservatively used (Figure 2-2.4-6).

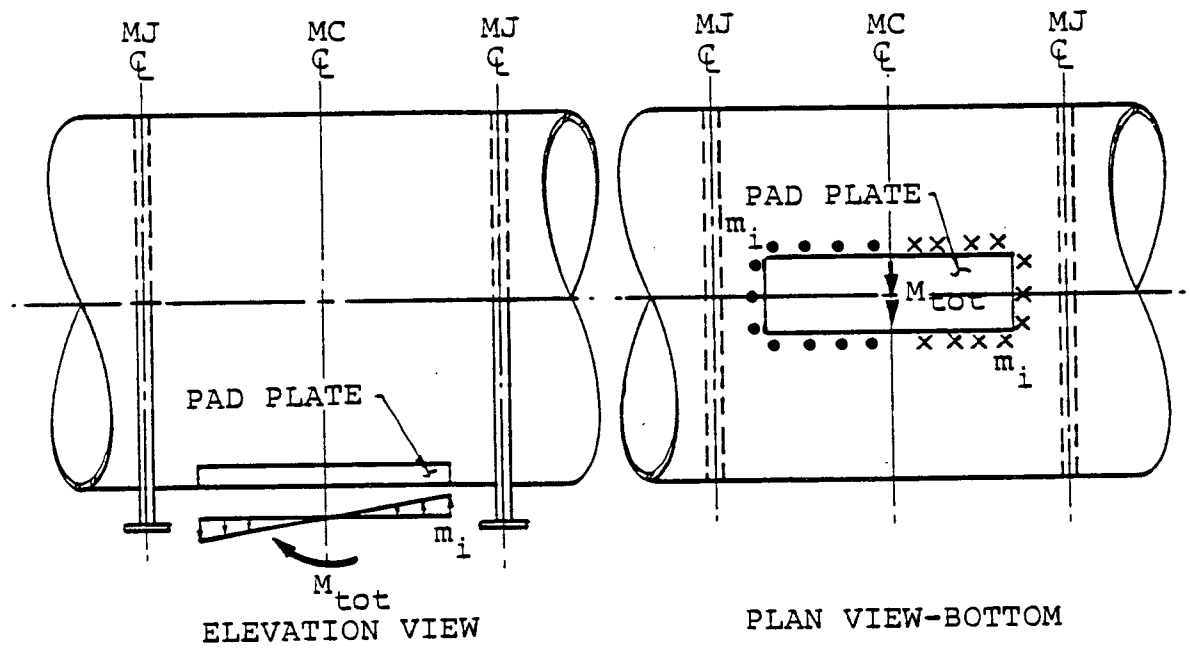
Use of the methodology described in the preceding paragraphs results in a conservative evaluation of suppression chamber shell stresses due to governing loads resulting in lateral loads on the suppression chamber.

IOW-40-199-2
Revision 0

2-2.119



For $V_{tot} = 1.0$ kip, $V_i = .0068$ k/in



For $V_{tot} = 1.0$ kip, $M_{tot} = 19.97$ in-k, $m_{i_{max}} = 0.0017$ k/in

Figure 2-2.4-4
METHODOLOGY FOR SUPPRESSION CHAMBER
LATERAL LOAD APPLICATION

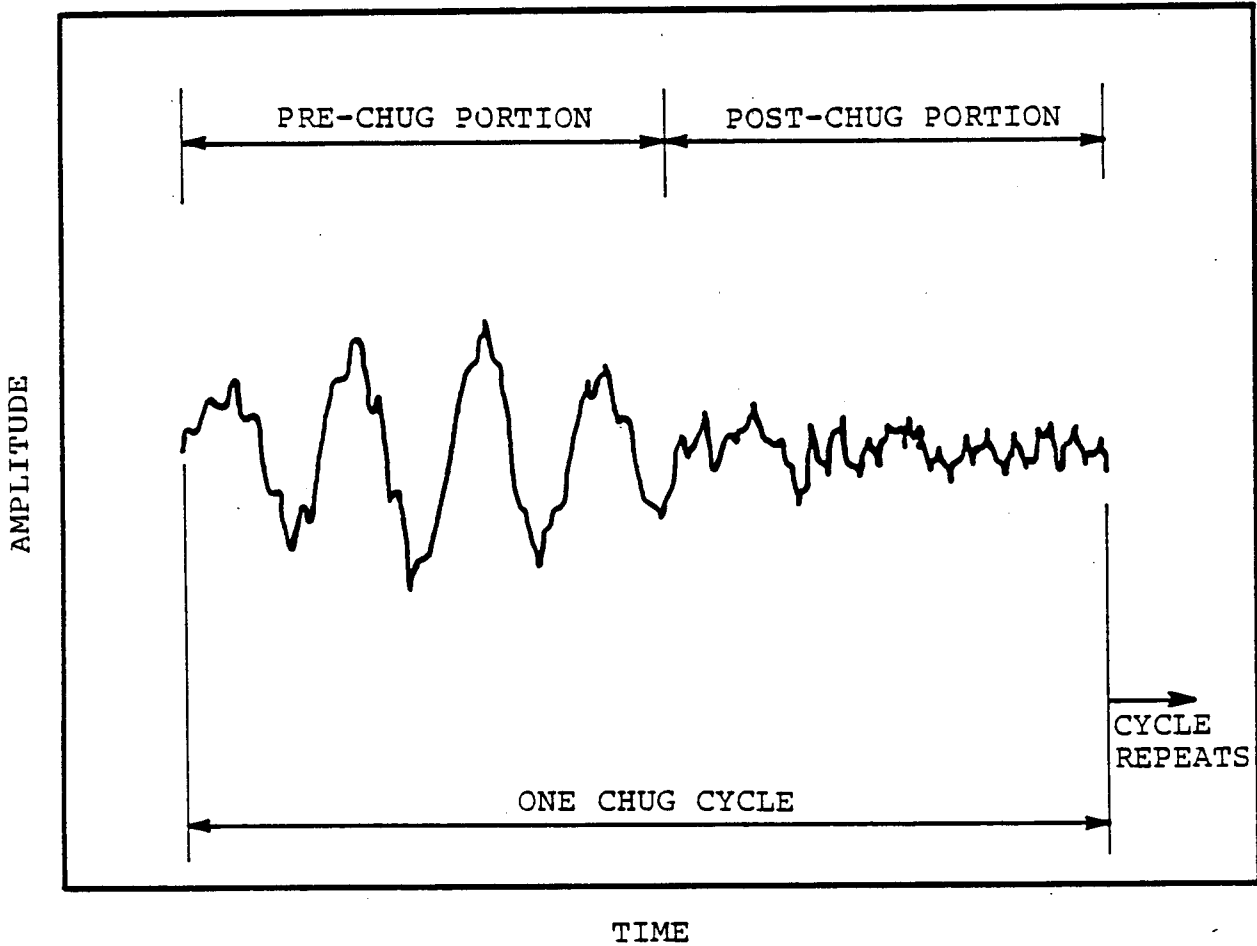


Figure 2-2.4-5

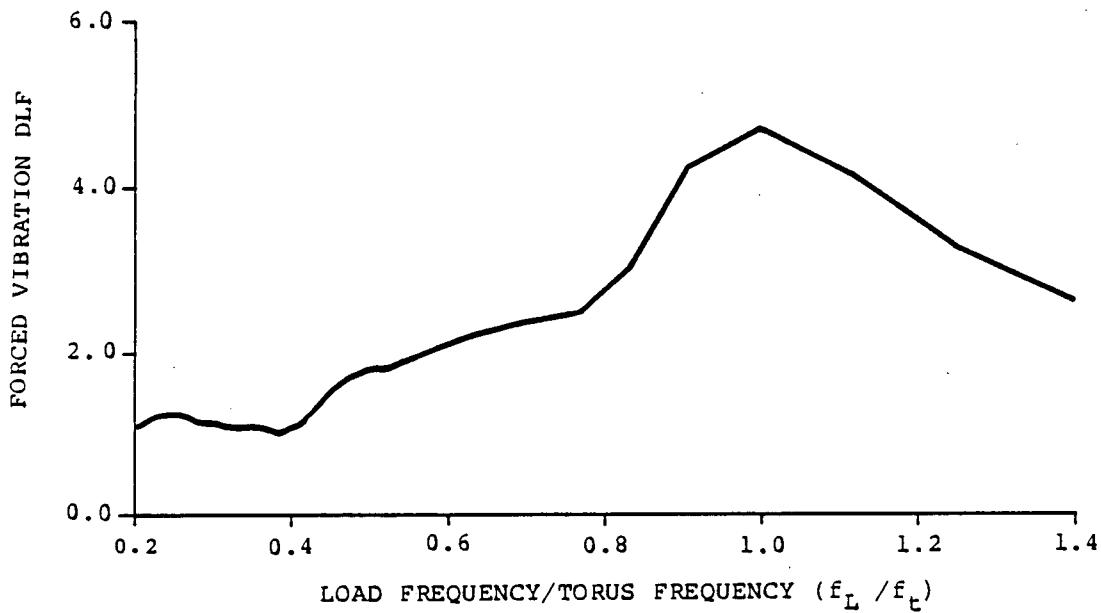
TYPICAL CHUGGING CYCLE LOAD TRANSIENT USED FOR ASYMMETRIC
PRE-CHUG DYNAMIC AMPLIFICATION FACTOR DETERMINATION

IOW-40-199-2
Revision 0

2-2.121

$$DLF_{max} = 2.25$$

TORUS FREQUENCY (f_t) (Hz)	LOAD FREQUENCY RANGE (f_L) (Hz)	FREQUENCY RATIO (f_L / f_t)	FORCED VIBRATION DLF RANGE	MODAL CORRECTION FACTOR (MCF)	DLF x MCF
8.0	6.00	0.75	2.46	0.52	1.29
	11.20	1.40	2.63	0.62	1.62
11.0	6.00	0.55	1.90	0.77	1.46
	11.20	1.02	4.61	0.36	1.65
14.0	6.00	0.43	1.32	1.00	1.32
	11.20	0.80	2.74	0.60	1.66
17.0	6.00	0.35	1.09	1.00	1.09
	11.20	0.66	2.29	0.98	2.25
23.0	6.00	0.76	1.23	1.00	1.23
	11.20	0.49	1.76	1.00	1.76
26.0	6.00	0.23	1.25	1.00	1.25
	11.20	0.43	1.35	1.00	1.35



1. SEE FIGURE 2-2.2-14 FOR FORCED VIBRATION LOADING TRANSIENT AND FREQUENCY RANGE.
2. SEE FIGURE 2-2.4-3 FOR MODAL CORRECTION FACTORS.

Figure 2-2.4-6

DYNAMIC LOAD FACTOR DETERMINATION FOR SUPPRESSION CHAMBER UNBALANCED LATERAL LOAD DUE TO SRV DISCHARGE

2-2.4.3 Methods for Evaluating Analysis Results

The methodology discussed in Sections 2-2.4.1 and 2-2.4.2 is used to determine element forces and component stresses in the suppression chamber components. The methodology used to evaluate the analysis results, determine the controlling stresses in the suppression chamber components and component supports, and examine fatigue effects is discussed in the following paragraphs.

Membrane and extreme fiber stress intensities are computed when the analysis results for the suppression chamber Class MC components are evaluated. The values of the membrane stress intensities away from discontinuities are compared with the primary membrane stress allowables (Table 2-2.3-1). The values of membrane stress intensities near discontinuities and localized regions are compared with local primary membrane stress allowables (Table 2-2.3-1). Primary stresses in suppression chamber Class MC component welds are computed using the maximum principal stress or resultant force acting on the associated weld throat. The results are compared with the primary weld stress allowables (Table 2-2.3-1).

In each of the controlling load combinations are many dynamic loads resulting in stresses which cycle with time, and which are partially or fully reversible. The maximum stress intensity range for all suppression chamber Class MC components is calculated using the maximum values of the extreme fiber stress differences which occur near discontinuities. These values are compared with secondary stress range allowables (Table 2-2.3-1). A similar procedure is used to compute the stress range for the suppression chamber Class MC component welds. The results are compared with the secondary weld stress allowables (Table 2-2.3-1).

When analysis results for the suppression chamber saddle supports are evaluated, membrane and extreme fiber stress components are computed and compared with the Class MC component support allowable stresses (Table 2-2.3-1). The reaction loads acting on the suppression chamber vertical support system column and saddle base plate assemblies are compared with the allowable support loads (Table 2-2.3-2). Stresses in suppression chamber Class MC component support welds are computed using the maximum resultant force acting on the associated weld throat. The results are compared with the weld stress limits discussed in Section 2-2.3.

The controlling suppression chamber load combinations evaluated are defined in Section 2-2.2.2. During load combination formulation, the maximum stress components in a particular suppression chamber component at a given location are combined for the individual loads contained in each combination. The stress components for dynamic loadings are combined to obtain the maximum stress intensities.

For evaluating fatigue effects in the suppression chamber Class MC components and associated welds, extreme fiber alternating stress intensity histograms are determined for each load in each event or combination of events. Stress intensity histograms are developed for the suppression chamber components and welds with the highest stress intensity ranges. Fatigue stress intensification factors of 2.0 for major component stresses and 4.0 for component weld stresses are conservatively used. For each combination of events, a load combination stress intensity histogram is formulated and the corresponding fatigue usage factors are determined (Figure 2-2.4-7). The usage factors for each event are then summed to obtain the total fatigue usage.

Use of the methodology described above results in a conservative evaluation of the suppression chamber design margins.

IOW-40-199-2
Revision 0

2-2.126

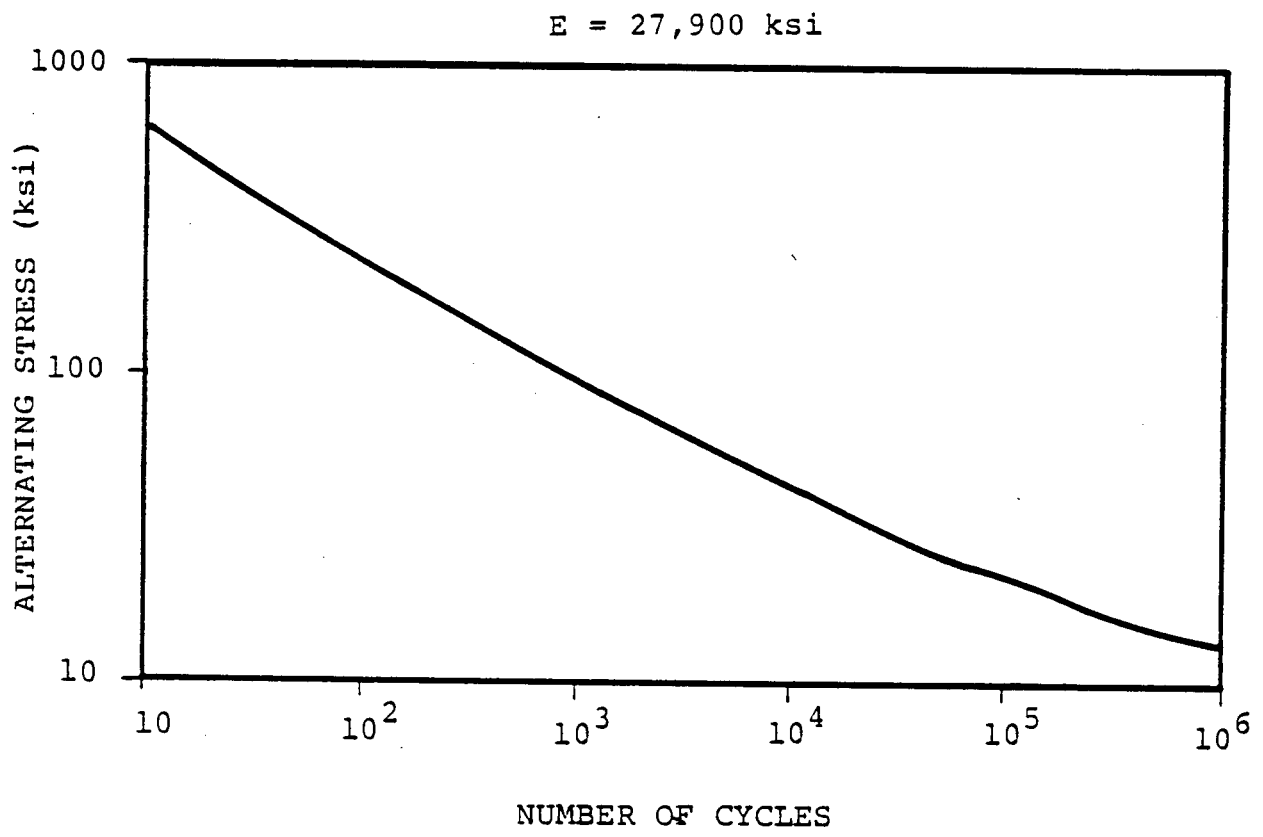


Figure 2-2.4-7

ALLOWABLE NUMBER OF STRESS CYCLES FOR SUPPRESSION
CHAMBER FATIGUE EVALUATION

IOW-40-199-2
Revision 0

2-2.127

2-2.5 Analysis Results

The geometry, loads and load combinations, acceptance criteria, and analysis methods used in the evaluation of the DAEC suppression chamber are presented and discussed in the preceding sections. The results and conclusions derived from the evaluation of the suppression chamber are presented in the following paragraphs.

Table 2-2.5-1 shows the maximum suppression chamber shell stresses for each of the governing loads. Table 2-2.5-2 shows the corresponding reaction loads for the suppression chamber vertical support system. Figures 2-2.5-1 through 2-2.5-3 show the transient responses of the suppression chamber for selected suppression chamber shell loads, expressed in terms of total vertical load per mitered cylinder.

Table 2-2.5-3 shows the maximum stresses and associated design margins for the major suppression chamber components and welds for the IBA III, IBA IV, DBA II, and DBA III load combinations. Table 2-2.5-4 shows the maximum reaction loads and associated design margins for the suppression chamber vertical support system for the IBA III, IBA IV, DBA II, and DBA III load combinations.

Table 2-2.5-5 presents the maximum suppression chamber shell stresses adjacent to the seismic restraints for each of the governing loads resulting in net lateral loads on the suppression chamber. Table 2-2.5-6 shows the corresponding reaction loads on the suppression chamber seismic restraints. Table 2-2.5-7 shows the maximum suppression chamber seismic restraint reactions and associated shell stresses adjacent to the seismic restraints for the IBA III and IBA V combinations. Table 2-2.5-8 shows the calculated and allowable stresses in each component of the seismic restraints for various loading conditions.

Table 2-2.5-9 shows the fatigue usage factors for the controlling suppression chamber component and weld. These usage factors are obtained by evaluating the normal operating plus SBA events and the normal operating plus IBA events.

The suppression chamber evaluation results presented in the preceding paragraphs are discussed in Section 2-2.5.1.

Table 2-2.5-1

MAXIMUM SUPPRESSION CHAMBER SHELL
STRESSES FOR GOVERNING LOADS

SECTION 2-2.2.1 LOAD DESIGNATION		SHELL STRESSES (ksi)		
LOAD TYPE	LOAD CASE NUMBER	PRIMARY MEMBRANE	LOCAL PRIMARY MEMBRANE	PRIMARY + SECONDARY STRESS RANGE
DEAD	1a +1b	3.12	3.98	5.90
SEISMIC	2a	0.63	0.78	2.17
	2b	1.26	1.56	4.33
PRESSURE AND TEMPERATURE	3b	10.89	10.89	16.02
	3d	0.69	1.36	2.20
POOL SWELL	4a	6.00	6.10	19.05
	4b	0.21	0.26	1.54
CONDENSATION OSCILLATION	5a	12.95	13.82	34.44
	5c	0.55	0.62	3.31
CHUGGING	6a	5.30	5.86	15.62
	6b	2.90	3.20	8.10
	6c	0.02	0.02	0.12
	6d	2.36	2.79	14.48
SRV DISCHARGE	7a	8.01	8.83	33.89
	7b	9.82	16.99	61.63
	7d	1.17	1.30	6.60

1. VALUES SHOWN ARE MAXIMUMS REGARDLESS OF TIME AND LOCATION AND MAY NOT BE ADDED TO OBTAIN LOAD COMBINATION RESULTS.

Table 2-2.5-2

MAXIMUM VERTICAL SUPPORT REACTIONS FOR
GOVERNING SUPPRESSION CHAMBER LOADINGS

SECTION 2-2.2.1 LOAD DESIGNATION			VERTICAL REACTION LOAD (kips)					
LOAD TYPE	LOAD CASE	DIRECTION	COLUMN		SADDLE		(1)	
			INSIDE	OUTSIDE	INSIDE	OUTSIDE	TOTAL	
DEAD	1a + 1b	UPWARD	0.00	0.00	0.00	0.00	0.00	
		DOWNWARD	14.12	6.16	118.62	151.60	290.50	
SEISMIC	OBE	2a	UPWARD	0.74	0.33	6.30	8.04	15.41
		DOWNWARD	0.74	0.33	6.30	8.04	15.41	
	SSE	2b	UPWARD	1.48	0.66	12.60	16.08	30.82
		DOWNWARD	1.48	0.66	12.60	16.80	30.82	
INTERNAL PRESSURE	3b	UP/DOWN	-7.38	4.26	7.46	-4.88	0.00	
THERMAL	3d	UP/DOWN	8.34	7.90	-8.36	-7.90	0.00	
POOL SWELL	4a	UPWARD	23.28	26.70	89.70	128.70	263.20	
		DOWNWARD	47.00	54.00	227.10	276.40	570.80	
CONDENSATION OSCILLATION	5a	UPWARD	96.46	104.29	319.10	426.30	946.10	
		DOWNWARD	99.44	102.76	348.98	403.34	950.48	
CHUGGING	PRE-CHUG	6a	UPWARD	20.92	41.18	51.30	77.10	190.50
		DOWNWARD	20.92	41.18	51.30	77.10	190.50	
	POST-CHUG	6b	UPWARD	23.24	28.44	75.70	92.98	220.36
		DOWNWARD	20.98	27.49	69.75	87.59	205.81	
SRV DISCHARGE	SINGLE VALVE	7a	UPWARD	40.81	51.42	347.23	476.58	650.00
		DOWNWARD	24.54	49.11	317.72	402.68	735.80	
	MULTIPLE VALVE	7b	UPWARD	100.14	159.84	577.75	740.96	1291.42
		DOWNWARD	72.42	128.25	475.27	679.22	1218.84	

(1) FOR DYNAMIC LOADS, REACTIONS ARE ADDED IN TIME.

Table 2-2.5-3

MAXIMUM SUPPRESSION CHAMBER STRESSES FOR
CONTROLLING LOAD COMBINATIONS

ITEM	STRESS TYPE	LOAD COMBINATION STRESSES (ksi)							
		IBA III ⁽¹⁾		IBA IV ⁽¹⁾		DBA II ⁽¹⁾		DBA III ⁽¹⁾	
		CALC. STRESS	CALC. ALLOW ⁽²⁾	CALC. STRESS	CALC. ALLOW ⁽²⁾	CALC. STRESS	CALC. ALLOW ⁽²⁾	CALC. STRESS	CALC. ALLOW ⁽²⁾
C O M P O N E N T S									
SHELL	PRIMARY MEMBRANE	18.8	0.97	19.6	1.0	14.6	0.76	16.2	0.46
	LOCAL PRIMARY MEMBRANE	27.3	0.94	28.0	0.97	18.1	0.63	16.0	0.30
	PRIMARY + SECONDARY STRESS RANGE	69.3	1.00	69.9	1.00	46.4	0.67	N/A	-
RING BEAM	PRIMARY MEMBRANE	13.2	0.68	13.7	0.71	11.3	0.59	24.4	0.69
	LOCAL PRIMARY MEMBRANE	18.2	0.63	22.3	0.77	18.2	0.63	29.1	0.55
	PRIMARY + SECONDARY STRESS RANGE	52.7	0.76	66.0	0.95	44.0	0.64	N/A	-
C O M P O N E N T S U P P O R T S									
COLUMN	MEMBRANE	(3)	-	15.5	0.73	16.5	0.77	21.3	0.75
	EXTREME FIBER	(3)	-	15.8	0.59	16.7	0.63	21.6	0.61
SADDLE	MEMBRANE	(3)	-	20.2	0.95	18.1	0.85	27.8	0.98
	EXTREME FIBER	(3)	-	21.8	0.82	19.7	0.74	29.4	0.83

Table 2-2.5-3

MAXIMUM SUPPRESSION CHAMBER STRESSES FOR
CONTROLLING LOAD COMBINATIONS

(Concluded)

ITEM	STRESS TYPE	LOAD COMBINATION STRESSES (ksi)							
		IBA III ⁽¹⁾		IBA IV ⁽¹⁾		DBA II ⁽¹⁾		DBA III ⁽¹⁾	
		CALC. STRESS	CALC. ALLOW ⁽²⁾	CALC. STRESS	CALC. ALLOW ⁽²⁾	CALC. STRESS	CALC. ALLOW ⁽²⁾	CALC. STRESS	CALC. ALLOW ⁽²⁾
W E L D S									
RING BEAM TO SHELL	PRIMARY	21.7	0.96	21.7	0.96	17.5	0.78	21.8	0.53
	SECONDARY	44.2	0.82	45.0	0.83	39.2	0.60	N/A	-
COLUMN CONNECTION TO SHELL	PRIMARY	(3)	-	15.5	0.80	16.5	0.85	21.3	0.60
	SECONDARY	(3)	-	37.0	0.53	34.6	0.50	N/A	-
SADDLE TO SHELL	PRIMARY	(3)	-	17.5	0.90	16.3	0.85	24.8	0.70
	SECONDARY	(3)	-	50.6	0.23	49.2	0.71	N/A	-

(1) SEE TABLE 2-2.2-12 FOR LOAD COMBINATION DESIGNATION.

(2) SEE TABLE 2-2.3-1 FOR ALLOWABLE STRESSES.

(3) IBA III CASE IS BOUNDED BY IBA IV.

Table 2-2.5-4

MAXIMUM VERTICAL SUPPORT REACTIONS
FOR CONTROLLING SUPPRESSION CHAMBER
LOAD COMBINATIONS

VERTICAL SUPPORT COMPONENT		DIRECTION	LOAD COMBINATION REACTIONS (kips)							
			IBA III ⁽¹⁾		IBA IV ⁽¹⁾		DBA II ⁽¹⁾		DBA III ⁽¹⁾	
			CALC. LOAD	CALC. ALLOW ⁽²⁾	CALC. LOAD	CALC. ALLOW ⁽²⁾	CALC. LOAD	CALC. ALLOW ⁽²⁾	CALC. LOAD	CALC. ALLOW ⁽²⁾
COLUMN	INSIDE	UPWARD	120.07	0.81	130.03	0.88	81.60	0.55	59.09	0.40
		DOWNWARD	118.17	0.24	120.35	0.25	114.32	0.24	95.40	0.20
	OUTSIDE	UPWARD	170.00	0.54	200.60	0.63	85.53	0.58	69.83	0.22
		DOWNWARD	188.33	0.39	209.01	0.43	121.52	0.25	155.41	0.32
SADDLE	INSIDE	UPWARD	608.44	0.89	582.60	0.86	202.80	0.40	329.36	0.48
		DOWNWARD	701.43	0.58	680.82	0.57	465.28	0.39	640.95	0.58
	OUTSIDE	UPWARD	817.93	0.96	803.86	0.95	266.73	0.52	458.85	0.54
		DOWNWARD	934.00	0.78	916.30	0.76	562.40	0.47	752.78	0.63
TOTAL		UPWARD	1501.62	0.75	1467.77	0.73	636.60	0.48	752.78	0.38
		DOWNWARD	1752.70	0.52	1739.98	0.52	1259.98	0.37	1672.30	0.50

- (1) SEE TABLE 2-2.2-12 FOR LOAD COMBINATION DESIGNATION.
 (2) SEE TABLE 2-2.3-2 FOR ALLOWABLE SUPPORT LOADS.

Table 2-2.5-5

MAXIMUM SUPPRESSION CHAMBER SHELL
STRESSES DUE TO LATERAL LOADS

SECTION 2-2.2.1 LOAD DESIGNATION		SHELL STRESS TYPE ⁽¹⁾ (ksi)		
LOAD TYPE	LOAD CASE NUMBER	LOCAL PRIMARY MEMBRANE	PRIMARY + SECONDARY STRESS RANGE	
SEISMIC	OBE	2a	4.57	10.23
	SSE	2b	9.11	N/A ⁽²⁾
PRE-CHUG		6a	4.78	10.78
SRV DISCHARGE		7b	6.47	14.52

(1) STRESSES SHOWN ARE IN SUPPRESSION CHAMBER SHELL
ADJACENT TO SEISMIC RESTRAINT PAD PLATE.

(2) EVALUATION NOT REQUIRED FOR SERVICE LEVEL C.

Table 2-2.5-6

MAXIMUM SEISMIC RESTRAINT REACTIONS
DUE TO LATERAL LOADS

SECTION 2-2.2.1 LOAD DESIGNATION		HORIZONTAL REACTION LOAD (kips)				
LOAD TYPE	LOAD CASE NUMBER	RESTRAINT AT AZIMUTH 22°-30'	RESTRAINT AT AZIMUTH 202°-30'	TOTAL	DYNAMIC LOAD FACTOR	
SEISMIC	OBE	2a	142.36	142.36	284.72	N/A ⁽¹⁾
	SSE	2b	284.72	284.72	569.44	N/A ⁽¹⁾
PRE-CHUG		6a	149.10	149.10	298.20	13.90
SRV DISCHARGE		7b	202.65	202.65	405.30	2.26

(1) MAXIMUM HORIZONTAL AND VERTICAL ACCELERATION FROM FSAR (REFERENCE 4) WERE USED.

Table 2-2.5-7

MAXIMUM SUPPRESSION CHAMBER SHELL
STRESSES AND SEISMIC RESTRAINT REACTIONS FOR CONTROLLING
LOAD COMBINATIONS WITH LATERAL LOADS

ITEM	STRESS/ REACTION TYPE	LOAD COMBINATION STRESSES/ REACTIONS (ksi, kips) (2)			
		IBA III		IBA V	
		CALC. VALUE	CALC. ALLOW.	CALC. VALUE	CALC. ALLOW.
SHELL (1)	LOCAL PRIMARY MEMBRANE	20.24	0.70	21.24	0.40
	PRIMARY + SECONDARY STRESS RANGE	58.66	0.84	(3)	(3)
SEISMIC RESTRAINT	MAXIMUM (4) REACTION LOAD	494.11	(4)	636.47	(4)

- (1) STRESSES SHOWN ARE IN SUPPRESSION CHAMBER SHELL ADJACENT TO SEISMIC RESTRAINT PAD PLATE.
- (2) REFERENCE TABLE 2-2.2-12 FOR LOAD COMBINATION DESIGNATION.
- (3) EVALUATION NOT REQUIRED FOR SERVICE LEVEL C.
- (4) REFERENCE TABLE 2-2.5-8 FOR ALLOWABLE AND CALCULATED STRESSES IN SEISMIC RESTRAINT COMPONENTS.

Table 2-2.5-8

MAXIMUM STRESSES IN SEISMIC RESTRAINT COMPONENTS
FOR CONTROLLING LOAD COMBINATIONS WITH LATERAL LOADS

COMPONENT	STRESS TYPE	LOAD COMBINATION STRESSES (ksi)			
		IBA III		IBA V	
		CALCULATED VALUE	(1) ALLOWABLE	CALCULATED VALUE	ALLOWABLE
8" DIAMETER PIN	SHEAR	5.05	14.40	6.50	28.80
	BENDING	6.67	27.00	8.56	36.00
2 1/4" DIAMETER ANCHOR BOLT	TENSION	9.64	18.96	12.42	36.00
UPPER TIE PLATE TO PAD PLATE WELD	SHEAR	6.48	15.80	8.31	21.06
LOWER TIE PLATE TO BASE PLATE WELD	SHEAR	7.60	15.80	9.77	21.06
PAD PLATE TO TORUS SHELL WELD	SHEAR	7.59	13.60	9.77	18.09
CONCRETE	BEARING	0.46	1.00	0.59	1.00

(1) ALLOWABLE STRESSES ARE FROM FSAR (REFERENCE 4).

Table 2-2.5-9

MAXIMUM FATIGUE USAGE FACTORS FOR SUPPRESSION CHAMBER
COMPONENTS AND WELDS

EVENT SEQUENCE ⁽¹⁾	LOAD CASE CYCLES ⁽¹⁾					EVENT USAGE FACTOR ⁽⁸⁾	
	SEISMIC	PRESSURE	TEMPERATURE	SRV DISCHARGE	PRE + POST CHUGGING (sec)	TORUS SHELL	WELD
NOC W/SINGLE SRV	0	150 ⁽²⁾	150 ⁽²⁾	740 ⁽³⁾	N/A	0.050	0.111
NOC W/MULTIPLE SRV	0	0	0	60 ⁽⁴⁾	N/A	0.181	0.051
SBA 0 to 600 sec	600 ⁽²⁾	1	1	50 ⁽⁴⁾	300 ⁽⁶⁾	0.227	0.062
SBA 600 to 1200 sec	0	0	0	2 ⁽⁵⁾	600 ⁽⁶⁾	0.009	0.002
IBA 0 to 900 sec	600 ⁽²⁾	1	1	25 ⁽⁴⁾	900 ⁽⁷⁾	0.116	0.031
IBA 900 to 1100 sec	0	0	0	2 ⁽⁵⁾	200 ⁽⁶⁾	0.009	0.002
MAXIMUM CUMULATIVE USAGE FACTORS				NOC + SBA		0.467	0.226
				NOC + IBA		0.356	0.195

- (1) SEE TABLE 2-2.2-12 AND FIGURES 2-2.2-15 THROUGH 2-2.2-17 FOR LOAD CYCLES AND EVENT SEQUENCING INFORMATION.
- (2) ENTIRE NUMBER OF LOAD CYCLES CONSERVATIVELY ASSUMED TO OCCUR DURING TIME OF MAXIMUM EVENT USAGE.
- (3) TOTAL NUMBER OF SRV ACTUATIONS SHOWN IS CONSERVATIVELY ASSUMED TO OCCUR IN SAME SUPPRESSION CHAMBER BAY.
- (4) VALUE SHOWN IS CONSERVATIVELY ASSUMED TO BE EQUAL TO THE NUMBER OF MULTIPLE VALVE ACTUATIONS WHICH OCCURS DURING THE EVENT.
- (5) NUMBER OF ADS ACTUATIONS ASSUMED TO OCCUR DURING THE EVENT.
- (6) EACH CHUG CYCLE HAS A DURATION OF 1.4 SECONDS.
- (7) CO LOADS, WHICH ARE THE SAME AS PRE-CHUG LOADS, OCCUR DURING THIS PHASE OF THE IBA EVENT.
- (8) USAGE FACTORS ARE COMPUTED FOR THE COMPONENT AND FOR THE WELD WHICH RESULT IN THE MAXIMUM CUMULATIVE USAGE.

MAX DOWNWARD REACTION = -570.4 kips

MAX UPWARD REACTION = 263.2 kips

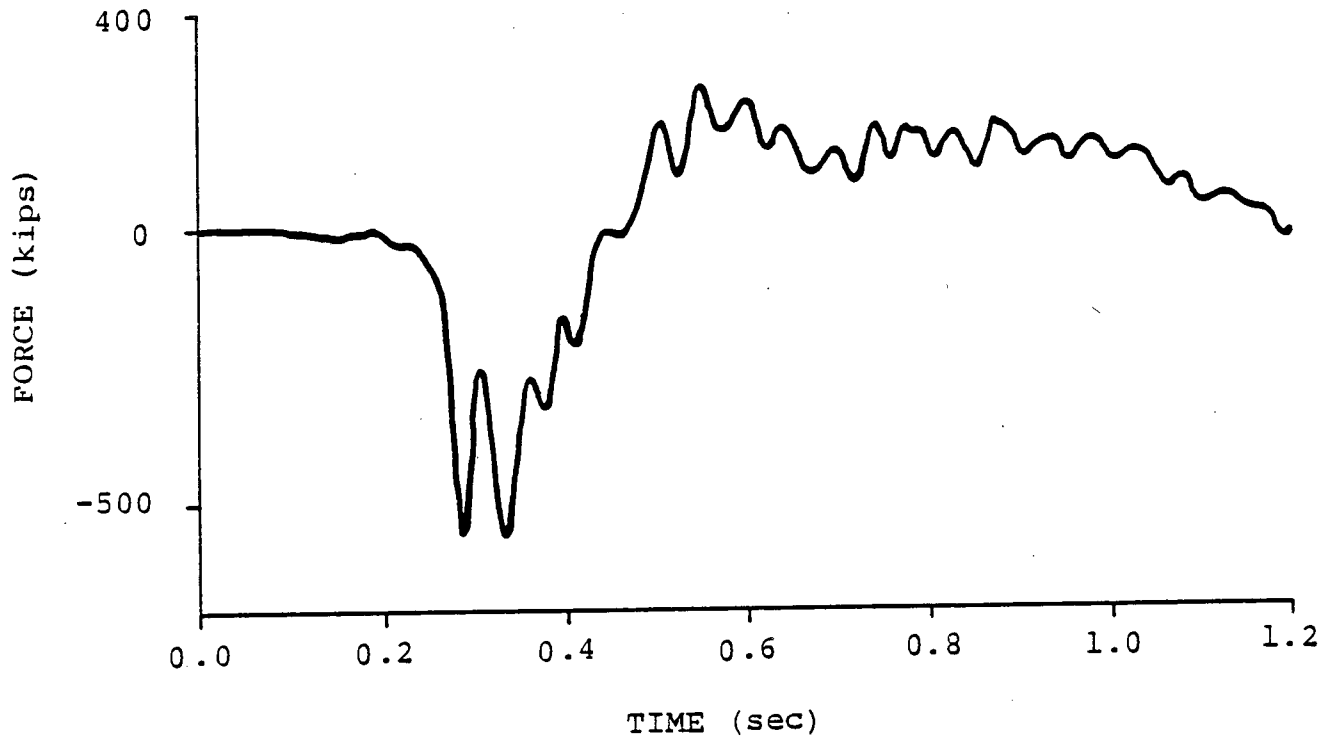


Figure 2-2.5-1

SUPPRESSION CHAMBER RESPONSE DUE TO POOL SWELL
LOADS-TOTAL VERTICAL LOAD PER MITERED CYLINDER

IOW-40-199-2
Revision 0

2-2.140

MAX DOWNWARD REACTION = -769.8 kips
MAX UPWARD REACTION = 680.0 kips

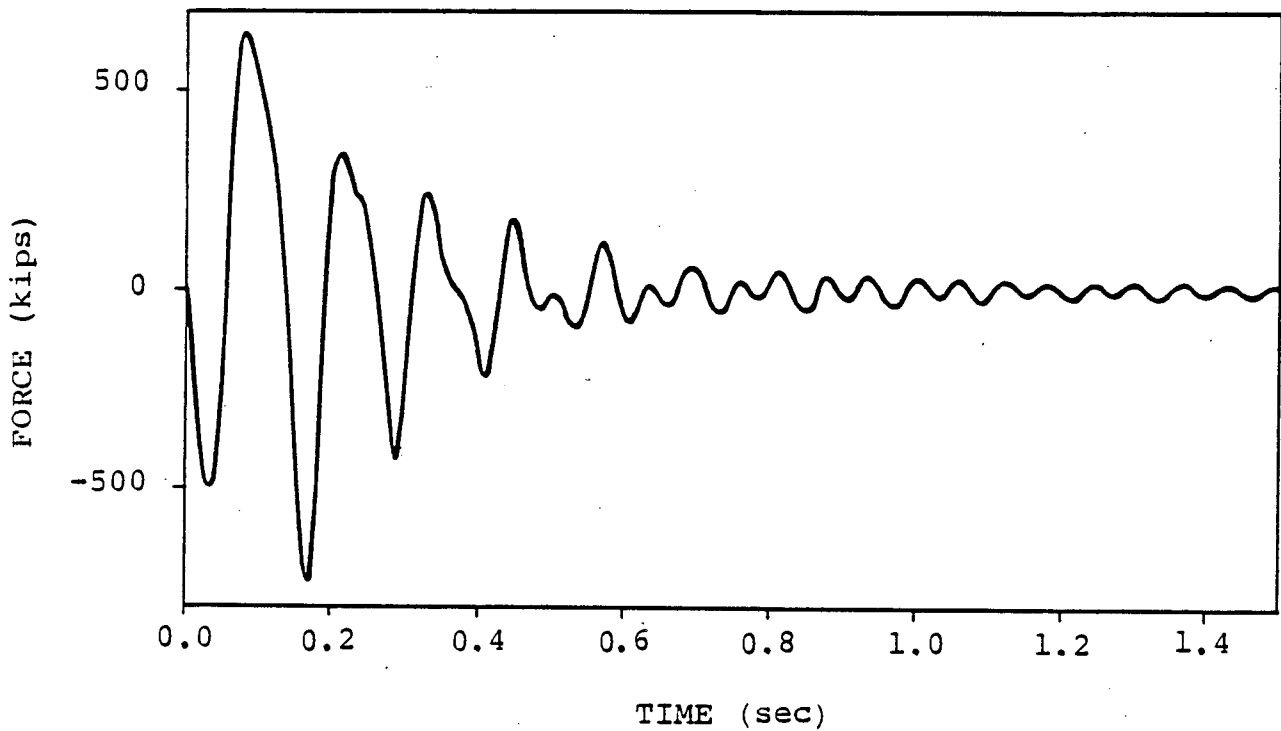


Figure 2-2.5-2

SUPPRESSION CHAMBER RESPONSE DUE TO SINGLE VALVE
SRV DISCHARGE TORUS SHELL LOADS-TOTAL VERTICAL LOAD
PER MITERED CYLINDER

IOW-40-199-2
Revision 0

2-2.141

MAX DOWNWARD REACTION = -966.66 kips

MAX UPWARD REACTION = 1045.84 kips

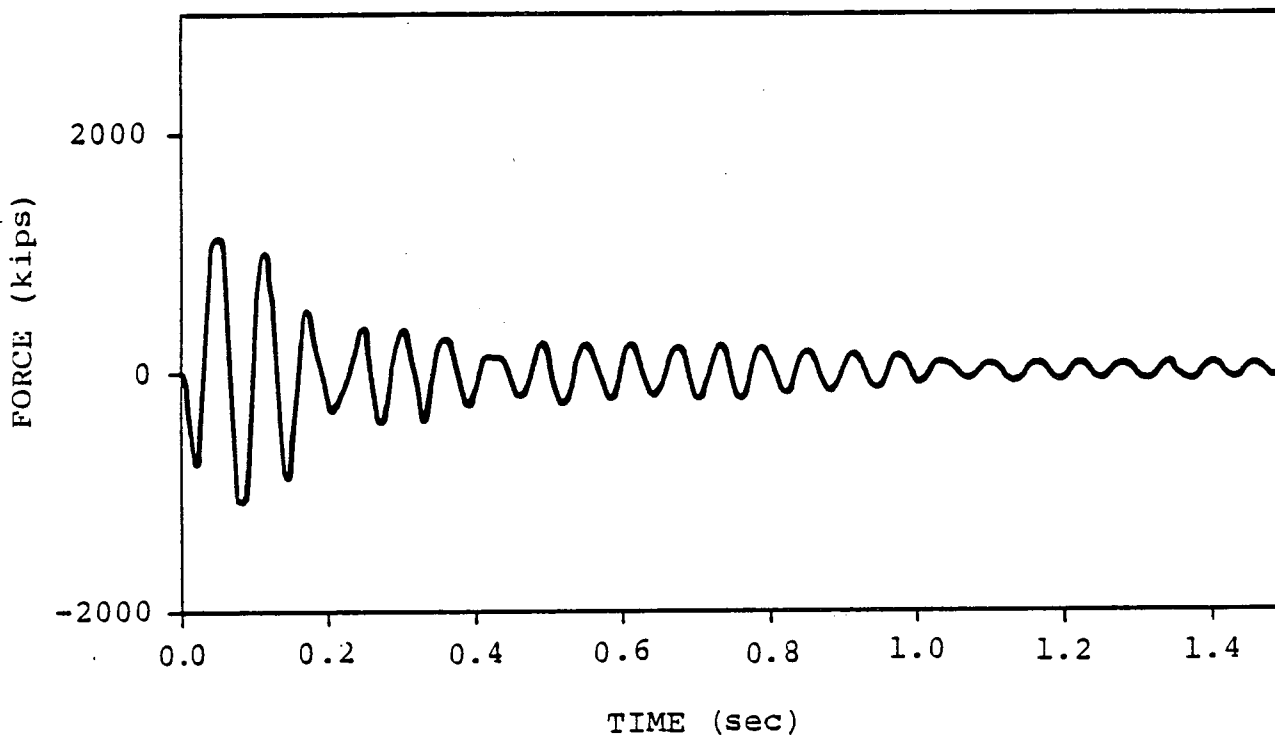


Figure 2-2.5-3

SUPPRESSION CHAMBER RESPONSE DUE TO MULTIPLE VALVE
SRV DISCHARGE TORUS SHELL LOADS-TOTAL VERTICAL LOAD
PER MITERED CYLINDER

IOW-40-199-2
Revision 0

2-2.142

2-2.5.1 Discussion of Analysis Results

The results shown in Table 2-2.5-1 indicate that the largest suppression chamber shell stresses occur for IBA internal pressure loads, pool swell suppression chamber shell loads, DBA condensation oscillation suppression chamber shell loads, and SRV discharge suppression chamber shell loads. The submerged structure loadings, in general, cause only local stresses in the suppression chamber shell adjacent to the quencher support beam and the ring beam.

Table 2-2.5-2 shows that the largest suppression chamber vertical support reactions occur for pool swell suppression chamber shell loads, DBA condensation oscillation loads, and SRV discharge suppression chamber shell loads. The saddle supports, in general, transfer a larger portion of the load to the basemat than do the support columns.

The results shown in Table 2-2.5-3 indicate that the largest stresses in the suppression chamber components, component supports, and associated welds occur for the IBA III and IBA IV load combinations. The suppression chamber shell stresses for the IBA III and IBA IV

combinations are less than the allowable limits, with stresses in other suppression chamber components, component supports, and welds well within the allowable limits. The stresses in the suppression chamber components, component supports, and welds for the DBA II, and DBA III combinations are also well within allowable limits.

Table 2-2.5-4 shows that the largest upward and downward vertical support reactions occur for the IBA III and IBA IV combinations. In general, the upward vertical support reactions are less than the downward vertical support reactions. The vertical support system reactions for all load combinations are less than allowable limits.

The results shown in Tables 2-2.5-5 and 2-2.5-6 indicate that the largest seismic restraint reactions and associated suppression chamber shell stresses occur for seismic loads and SRV discharge loads. Table 2-2.5-7 shows that the seismic restraint reactions and suppression chamber shell stresses adjacent to the seismic restraints for IBA III and IBA V load combinations are less than allowable limits. Table 2-2.5-8 shows that the calculated stresses in the seismic restraint components are less than the allowable stresses.

The results shown in Table 2-2.5-9 indicate that the largest contributor to suppression chamber fatigue effects are SRV discharge loads which occur during normal operating conditions. The largest total fatigue usage occurs for the normal operating plus SBA events, with usage factors for the suppression chamber shell and associated welds less than allowable limits. The usage factors for the normal operating plus IBA events are also less than allowable limits.

2-2.5.2 Closure

The suppression chamber loads described and presented in Section 2-2.2.1 are conservative estimates of the loads postulated to occur during an actual LOCA or SRV discharge event. Applying the methodology discussed in Section 2-2.4 to evaluate the effects of the governing loads on the suppression chamber results in bounding values of stresses and reactions in suppression chamber components and component supports.

The load combinations and event sequencing defined in Section 2-2.2.2 envelop the actual events postulated to occur during a LOCA or SRV discharge event. Combining the suppression chamber responses due to the governing loads and evaluating fatigue effects using this methodology results in conservative values of the maximum suppression chamber stresses, support reactions, and fatigue usage factors for each event or sequence of events postulated to occur throughout the life of the plant.

The acceptance limits defined in Section 2-2.3 are as restrictive or more so, as those used in the original containment design documented in the plant's FSAR.

Comparing the resulting maximum stresses and support reactions to these acceptance limits results in a conservative evaluation of the design margins present in the suppression chamber and suppression chamber supports. As demonstrated in the results discussed and presented in the preceding sections, all suppression chamber stresses and support reactions are within these acceptance limits.

As a result, the suppression chamber components described in Section 2-2.1, which are specifically designed for the loads and load combinations used in this evaluation, exhibit the margins of safety inherent in the original design of the primary containment as documented in the plant's FSAR. The NUREG-0661 requirements, as they relate to the design adequacy and safe operation of the DAEC suppression chamber, are therefore considered to be met.

LIST OF REFERENCES

1. "Mark I Containment Long-Term Program," Safety Evaluation Report, USNRC, NUREG-0661, July 1980.
2. "Mark I Containment Program Load Definition Report," General Electric Company, NEDO-21888, Revision 2, November 1981, including Errata and Addenda No. 1, April 1982.
3. "Mark I Containment Program Plant Unique Load Definition," Duane Arnold Energy Center, General Electric Company, NEDO-24571, Revision 1, March 1982, including Errata and Addenda No. 1, October 1982.
4. DAEC Final Safety Analysis Report (FSAR) and Supplementary Amendments #1 through #14 dated May 1972 to August 1973, respectively.
5. "Mark I Containment Program Structural Acceptance Criteria Plant Unique Analysis Application Guide," Task Number 3.1.3, General Electric Company, NEDO-24583-1, October 1979.
6. ASME Boiler and Pressure Vessel Code, Section III, Division 1, 1977 Edition with Addenda up to and including Winter 1978.
7. American Concrete Institute (ACI) Code, Code Requirements for Nuclear Safety-Related Concrete Structures, ACI-349-80.
8. "Damping Values for Seismic Design of Nuclear Power Plants," U.S. Atomic Energy Commission, Regulatory Guide 1.61, October 1973.